UNIVERSIDADE FEDERAL DO PARANÁ

LUCAS CHAGAS LIMA DO CARMO

COSMETIC EMULSION PHYSICAL STABILITY SCREENING BY MEANS OF RHEOLOGY

CURITIBA

2020

LUCAS CHAGAS LIMA DO CARMO

COSMETIC EMULSION PHYSICAL STABILITY SCREENING BY MEANS OF RHEOLOGY

Dissertação apresentada ao Programa de Pós-Graduação em Ciências Farmacêuticas para obtenção de grau de Mestre em Ciências Farmacêuticas pelo setor de Ciências da Saúde da Universidade Federal do Paraná .

Supervisor: Dr. Rilton Alves de Freitas

CURITIBA

2020

Carmo, Lucas Chagas Lima do
Cosmetic emulsion physical stability screening by means of rheology [recurso eletrônico] / Lucas Chagas Lima do Carmo – Curitiba, 2020.

Dissertação (mestrado) – Programa de Pós-Graduação em Ciências Farmacêuticas.
Setor de Ciências da Saúde, Universidade Federal do Paraná, 2020.
Orientador: Dr. Rilton Alves de Freitas

1. Reologia. 2. Estabilidade de cosméticos. 3. Emulsões. 4. Triagem. 5. Emulsão O/A. I. Freitas, Rilton Alves de. II. Universidade Federal do Paraná. III. Título.

CDD 531.1134

Leonardo Talone Neto CRB 9/1977

TERMO DE APROVAÇÃO

Os membros da Banca Examinadora designada pelo Colegiado do Programa de Pós-Graduação em CIÊNCIAS FARMACÊUTICAS da Universidade Federal do Paraná foram convocados para realizar a arguição da Dissertação de Mestrado de **LUCAS CHAGAS LIMA DO CARMO** intitulada: **Cosmetic emulsion physical stability screening by means of rheology**, sob orientação do Prof. Dr. RILTON ALVES DE FREITAS, que após terem inquirido o aluno e realizada a avaliação do trabalho, são de parecer pela sua APROVAÇÃO no rito de defesa.

A outorga do título de mestre está sujeita à homologação pelo colegiado, ao atendimento de todas as indicações e correções solicitadas pela banca e ao pleno atendimento das demandas regimentais do Programa de Pós-Graduação.

CURITIBA, 16 de Março de 2020.

Avaliador Interno (UNIVERSIDADE FEDERAL DO PARANÁ)

Assinatura Eletrônica
30/03/2020 16:20:50.0
RILTON ALVES DE FREITAS
Presidente da Banca Examinadora (UNIVERSIDADE FEDERAL DO PARANÁ)

Assinatura Eletrônica
25/03/2020 15:32:40.0
AGNES DE PAULA SCHEER
Avaliador Externo (UNIVERSIDADE FEDERAL DO PARANÁ)

Assinatura Eletrônica
13/04/2020 16:55:29.0
SAAD AKHTAR KHAN
Avaliador Externo (NORTH CAROLINA STATE UNIVERSITY)

Assinatura Eletrônica
25/03/2020 15:40:49.0
FÁBIO SEIGI MURAKAMI
Avaliador Interno (UNIVERSIDADE FEDERAL DO PARANÁ)

ACKNOWLEDGEMENTS

I would like to express my gratitude for all the help and support put forth by my supervisor Dr. Rilton Alves de Freitas, who kept challenging me up to the final stages of the master's degree completion. I also am thankful for the participation of Dr. Izabella Maria F. Campos from Grupo Boticário, who helped in the experiments and provided excelent advice based on her experience.

My gratitude goes to Dr. Silvia S. Guterres and Dr. Karina Paese from the Federal University of Rio Grande do Sul, for providing the raw materials needed and the help in the development of the formulations. My colleagues also deserve my gratitude for providing a safe and just workplace and support despite all the friendly bickering. I would like to thank all the participants of the evaluation board, Dr. Fábio Murakami from the Pharmaceutical Sciences Post-graduation Program, Dr. Agnes de Paula Scheer from the Chemistry Engineering Department and Dr. Saad Khan from the Department of Chemical and Biomolecular Engineering of North Carolina State University.

I acknowledge and am grateful for the financial support provided by CAPES, the Pharmaceutical Sciences Post-graduation Program, the Chemistry Department and Grupo Boticário for granting access to their facilities, which were imperative to the development of this project.

I would like to thank my brother Augusto who actively helped me in the development of scripts to automate data organization and plotting and for his input on the creation of the figures. My parents deserve my gratitude for providing emotional and financial support as well as advice throughout my professional and academic development, their role in my formation was of the utmost importance and my accomplishments are a result of their education. Last but not least I am thankful for my companion Flávia who is constantly reminding me what I'm capable of.

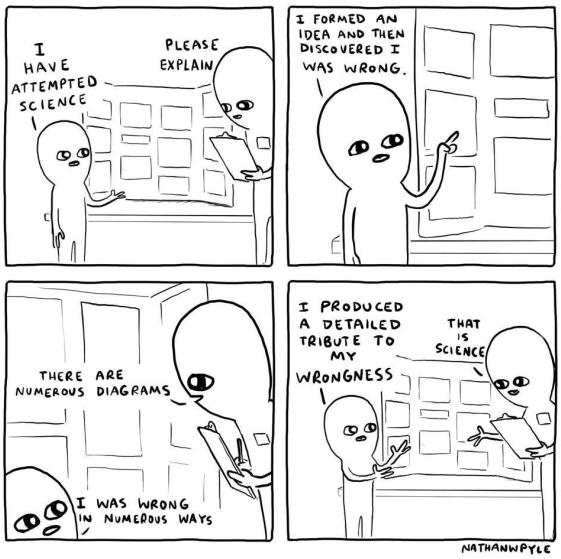

– Nathan W. Pyle

RESUMO

Estabilidade é uma das primeiras condições que se deve ser avaliada no desenvolvimento de produtos cosméticos. Entretanto a avaliação da estabilidade física é um processo longo onde formulações nas etapas iniciais, é preparada em escala laboratorial e armazenado em diferentes condições de temperatura e iluminação para ser analisado sob vários parâmetros em períodos de tempo de armazenamento específicos. Emulsões cosméticas são sistemas termodinâmicamente instáveis formados pela mistura de duas fases líquidas imiscíveis. O estudo presente se propõe em verificar a correlação entre parâmetros reológicos e a estabilidade de emulsões cosméticas para propor um protocolo de identificação de instabilidade física prematura. Para os experimentos, uma fórmula do formulário Nacional da farmacopéia brasileira foi selecionada e a instabilidade foi simulada através do aumento do conteúdo da fase oleosa em relação com a fase aquosa. Logo, oito formulações foram preparadas para que se fossem avaliados durante um período de 182 dias os parâmetros reológicos com ciclos aquecimento e resfriamento; medidas de tamanho de gotículas por microscopia óptica e pelo método de difração de Fraunhofer; medidas de pH e condutividade e centrifugação. Os perfis de varreduras de amplitude demonstram que após 14 dias de produção ainda há efeito de amadurecimento. Varreduras de frequência mostram que o ponto de relaxação não é afetado pelo tempo de armazenamento apesar de haver um aumento em ambos módulo elástico e viscoso ser aparente em função do tempo. As varreduras de temperatura possibilitam inferir que a maioria das amostras são sensíveis à temperatura porém algumas não desestabilizam em função da mesma. A razão entre G'' e G' (tan δ) aumenta em função da temperatura e reflete um *loop* para temperaturas maiores que 35 °C, indicando efeito de histerese térmica. Medidas de tamanho de gotículas indicam distribuição multimodal com a presença de agregados para fórmulas com maior conteúdo de óleo. Valores de condutividade e pH apresentam alta variância ao longo do tempo e pH apresenta uma tendência de diminuir ao longo do tempo de armazenamento. O uso de métodos reológicos como peça central no estudo da estabilidade de emulsões cosméticas pode vir a garantir a redução da avaliação da estabilidade física, também como aumentar os padrões de qualidade e aceitação dos consumidores do produto.

Palavras Chave: reologia; estabilidade; emulsão; triagem; O/A.

ABSTRACT

Stability is one of the first conditions that require investigation when developing new cosmetic products. However, stability assessment is a long process whereas formulations still in initial stages are prepared in laboratory scale, stored in different temperature and lighting conditions to by analyzed under various parameters in specific periods throughout storage time. Cosmetic emulsions are thermodynamically unstable systems formed by the mixture of two liquid immiscible phases. This study proposes to verify the correlation between rheological parameters and cosmetic emulsions stability, establishing a protocol to prematurely identify instability potential. For the experiments a formula from the National Form of the brazilian pharmacopoeia was selected and instability was simulated by increasing the content of the oily phase in relation to aqueous phase. Thus, eight formulations were prepared to be evaluated over a period of 182 days by oscillatory rheological parameters, with cycles of increasing and decreasing temperature; droplet size measurements by optical and polarized microscopy and Fraunhofer diffraction method; pH and conductivity measurements and centrifugation. Amplitude sweep curve profile demonstrate that after 14 days of creamy emulsion production there is still a ripening effect. Frequency sweeps shown that relaxation point is not affected by storage time, however a slight increase in the both elastic and viscous moduli is apparent over time. Temperature sweeps allow to infer that most samples are sensitive to temperature but some do not destabilize. The ratio between G'' and G' (tan δ), increases as a function of temperature and presents a loop for temperatures above 35 °C, indicating a thermal hysteresis effect. Droplet size measurementes indicate multimodal distribution with the presence of aggregates in the formulations with higher oil content. Conductivity and pH values present a high variance and pH presents a small tendency in decrease for all formulas over the period of 182 days. The use of rheological methods as the centerpiece in the study of cosmetic emulsion stability may guarantee a reduction in stability assessment time as well as increase the quality standards and consumer acceptance of the product.

Keywords: rheology; stability; emulsion; screening; O/W.

LIST OF FIGURES

LIST OF TABLES

LIST OF SYMBOLS

α	Angular coefficient
γ	Strain
γ_y	Yield Strain
$\dot{\gamma}$	Shear rate
δ	Phase angle
η	Viscosity
η^*	Complex Viscosity
Ξ	Ratio between i^{th} G' max value and first G' max value in temperature swings test
π	Mathematical constant
ρ	Density
σ	Interfacial tension
τ	Shear stress
τ_y	Yield point
ϕ	Volume fraction
ω	Oscillation frequency
ω_c	Crossover frequency
w_i	Mass fraction
G^*	Complex shear modulus
G'	Elastic component of the complex shear modulus – storage modulus
G''	Viscous component of the complex shear modulus – loss modulus
$\mathcal{A}$	Value that represents strength between rheological units
z	Value that represents number of interactions between rheological units

R	Gas universal constant
g	Gravity force
r	Radius
t	Time
E_{coh}	Cohesive energy
k_B	Boltzmann constant
T	Temperature – [K]
∞	Infinity
°C	Celsius degree
µ	Micro – 10^{-3}
m	Meter
g	Gram
rpm	Revolutions per minute
SD	Standard Deviation
mL	Milli litre
mm	Milli meter
s	Seconds
Pa	Pascal
Hz	Hertz
min	Minute
px	Pixel

CONTENTS

1 INTRODUCTION

Coming into any pharmacy or store in a mall we come to face an infinity of cosmetic products with many applications. A large majority of these products are creams, lotions, personal hygiene and cosmeceuticals. Incompatibilities in formulations are very common when developing new products and a great deal of work, study and time is invested to try to outline these problems. Production line delays can backlog sales, generate waste of raw materials and result in environmental and economic impairment, however the industry wastes no time in supplying the market constantly with new releases (ABIHPEC, 2018).

Cosmetic and pharmaceutical semi-solid formulations are most commonly formed when two immiscible liquid phases are mixed by applying energy onto them, until one liquid is separated as droplets spread inside the other liquid (SJÖBLOM, 2006). Such formulations can be as complex as the amount and variety of raw materials used to produce and stabilize them, therefore complex and unpredictable behavior are expected.

Even though there are methods to assess instabilities over the period of weeks, those are technologically belated when it comes to predicting stability over long periods of time. As a result, to evaluate product physical stability it must be done over longer time spans. That being the case, it is not very attractive for companies to have to delay releases in spite of stability studies so new methods must be developed to shorten that time and meet market demands (ISAAC et al., 2008).

Ideally a solution to such a problem would be to develop a experimental protocol based on current and new technologies that would provide the possibility to predict formulations structural stability over time, however not much has been published with standardization in mind. Thus, based on the presented, through rheological analysis the current work seeks to apply concepts and methods to expand the knowledge about emulsion properties and which characteristics are ideal to ensure long term stability.

1.1 OBJECTIVES

The main objective of this work is to establish a rheological experiment protocol that allows the possibility of predicting cosmetic creams shelf-life stability.

1.2 SPECIFIC OBJECTIVES

- Prepare oil-in-water emulsions based on brazilian pharmacopoeia that remains stable over the experiment duration;
- Promote emulsion structural instability;
- Conduct accelerated structural stability and long-term shelf-life structural stability assays;
- Propose rheological assays protocol to assess structural stability;
- Correlate rheological parameters with emulsion stability.

2 LITERATURE REVIEW

2.1 COSMETIC MARKET

The cosmetics industry has grown constantly between 2006 and 2014, with an deflated average of 11.4 % in this interval (ABIHPEC, 2015). In 2016 the ex-factory revenue summed a total of 45 billion *reais* and among the main reasons for this growth is the increase in life expectancy; increase of women in the workforce and the constant launch of new products that meet consumer needs and expectations (ABIHPEC, 2018).

Cosmetic industry sector was the one with highest investments in advertising from 2015 to 2016, just under retail and services respectively (KANTAR IBOPE MEDIA, 2016, 2017). Acording to ABIHPEC (2018), less than 2 % of the billing was invested in R&D while in advertising it was of 9.3 %. These values when associated with data from revenue increase can indicate that new formulations are not necessarily product of technological advancements in the cosmetics industry but likely due to a demand from the marketing departments of the large personal hygiene and cosmetics industry.

The increase in the sheer number of new formulations represents a series of challenges. How can one guarantee that quality criteria will be met in all new formulations? How to assert that these products will be competitive in the market and meet consumer expectations? There are methods recommended by public agencies that establish minimum quality parameters for cosmetics and perfumery, but they are costly in human, economic and financial resources (ANVISA, 2004), however no legislation or norm are in place.

To solve these issues, companies require the development of experimental protocols that assist in the savings of all these resources. Additionally, the advent of consumers interest in sustainability and *green* cosmetics has increased the difficulty of developing new products that have the same performance as the old ones (BOM et al., 2019). Sustainability is not only relevant in selection of materials but also in production scaling and manufacturing. Predicting the stability of formulations can be a tool to help reduce waste of raw materials as well as spoilage and emissions.

2.2 PRODUCTS AND PERFUMERY

Any product used for beauty and some for toiletry can be considered cosmetics. Within this category there are: creams; lotions; gels; ointments; pastes; solutions and others (EUROPEAN COMMISSION, 2009; ANVISA, 2018). Among the most common are oil-in-water emulsions, whose functions are to keep the skin hydrated through three

distinct mechanisms: occlusion; wetting and active hydration. Occlusion is the formation of a thin layer of a material over the skin to inhibit water evaporation; wetting is the attraction of water vapour to the skin and the active hydration is the recovery of the natural emulsion of the skin (GARRETT, 1962).

These products must meet some stability criteria: long storage times, physical stability under temperature variations and mechanical stress, (e.g., in transportation), as well as sensory properties for application to the skin and also the safety of the raw materials used (TADROS, 2004).

2.3 EMULSIONS

The author acknowledges that phenomena occuring in both *droplets* and *particles* are distinct but to simplify the text, in some cases, these terms will be used interchangeably in this document.

Emulsions are the class of colloidal systems made from the mixture of two liquid immiscible phases and a surfactant. The mixture is composed of droplets of the dispersed phase spreaded within the continuous phase. There are several types of emulsions: simple, multiple, macroemulsions, nanoemulsions and microemulsions, to cite some (MYERS, 2005; TADROS, 2010). They are also classified by the nature of its dispersed and dispersing phases. Oil-in-water (O/W) are the emulsions that contain oily phase dispersed droplets in an aqueous phase, they are te opposite of water-in-oil emulsions. Here the term *oil* means any water-insoluble liquid. There has also been described in literature oil-in-oil (O/O) and water-in-water (W/W) emulsions (ESQUENA, 2016; WAQAS et al., 2014; CHABNI et al., 2018; LU et al., 2018; DE FREITAS et al., 2016; HAZT et al., 2020).

Simple emulsions are the ones formed by only two immiscible phases, and are commonly found in cosmetic products. Droplets usually have a diameter larger than 0.1 µm resulting in opaque systems that can be stable for long periods of time when formulated properly (MITSUI, 1997).

Multiple (double) emulsions occur when there are droplets within dispersed droplets. They can either be classified by having a single droplet within (Fig. 1A) or multiple (Fig. 1B). Usually, in systems with multiple emulsions both are observed (MITSUI, 1997; PAL, 2008). Just as simple emulsions they can also be classified by the nature of the dispersing and dispersant phase: either W/O/W or O/W/O.

Macroemulsions do not form spontaneously therefore they are thermodinamically unstable, however microemulsions can be stable due to extremely low interfacial tension (TAYLOR, 1998; FRYD; MASON, 2012). They are transparent or semi-transparent systems formed by water, oil, an ionic surfactant and a medium-length

Figure 1 – MULTIPLE EMULSION DIAGRAM

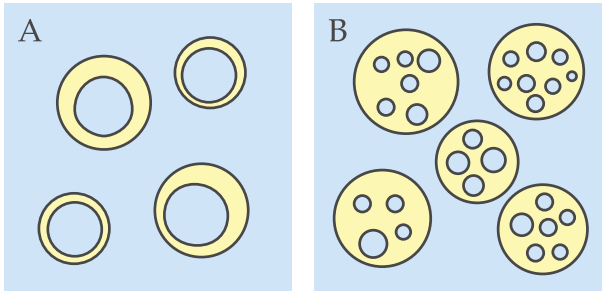

SOURCE: the author, (2020).

alcohol (MITSUI, 1997). Microemulsions are good drug carriers in topical, ocular and parenteral formulations (FANUN, 2012).

Nanoemulsions are denominated as such because it only contains droplets with a diameter smaller than 0.1 µm (TADROS, 2010), achieved by a high surfactant concentration and energy input (TADROS, 2005). They have applications in pharmaceutical, food and cosmetics industries and are very stable due to its reduced droplet size, result of high pressure homogenization or ultra sonication (GUPTA; SBRAGAGLIA; SCAGLIARINI, 2015).

Another class are the concentrated and highly concentrated emulsions (CHABNI et al., 2018) they are named this way according to the high concentration of dispersed droplets (KIM; MASON, 2017). In both there is packing and jamming of droplets that form a gelled macrostructure that has effects on its consistency (PAL, 2011). In these systems, monodispersed droplets can make up to 74 % of the total volume when not deformed, while this number can be higher for deformable or polydispersed droplets. The jammed droplets have solid-like properties (LANGENFELD; SCHMITT; STÉBÉ, 1999), hence they are used in food and cosmetic industries especially in the formulation of semi-solid creams (MOULAI MOSTEFA et al., 2006).

2.3.1 Emulsions stability mechanisms

Emulsions are considered themodinamically unstable systems because in the emulsification step, as a result of the increase in interface between immiscible liquids area, both the surface energy term ($\Delta A\sigma$) and the entropy dispersion term (ΔS) are positive, resulting in a positive Gibbs free energy term (ΔG), (Eq. 2.1). Generally for most emulsified systems $\Delta A\sigma$ is much greater than $\mathrm{T}\Delta S$, so even with the increase in entropy, the Gibbs free energy will be positive. In order to reduce free energy, the system will tend to reduce the interfacial area by coalescence, flocculation and Ostwald

ripening, unless some other mechanism of stability is present (TADROS, 2013).

$$\Delta G = \Delta A\sigma - \mathrm{T}\Delta S \tag{2.1}$$

The stabilization mechanisms present are kinetic, which grants emulsions a metastability. In order to reduce flocculation, coalescence and Ostwald ripening there are some strategies based on the Stokes equation (Eq. 2.2) (MIKKONEN et al., 2016) where it is observed that the density difference between dispersed and dispersant phases ($\Delta\rho$); gravity acceleration (g); and droplet radius (r) are all directly proportional to sedimentation (or creaming) velocity (v_0) and the viscosity of the continuous phase (η) is inversely proportional, however this relationship can only be assumed when there are no interactions between neighboring droplets i.e., volume fraction $\phi < 0.02$ (MASON, 1999; TADROS, 2011). For emulsion droplets that behave like close packing spheres, Stokes equation (Eq. 2.2) becomes invalid for determining sedimentation velocity because they are arrested in place (DATTA et al., 2011). However, in emulsions with smaller volume fraction (therefore smaller droplet packing), the strategies to grant emulsion kinetic stability are based on the modification of said variables.

$$v_0 = \frac{2}{9}\frac{\Delta\rho\ g\ r^2}{\eta_0} \tag{2.2}$$

Some example methodologies to assess emulsions stability have been developed using the aforementioned parameters. These include: phase separation kinetics as function of time (Eq. 2.3); flocculation studies as function of cohesive energy (Eq. 2.4) (TADROS, 2004, 2010); droplet size distribution (MCCLEMENTS, 2007); accelerated coalescence tests based on centrifugation (KREBS; SCHROËN; BOOM, 2012); zeta-potential measurements (CARLOTTI et al., 2005; ARAB; KANTZAS; BRYANT, 2018) and the widespread DLVO theory for electrical repulsion systems (MITSUI, 1997; SANFELD; STEINCHEN, 2008).

$$\frac{t}{V} = \frac{1}{b\ V_\infty} + \frac{t}{V_\infty} \tag{2.3}$$

Where: t = time; V = dispersed phase separated volume at time t; V_∞ = separated volume at $t \to \infty$; b = constant.

$$\mathrm{E}_{coh} = \int_0^{\gamma_y} G'\gamma_y\ \partial\gamma \tag{2.4}$$

Where: G' = storage modulus; γ = shear deformation; γ_y = critical shear deformation (where above this point, the material no longer displays viscoelastic linear behaviour).

2.3.1.1 Creaming and Sedimentation

Creaming and sedimentation are the simplest phase separation process, as they are dependant on simple to describe variables. Droplets can either cream or sediment based on the density differece between dispersed and continuous phases, as an example O/W emulsions tend to present creamed phase at the surface (MYERS, 2005). However, depending on the surfactant or polymer system used to stabilize droplets, repulsion forces can be reduced, facilitating aggregation and thus creaming (ROBINS; WATSON; WILDE, 2002; MOSCHINI DAUDT et al., 2018). This mechanism is reversible and to prevent it the viscosity of continuous phase is modified by the use of thickeners to reduce droplet velocity (FLICK, 1989; DAHER et al., 2014; MEDINA-TORRES et al., 2014; SAKAMOTO et al., 2017). When the thickener agent is polymeric, they can act in distinct ways:

I. Modification of the rheological properties of continuous phase, (e.g., increased viscosity) (ESTANQUEIRO; AMARAL; SOUSA LOBO, 2016);

II. Adsorption at the liquid-liquid interface forming a steric or eletrostatic barrier (CHUN; POLOSKI; HANSEN, 2010; TADROS, 2011; OZTURK et al., 2015; BUCHOLD et al., 2017);

III. Formation of a three-dimensional matrix that fixates dispersed structures in place (BAIS et al., 2005; SCHRAMN, 2005; ALBUQUERQUE et al., 2016; ANDRADE et al., 2007);

IV. A combination of all these effects.

Another method to reduce creaming rate is to minimize difference between densities of internal and external phases, however this is rarely possible depending on the raw materials utilized (HAJ-SHAFIEI; GHOSH; ROUSSEAU, 2013). Lastly, droplet size diamater can be modified by tuning homogenization time and intensity during emulsification steps (SHARU et al., 2017), emulsifier system choice (HONG; KIM; LEE, 2018) and emulsification method (SUGIURA et al., 2004; VAN DER GRAAF et al., 2004).

2.3.1.2 Ostwald ripening

Ostwald ripening is a phenomena observed as a gradual growth of larger particles at the expense of smaller ones by molecular diffusion (KABALNOV; SHCHUKIN, 1992; ALEMÁN et al., 2007). It can be explained by Kelvin's equation (2.5)

$$\ln \frac{S_1}{S_2} = \frac{2\sigma\, V}{\mathrm{R\,T}} \left(\frac{1}{r_1} - \frac{1}{r_2} \right) \tag{2.5}$$

Where S_1 and S_2 are the solubilities of the particles of radius r_1 and r_2, σ the interfacial tension, V the molar volume of the disperse phase, R the gas constant, and T the absolute temperature. This equation shows that the solubility of molecules inside droplets is inversely proportional to its radius, which results in the migration of molecules from smaller droplets to bigger ones (MITSUI, 1997). With this relationship it is expected that the average size of droplets increase over time hence causing a higher sedimentation or creaming velocity and finally phase separation (FARN, 2006; SCHRAMN, 2005; TADROS, 2010).

2.3.1.3 Coalescence and flocculation

Coalescence occurs when two or more droplets merge together due to a loss of the layers of the interface that separates them. Contrary to flocculation it is an irreversible process (TADROS, 2004). When in concentrated emulsions, packing increases the area of interaction between droplets, this packing results in accomodation and deformation of droplets. Depending on the degree of such deformation, drops can present polyhedral shapes that have portions of the interface with a smaller radius than other portions (Fig. 2). Based on the LaPlace equation (Eq. 2.6), the pressure difference between external and internal phase is inversely proportional to the curvature radius of the interface, hence smaller droplets have a higher pressure difference than bigger ones. Similarly, parts of the deformed droplet also have a higher pressure difference (MASON, 1999). In higher pressure points, surfactant concentration in the interface becomes depleted (Marangoni Effect) which in turn enables a closer interaction between internal phase of the droplets, therefore coalescence and molecule migration to continuous phase (SAKAMOTO et al., 2017).

Figure 2 – DROPLET DEFORMATION AS FUNCTION OF VOLUME FRACTION

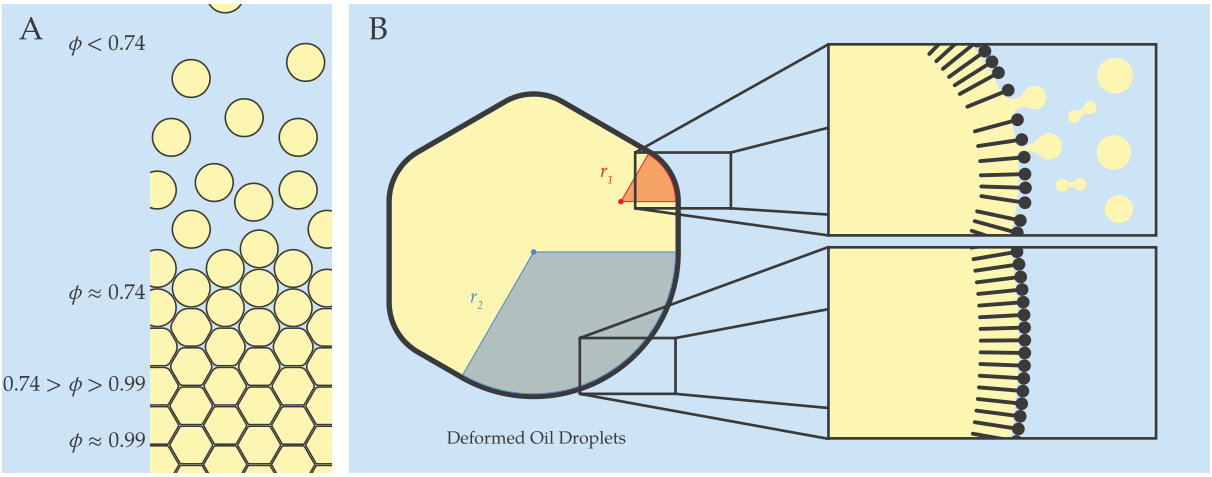

SOURCE: the author, (2020).

$$\Delta P = \frac{2\sigma}{r} \tag{2.6}$$

Flocculation occurs whenever particles of the dispersed phase aggregate. In emulsions, flocculation phenomena generates bigger particles that will tend to cream or sediment with increased rate due to its larger radius (FARN, 2006; MYERS, 2005). Flocculation occurrence can be explained through the perspective of the repulsion and attractive potentials in DLVO theory (DERJAGUIN; LANDAU, 1993; LERCHE; SOBISCH, 2011). This theory uses the concepts of repulsion electrostatic potential and attractive Van der Waals potential to give a total potential that is dependent on the distance between particles (MITSUI, 1997). As particles approach, the repulsion potential increases because of the increase in the interference between the double-layer creating a barrier against flocculation, however if the kinetic energy of the particles can overcome this barrier coagulation can occur (MITSUI, 1997). Colloidal systems with higher zeta potential values can be more stable when compared with systems without a eletrostatic repulsion mechanism (XU, 2002).

The flocculation process can be irreversible or reversible depending on the intermolecular interactions between substances in the liquid-liquid interface (SAVIĆ; TAMBURIĆ; SAVIĆ, 2010; MIRSHEKARI; PAKZAD; FATEHI, 2019).

In real colloidal systems all the instability mechanisms can occur concomitantly. The Figure 3 is a schematic diagram representing the mechanisms of loss of stability for emulsions.

Figure 3 – EMULSION BREAKAGE MECHANISMS DIAGRAM

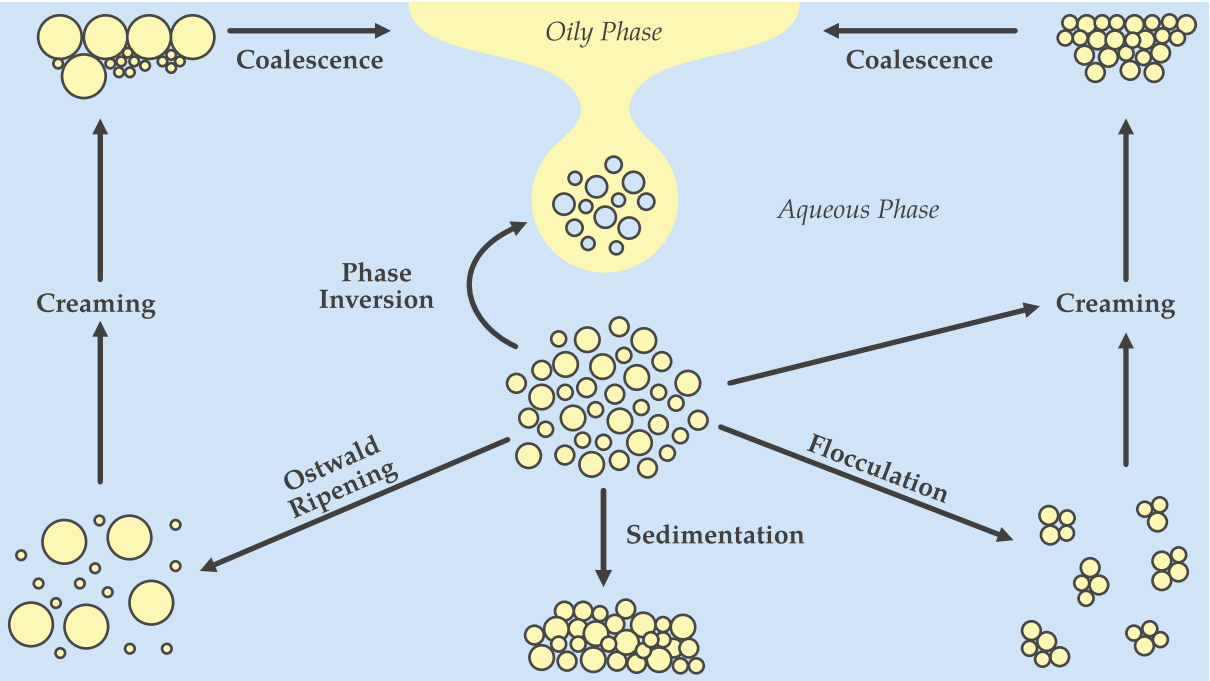

SOURCE: adapted from Tadros (2005).

2.3.2 Surfactants

Assuming that macroemulsions are thermodynamically unstable and the reduction of interfacial tension is not enough to stabilize them, surfactants must have properties that aid in the kinetic stabilization of emulsions (DERKACH, 2009; MCCLEMENTS; JAFARI, 2018). The most common mechanisms are electrostatic repulsion and steric hindrance. In the Figure 4 there are displayed four surfactant systems. In 4A, emulsions are stabilized by the electrostatic repulsion of ions adsorbed at the interface. In 4B droplets have colloidal particles with surface properties adsorbed at the interface. 4C represents polymer molecules adsorbed at the globules interface that can grant steric hindrance against droplet interaction and in 4D, the emulsion is stabilized by molecular surfactants that can be ionic or non-ionic (TADROS, 2005; MYERS, 2005).

Figure 4 – EMULSIFIER TYPES DIAGRAM

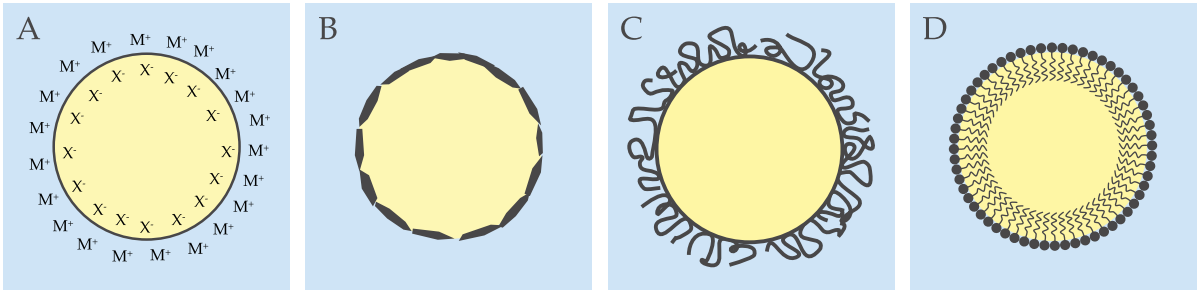

SOURCE: adapted from Tadros (2005).

2.3.2.1 Ionic molecular surfactants

The structure of molecular surfactants is characterized by extremities having opposite hydrophilic properties. Usually for O/W emulsifiers, the extremity with a larger group is called the “head” and the other, hydrophobic portion is called the “tail”. In ionic surfactants the hydrophilicity is given by ionic groups, either positive or negative. The charge present in the “head” will cause an electrostatic repulsion when droplets covered by the emulsifier come too close, and they will repel each other (HUANG; KIM, 1981; ROSEN, 2004)

Within ionic surfactants, anionic have a negatively charged “head”. The most common have “heads” with sulfates, sulfonates, phosphate esters and carboxylic acid salts as their ionic groups. This is the class with the higher number of surfactant substances and are also the most used. They are mostly used as detergents (FARN, 2006; KRALCHEVSKY; DANOV; DENKOV, 2009).

Cationic surfactants have a positive charge in the hydrophilic portion of the molecule. Most of them are formed with primary, secondary or tertiary amines, that usually need to be in low pH medium to be protonated or quaternary ammonium salts

that are permanently protonated. Only 10 % of surfactants are cationic and they are used in solid particles coating to create a hydrophobic layer (ROSEN, 2004; FARN, 2006).

Another class of surfactants are the amphoteric, that possess both anionic and cationic groups in its hydrophilic portion. Predominant charge will be pH-dependent, therefore in acid media the molecule will have a positive net charge and in basic media it will have a negative net charge (MYERS, 2005; SJÖBLOM, 2006).

2.3.2.2 Non-ionic molecular surfactants

For non-ionic surfactants water-solubility is governed by hydrogen bonds between the functional groups: sugars, alcohols, etoxilated amines, amine oxides and alkanolamines, present in the hydrophobic “head” and aqueous phase (MYERS, 2005; SCHRAMN, 2005). The repulsion mechanism is no longer by electrostatics repulsion but by steric mechanisms hence flocculation can be pronounced (SJÖBLOM, 2006; TADROS, 2010). They have some advantages over ionic surfactants because they are less sensitive to the presence of electrolites and pH changes (MYERS, 2005).

2.3.3 Cosmetic cream structure

Aside from stability granted by the reduction of interfacial tension, non-ionic surfactants can form structures with a mesomorphic behaviour with lipophilic and hydrophilic liquid cystals that organize in the interface of the droplet. This thicker surfactant layer has the capacity to reduce droplet coalescence thus generating more stable systems (SAVIC; VULETA, et al., 2005; SAVIC; TAMBURIC, et al., 2008). However, these liquid crystals can swell over time, as a result of the water bonding to the hydrophilic groups which will change sensory, macroscopic and rheological parameters (ECCLESTON, 1997; LUKIC; PANTELIC; SAVIC, 2014).

For a long time, it was presumed that cosmetic creams produced with emulsifying waxes were exclusively composed by emulsified droplets, so *cream* became a synonym for *emulsion*, however it was demonstrated by Junginger (1984) that creams produced with non-ionic surfactants and cetostearyl alcohol have much more complex structures with multiple phases. These systems can have lamellar gelled networks and contain more phases than emulsions (FUKUSHIMA; TAKAHASHI; YAMAGUCHI, 1976; ANDRADE et al., 2007; KARL et al., 2016; SAKAMOTO et al., 2017). The phases are shown in Figure 5 that shows that a is a surfactant bilayer; a + b is a hydrophilic gel that can present branches; c is a lipophilic gel; d is the bulk water of the system and e represents the emulsified lipophilic phase (JUNGINGER, 1984).

Figure 5 – DIAGRAM OF THE STRUCTURES FOUND IN COSMETIC CREAM CONTAINING NON-IONIC SURFACTANT AND CETOSTEARYL ALCOHOL

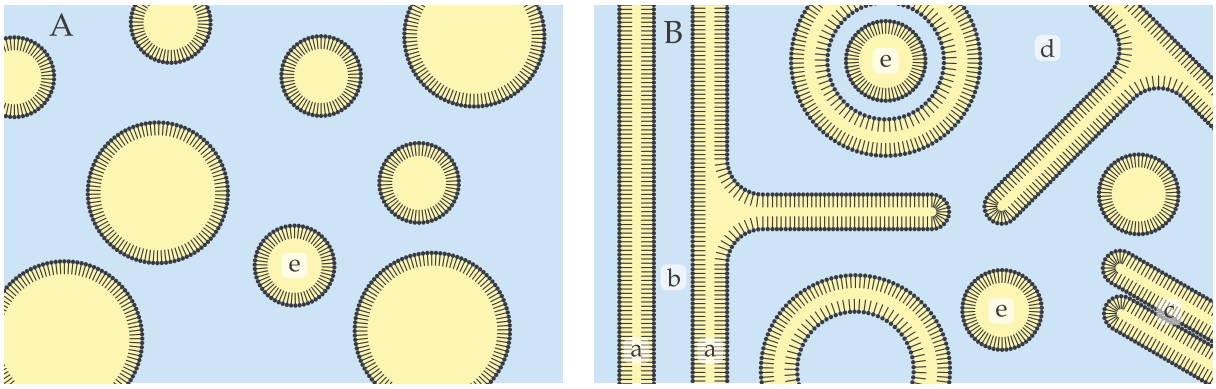

LEGEND: Subfigure A illustrates a simple emulsion whilst B illustrate the other structures found in cosmetic creams that are listed below:

- a, surfactant bilayer;
- b, interlamellar fixed water;
- a + b, hydrophilic gel that can be branched;
- c, lipophilic gel;
- d, bulk water phase
- e, emulsified droplets.

SOURCE: adapted from Junginger (1984)

2.4 RHEOLOGY

Rheology is defined as the study of matter flow and deformation behaviour wether in the solid, liquid or gaseous state, when a force is applied over it (SCHRAMM, 1994; BRUMMER, 2006; MEZGER, 2014). This behaviour can be viscous or elastic depending on the nature of the material (STEFFE, 1996; BOURNE, 2002).

Rheometry is a powerful tool in the development of products with ideal sensory and textural properties. It can be used in the development and optimization of food and cosmetic poducts (GALLEGOS; FRANCO, 1999; BRUMMER, 2006; DICKINSON, 2010).

Within the cosmetics industry context, rheological analysis have already been used to correlate product sensory properties to samples rheological profiles (LUKIC; JAKSIC, et al., 2012; MORAVKOVA; FILIP, 2014; CALIXTO; MAIA CAMPOS, 2017; CALIXTO; INFANTE; MAIA CAMPOS, 2018). It is possible that rheological analysis will replace sensory analysis that are time; financially and human resources consuming (ESTANQUEIRO; AMARAL; SOUSA LOBO, 2016; FILIPOVIC et al., 2017).

Through rheological assays it is possible to verify which parameters have changed over time (PY et al., 1994; AFIFAH et al., 2018) and what are the emulsion properties even before it reaches the consumer, however to understand this parameters

it is necessary to understand the physico-chemical properties that grant emulsions these traits.

2.4.1 Viscosimetry

Viscosity is a property of fluids that can be simplified as the resistance to flow given by the friction between molecules, macromolecules and other structures that can be dispersed within the fluid. Therefore intermolecular forces play a fundamental role in flow characteristics (BOURNE, 2002).

Depending on its composition, fluids present different viscosity characteristics. Newtonian (ideal) fluids follow the Newton's viscosity law, in which viscosity is constant regardless of the shear rate applied, whilst non-Newtonian fluids can have apparent viscosity vary as a function of shear rate (DERKACH, 2009). In the Figure 6 the many types of fluids are exemplified in simplified manner, according to their viscosity behaviour.

Figure 6 – FLUID CLASSIFICATION SCHEME

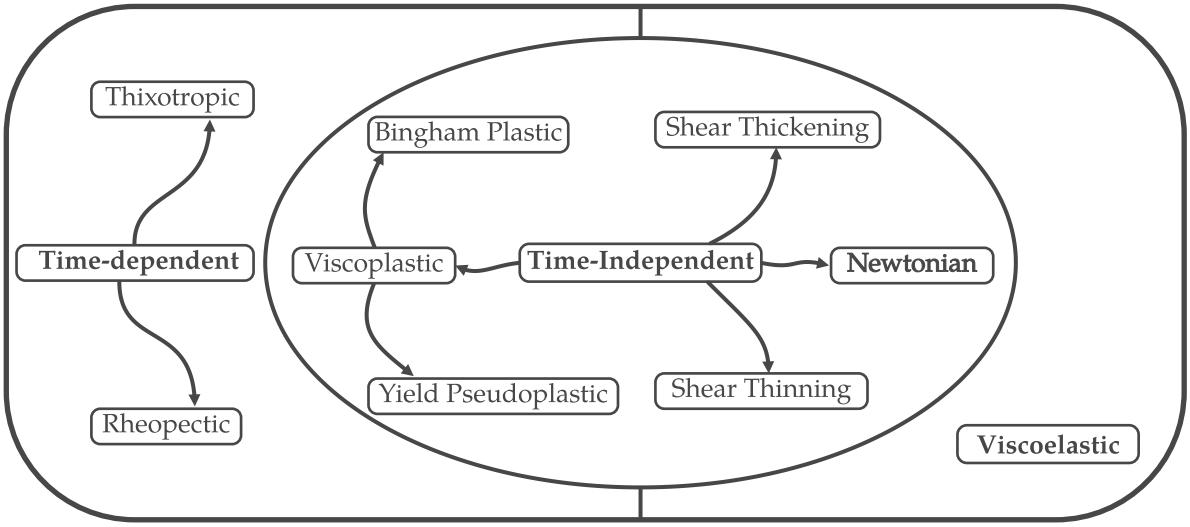

SOURCE: adapted from Lieberman and Lieberman (2014).

For fluids with dilatant and pseudoplastic it is observed that viscosity (η) varies as a function of shear rate ($\dot{\gamma}$) hence they are classified as non-Newtonian. In pseudoplastic fluids it is observed that increasing shear rates cause the reduction of viscosity and the opposite is true for dilatant fluids (TADROS, 2005). This relationship can be seen in Figure 7, along with other viscosity behaviours.

Fluid behaviour when under a tangential shear force can be mathematically described through the parallel plate model (Eq. 2.7). The model represented in Figure 8, shows two horizontally oriented plates with area (A) calculated by radius (r), with a gap height of h. The upper plate is under a force (F) that moves it with a velocity (v) in a specified direction. The arrows in the blue material indicate layers of the fluid under shear and the closer the layer relative to the upper plate, the higher the deformation

Figure 7 – FLUID BEHAVIOUR CURVES SCHEME

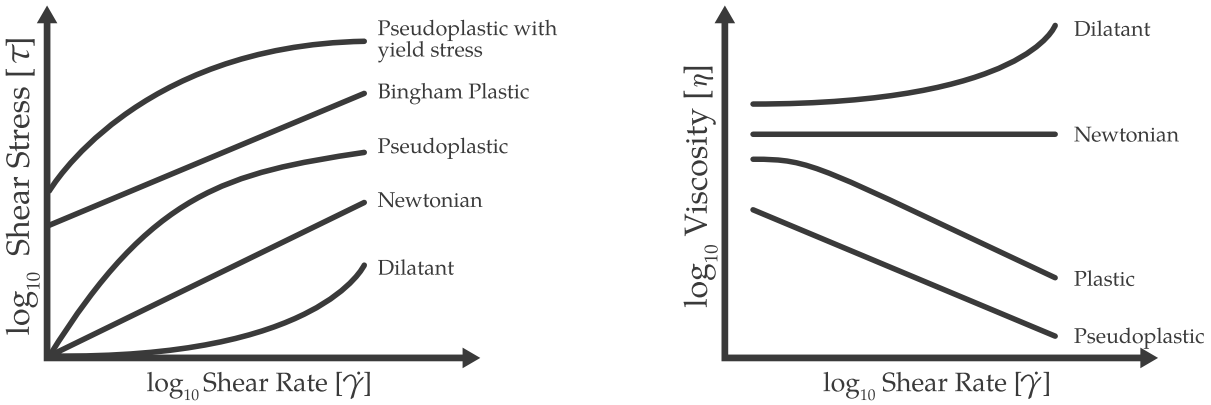

SOURCE: adapted from Brummer (2006).

this layer suffers. The deformation gradient is directly related to the material viscosity, if this gradient is linear it is said that que fluid exhibits a Newtonian flow (MITSUI, 1997; BRUMMER, 2006; MEZGER, 2014).

Figure 8 – PARALLEL PLATES MODEL DIAGRAM

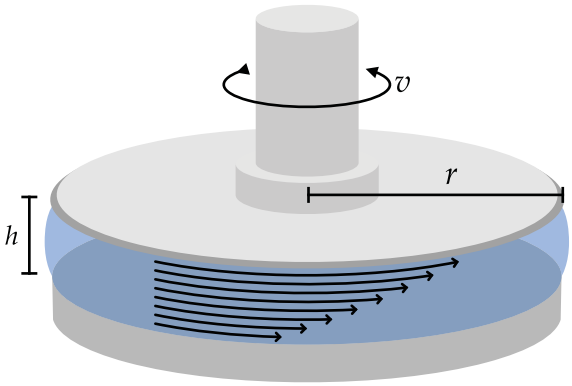

SOURCE: adapted from Brummer (2006).

$$\eta = \frac{F/A}{v/h} \tag{2.7}$$

Where: η = viscosity; F = force; A = upper plate area as function of radius (r) ; v = velocity; h = height of the layers.

This model is a simplified way to demonstrate variables measured in fluid viscosity, however there are other methods models and equipments that use similar mathematical principles but with higher sofistication. Among these the most common are: concentric cilinder viscosimeter; capillary viscosimeter; cone-plate and plate-plate systems; and viscosimeters that use spindles and paddles with various shapes (BRUMMER, 2006; SCHRAMN, 2005; MEZGER, 2014).

2.4.2 Newtonian fluids

By definition Newtonian fluids are the ones whose relationship between shear rate and deformation is linear. This means that the viscosity is independent on shear rate therefore Newtonian fluid viscosity is dependant only temperature and intermolecular forces. The materials that exhibit this behaviour are tipically water, diluted solutions and liquid oils of low molar mass (FARN, 2006; SCHRAMN, 2005).

2.4.3 Non-newtonian fluids

All fluids that do not represent a linear relationship between shear rate and shear stress can be classified as non-newtonians, nevertheless, fluids within this class can present varied rheological behaviours (TADROS, 2005). In the next sections their properties will be explored.

2.4.3.1 Time independent fluids

The fluids classified as time independent also have a non-linear shear stress to shear rate relationship. In pseudoplastic fluids (rheo-thinning), shear tension increases until it reaches a plateau as function of shear rate, which translates to the decrease in apparent viscosity as a function of shear rate. The Figure 9 exemplifies how flow behaviour can change according to the fluid composition.

Depending on the type of material that is dispersed in the fluid different phenomena occur. In 9A after flow initiation, particles orient themselves in the same orientation and direction as flow, reducing collisions, hence flowing with less resistance. In 9B polymeric chains in resting state are entangled and stretch as the shear tension is applied, reducing interaction between the polymer molecules. In 9C emulsion droplets become deformed as shear tension is applied which facilitates droplet sliding over themselves and in 9D the shear tension causes disaggregation of particles that when smaller have lower resistance to flow.

The behaviour of dilatant fluids (rheo-thickening), is the opposite of pseudoplastic. Its apparent viscosity increases as shear rate increases. This non-linear behaviour can be observed in clays and suspensions with a high concentration of hard particles (SCHRAMN, 2005).

Bingham plastics have a similar behaviour to Newtonian, however they have a yield point where for shear tensions applied under this value, the material behaves as a solid and for tensions above it starts to flow as a newtonian fluid. Unlike Bingham plastics, pseudoplastic materials with yield stress do not have a linear shear rate and shear stress relationship after yield stress is applied, and behave as pseudoplastic fluids (BRUMMER, 2006).

Figure 9 – DIAGRAM OF DISPERSION BEHAVIOUR IN RESTING AND FLOW STATE

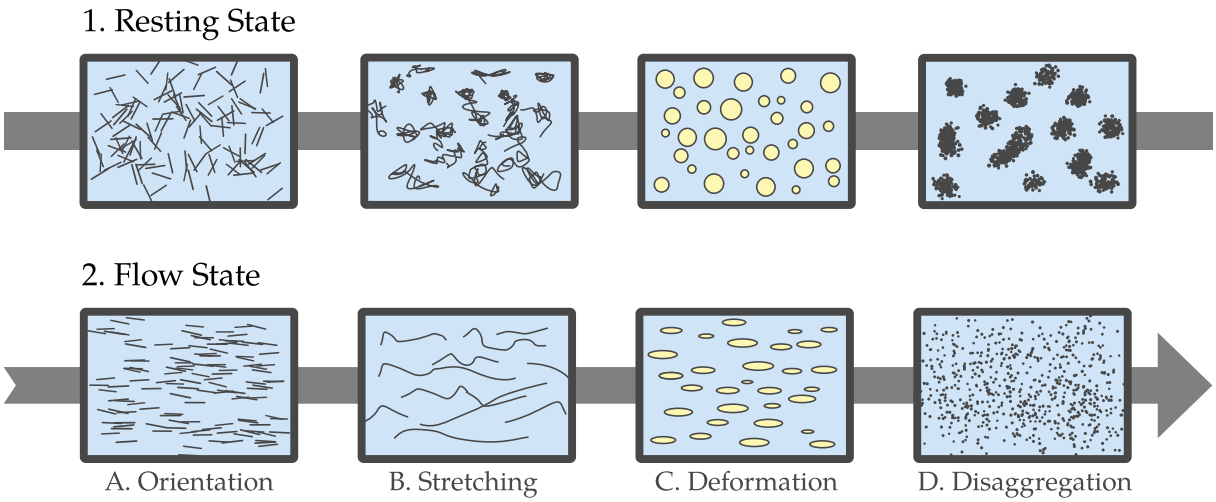

SOURCE: adapted from Schramn (2005).

2.4.3.2 Time-dependent fluids

There are two main types of fluids that present time-dependency: thixotropic and rheopetic. In both, at constant temperature, when a constant shear tension is applied for a period of time, apparent viscosity changes but when this tension is removed, viscosity returns to its original resting state (BRUMMER, 2006).

In thixotropic fluids viscosity decreases over time as tension is applied. Usually, materials containing polymers that form gels present this behaviour. When in the resting state, viscosity is high due to the solid-like, three-dimensional network created by the polymer cross-linking. Viscosity decreases when the structure yields to the tension that surpassed the reticulation forces of the gel, which in turn allows flow. After the tension is removed the structure recovers itself over time and viscosity is restored as the gelled network is re-established (STEFFE, 1996; SCHRAMN, 2005).

Not as common as thixotropy, rheopexy is its opposite. For rheopetic materials apparent viscosity increases with shear tension, a phenomena that can be explained through increase in collisions between particles dispersed in the fluid thus increasing resistance to flow. Once tension is removed, particles relax and viscosity decreases (BARNES; HUTTON; WALTERS, 1989).

2.4.4 Rheometry

Up until now, viscosimetry, a measure of material flow, has been discussed, but rheology covers a larger scope than just the study of flow. Rheometry includes the study of deformation of solids and semi-solids, as well as flow of liquids and gases, suspensions and dispersions. Most materials not only have solid or fluid properties,

there is a spectrum between solids and fluids where these properties are combined (SCHRAMM, 1994).

2.4.5 Viscoelasticity

To understand viscoelasticity, one must comprehend that fluids can have elastic properties as well as flow properties. Ideal solids, also called Hookean solids, are materials that do not flow and deform in a perfectly elastic way; linearly and proportionally to the applied force. Once the force is removed they return to its original form and volume (BARNES; HUTTON; WALTERS, 1989), yet, there are other forms of elasticity, including elastoplastic and non-linear elastic materials. Elastoplastic are materials that deform permanently after a critical deformation and non-linear elasticity is characterized by a delayed response to the force applied (STEFFE, 1996).

Ideal solid behaviour can be explained as a spring that when under stress, deforms proportionally to the force applied and the ideal liquid (Newtonian) behaviour can be simplified as an hydraulic dampener, a dashpot. The elastic deformation of a Hookean solid is dependent only on the force applied and independent on the time duration in which the force is being applied, whilst for fluids, the deformation of ideal fluids is dependent on the duration. Viscoelastic materials are between these extremes, almost no single material is perfectly solid or liquid, thus viscoelastic properties are stress and time-dependent (STEFFE, 1996; BRUMMER, 2006; SCHRAMN, 2005).

To model viscoelasticity, the spring and dashpot models were used. In Figure 10 some of the simplest viscoelasticity models are exemplified. In 10A, the Maxwell model is the combination of a spring and a dashpot connected in series (BARNES; HUTTON; WALTERS, 1989), while 10B represents the Kelvin-Voigt model that chooses to connect the solid and viscous elements in parallel (SARAMITO, 2009). Other, more complex models were created with different combination of these elements to elucidate the distinct behaviors of the materials being tested, including the Burguers model (Fig. 10C) (GILBERT; PICARD, et al., 2013).

Figure 10 – SIMPLE VISCOELASTIC MODELS DIAGRAM

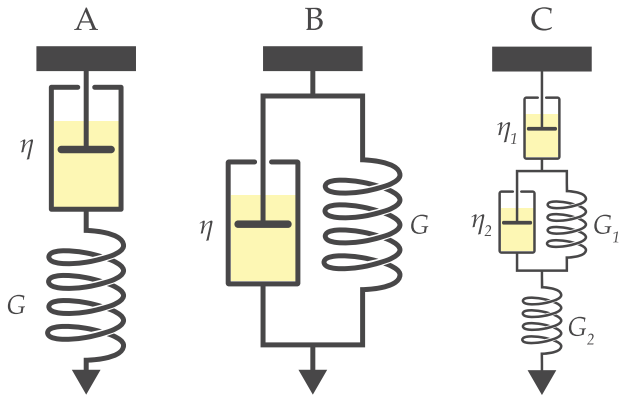

LEGEND: Maxwell, Kelvin-Voigt and Burguers models are represented by A, B and C respectively. Viscous (dashpot) elements are indicated with the symbol η and elastic (spring) elements are indicated by the symbol G.

SOURCE: adapted from Schramm (1994).

Viscoelasticity is the property of materials that exhibit viscous and elastic characteristics simultaneously, i.e., flow behavior and resistance to deformation, which is the tendency to return to original volume and shape (STEFFE, 1996; MARKOVITZ, 2008; TADROS, 2010).

As shown in Figure 7, flow behaviour is classified according to the viscosity of materials when in flow, but at that point the internal structure has been deformed and in some cases destroyed. Viscosimetric methodologies disrupt the materials internal structure, therefore should not be used for the stability of products in its resting state. With rheometry and the measurement of elastic properties it is possible to extract information from the samples internal structure in the resting state via the dynamic method (STEFFE, 1996).

Dynamic testing, or oscillatory testing is conducted with rheometers where applied tension oscillates in a senoidal fashion with determined frequency (ω) and amplitude (τ). The Equation 2.8a shows that complex shear modulus is calculated based on the ratio between complex tension (τ^*) applied and the response deformation of the material (γ) (BARNES; HUTTON; WALTERS, 1989; FARN, 2006). The complex shear modulus (G^*) can be understood as the sum of the elastic and viscous modulus, the real and imaginary components respectively (Eq. 2.8b), which are calculated based on the phase angle between applied stress and deformation response (Fig. 11B, Eqs. 2.8c; 2.8d). Elastic modulus (G') is also called storage modulus because it represents the energy applied that is stored and can be potentially recovered. The viscous modulus (G'') is called loss modulus because it represents the energy applied that has been dissipated, mainly as shear heat. The value of δ can be defined as the lag between maximum stress applied and maximum strain response (Eq. 11). If $\tan\delta > 1$ it means

that $G'' > G'$ therefore it is said that the material is flowing (SCHRAMM, 1994; MEZGER, 2014).

In Figure 11A the behaviour of ideal solids and liquids is represented. The black line represents the stress being applied by the rheometer. The blue line represents an ideal liquid and the orange line represents an ideal solid. Ideal solids deform without time-dependence so the strain response is always in phase with the stress, which means that the phase angle is equal to 0°, contrarily, ideal fluids have a 90° degree phase angle, that is, completely out of phase. Viscoelastic materials δ value lie between these extremes.

Figure 11 – IDEAL SOLID AND LIQUID STRAIN RESPONSE AGAINST APPLIED SHEAR TENSION

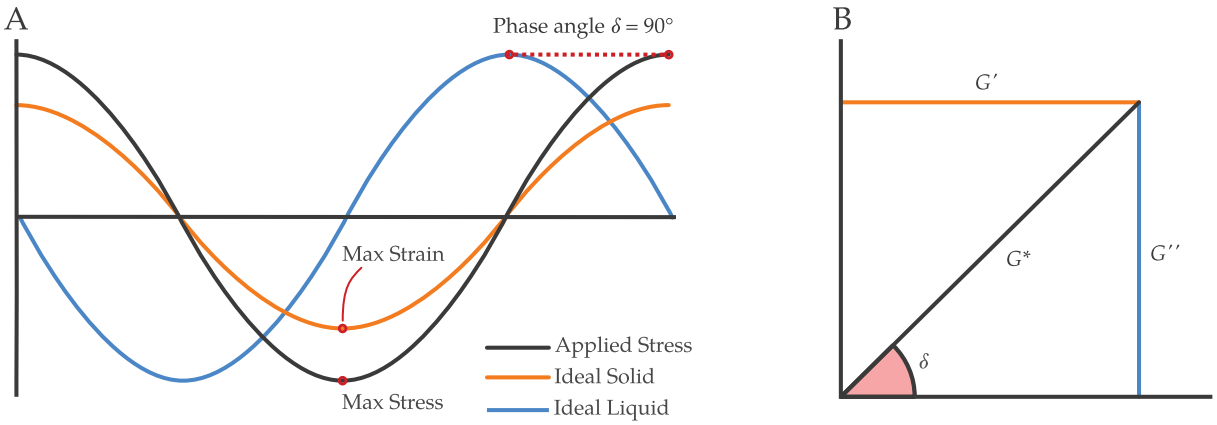

SOURCE: adapted from Schramm (1994).

Complex modulus:

$$G^* = \frac{\tau^*}{\gamma} \tag{2.8a}$$

$$G^* = \underbrace{G'}_{\text{real}} + \underbrace{iG''}_{\text{imaginary}} \tag{2.8b}$$

Elastic and viscous modulus:

$$G' = G^* \cos\delta \tag{2.8c}$$

$$G'' = G^* \sin\delta \tag{2.8d}$$

Delta and delta tangent:

$$\delta = \omega\Delta t \tag{2.8e}$$

$$\tan\delta = \frac{G''}{G'} \tag{2.8f}$$

2.4.5.1 Amplitude sweeps

Amplitude sweeps are the first oscillatory test that needs to be performed in the rheological characterization because it will show the material's *Linear viscoelastic region* (LVER). This is the region of stresses the material can withstand before it is irreversibly deformed or completely destroyed (MEZGER, 2014). Experiments conducted in this region are called small-amplitude oscillatory shear tests (SAOS). In this experiment the equipment applies a tension in log-spaced intervals and measures G^* and δ as function of the ocillatory tension. The plateau indicates LVER (Fig. 12) and the critical tension (τ_y) is defined as the tension in which G' starts to decrease. The tolerance to determine at which τ, G' is outside of the plateau is determined by the user but it usually dwells between 5 to 10 % of the G' value in the plateau (MEZGER, 2014).

Data obtained from amplitude sweeps reveal values of G' and G''. When $G'' > G'$, the material is flowing and when $G'' < G'$ it is not (PALIERNE, 1990; PAL, 2008). The profile of elastic and viscous moduli curves can be used to differentiate emulsions properties (LI; ZHANG, 2015), stability (DERAKHSHANDEH et al., 2018), flocculation and deformation (SANFELD; STEINCHEN, 2008) and shelf-life physical stability (BRUMMER, 2006).

Figure 12 – AMPLITUDE AND FREQUENCY SWEEPS DIAGRAM

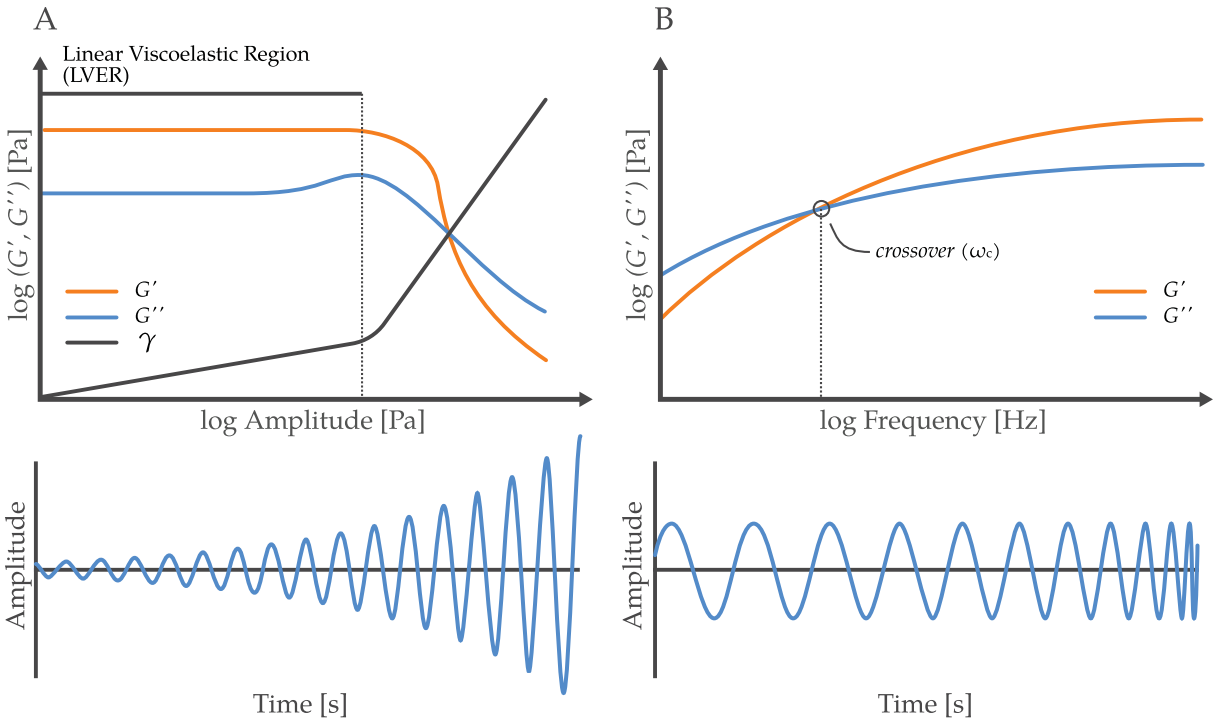

SOURCE: adapted from Vader and Wyss (2018).

Another data point that can be extracted from amplitude sweeps is the Cohesive Energy Density (E_{coh}), cited on page 21 and simplified in the Equation 2.9 to observe

the strength of emulsion structure (TADROS, 2010; GOLEMANOV et al., 2013).

$$\mathrm{E}_{coh} = \frac{1}{2}\,\gamma_y^2\,G'_y \tag{2.9}$$

Where: γ_y is the critical strain at which G' starts to decrease and G'_y is the G' value at the same point.

In this document, yield stress, yield point and critical tension are all synonyms and represent the point at which the structure of the emulsion starts to breakdown as a function of the stress being applied over it (MEZGER, 2014). This point can be determined by rotational and oscillatory methods.

2.4.5.2 Frequency sweeps

The frequency sweep, identified in Figure 12B is a test performed under constant shear tension and temperature within the LVER, where the angular oscillation frequency (ω) varies (MEZGER, 2014). These tests are performed to investigate the deformation as a function of time. Fast frequencies correspond to short time periods while slow frequencies correspond to long time periods. The frequency where G' and G'' meet is called the crossover point. At frequencies greater than crossover, if $G' > G''$ the material is said to have solid properties, or to be gelled (ALMDAL et al., 1993). The point of crossover is given in the frequency unit that the experiment was conducted, it can be either Hz or rad s^{-1} the inverse of this value is the relaxation time in seconds. The relaxation time is the time required for the material to be in the transition between sol and gel under the stress that is subjected. Another way to observe the crossover phenomenon is to measure elastic and viscous moduli for a long time with constant frequency and tension (GABRIELE; DE CINDIO; D'ANTONA, 2001).

Materials can be categorized as gels, viscoelastic solids or viscoelastic liquids through frequency sweeps. For gels, G' and G'' have little frequency dependence, always with G' predominant, viscoelastic solids have predominance of G'' over G' at higher frequencies and viscoelastic liquids have G' predominance at higher frequencies (LARSON, 1998).

2.4.5.3 Tension curves

Tension curve is not necessarily an experiment that allows the stability assessment for emulsions, however it is useful in caracterizing maturation and to compare to primary sensory properties (MORAVKOVA; FILIP, 2014).

This experiment is conducted in a *control stress* rheometer where the critical tension (τ_y) is determined at the point where there is a change in the angular coefficient of the curve produced by the deformation as function of tension applied. There are other

methods to calculate the yield point but they depend on mathematical fitting such as the Herschel-Buckley that might not represent the real behaviour of the sample (SCHRAMM, 1994; DINKGREVE et al., 2016).

2.4.5.4 Temperature swings

Accelerated studies with temperature increase are used in the determination of cosmetic stability (ANVISA, 2004; TADROS, 2004; GUARATINI; GIANETI; CAMPOS, 2006) and medicaments alike (ANVISA, 2012). Freeze-thaw methodology described in the Cosmetic Product Stability Guide (2004) have been used and improved in the determination of stability of colloidal systems (MCCLEMENTS, 2007; BALLMANN; MÜELLER, 2008; LERCHE; SOBISCH, 2011) and are considered the most adequate in determining cosmetic stability along with centrifugation tests (ONDRACEK et al., 1985). Therefore, there has been an increased interest in applying temperature variations with other methods to expand even more the range of accelerated tests.

A dynamic oscillatory, within LVER, with constant τ and ω and variable temperature, experiment can be used to assess the material's elastic and viscous properties over consecutive increasing and decreasing temperature ramps. This experiment seeks to perform multiple freeze-thaw cycles in a duration of under 3 hours, contrary to the described in cited literature methodology that takes over 12 days (ANVISA, 2004).

Until now, few citations to a thermal analysis concomitantly with rheology have been found. One of the first mentions to such a method with consecutive temperature ramps was from Brummer (2000), where he concluded that it is possible to reduce stability assessment duration drastically when in comparison to the conventional stability assessment methods. Later, Tadros (2004), claimed that a rheological thermo analysis with cycling temperature is essential to the complete evaluation of emulsions stability and Brummer published in his book Rheology Essentials of Cosmetic and Food Emulsions (2006) a larger scale study where a direct relationship is detected between the thermo analysis results and shelf-life stability for both O/W and W/O cosmetic and food emulsions.

Posteriorly, this technique was used by Laca, Paredes, and Díaz (2012) in many storage times to evaluate cosmetic emulsions formulations. According to the authors, G' and G'' variation as a function of temperature cycles can be interpreted as an index of the emulsion stability. Thomas Mezger compiled the information found about this test in his book The Rheology Handbook (2014) with examples of experiments that could be performed for stability assessment citing Brummer (2006) and Bernzen (2008).

In the field of the food industry this technique was applied to evaluate the stability of "creamed honey" where the authors concluded through G' and G'' values over temperature cycles, that the product did not mantained its structural properties as

the temperature cycles were applied (KARASU et al., 2015).

The most recent study, compares this method to a conventional freeze-thaw experiment realized in climatized chambers. According to the authors, it was possible to find statistical evidence that both methods are comparable for the five W/O emulsions tested, however to obtain more consistent conclusions, it is necessary to increase sample number and test different types of formulations (CEKIC; SAVIC; SAVIC, 2019).

There is still no consensus in the academic community about the feasibility of using this method in conjunction with other rheological methods to draw conclusions about emulsion stability. Cosmetic creams and foods are very complex systems that have several phases and behave unpredictably, however, rheology has proven useful in characterizing and analyzing these materials.

2.5 DROPLET SIZE DETERMINATION

Droplet and particle size can be determined and reported in many ways. Most particles generally have irregular shapes so summarizing its size is hardly a simple task. There are several particle sizing methods available, each with its own advantages and disadvantages, however to summarize particle size the concept of an equivalent sphere is used. The equivalent sphere is the theoretical concept in which a particle and its equivalent sphere have identical properties given a specific parameter (MERKUS, 2009). Figure 13 exemplifies a particle with irregular shape that can have multiple sizes according to which parameter is being measured.

Each method uses these parameters to determine particle size. Optical microscopy is used to identify particle morphology and can be used to determine the average between maximum and minimum diameters. Laser diffraction determines size by detecting the diffraction patterns a population of particles produces when a He-Ne laser incides over them. In dynamic laser scattering, the hydrodynamic diameter is calculated based on the particles diffusion coefficient through Stokes-Einstein equation (2.10) (MERKUS, 2009).

$$D_H = \frac{k_B \, \mathrm{T}}{3\pi \, \eta \, D_t} \tag{2.10}$$

Where: D_H = hydrodynamic diameter; k_B = Boltzmann constant; T = temperature [K]; π = constant; η = dynamic viscosity; D_t = translational diffusion coefficient.

Each of the techniques have some type of limitation. While some are faster cheaper and more practical, others can minimize errors and return more precise and accurate data (XU, 2002). There are several ways to report the measured size, namely: mean diameter with standard deviation; median; mode and weighted mean diameter

Figure 13 – EQUIVALENT SPHERE DIAMETER TYPES

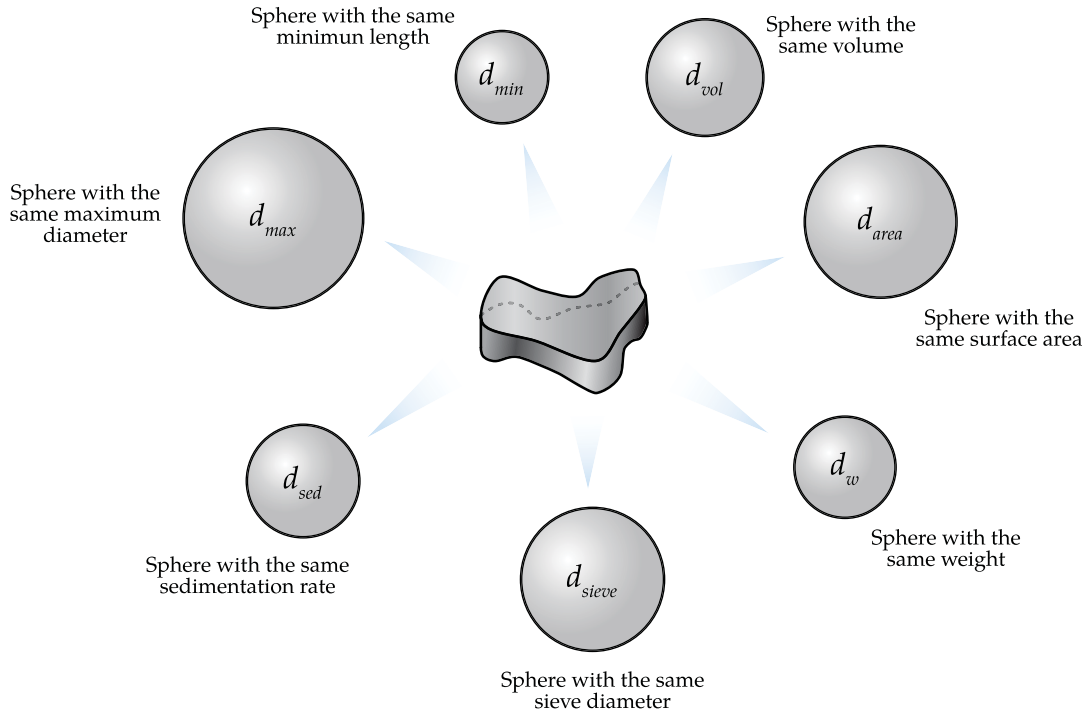

SOURCE: the author, (2020).

(XU, 2002). The equation 2.11 is the general equation used to report average particle size. The terms m and n are algebraic powers. The most common diameters are:

$$D_{m,n} = \left[\frac{\sum n_i \, D_i^m}{\sum n_i \, D_i^n}\right]^{\frac{1}{m-n}} \tag{2.11}$$

- $D_{[1,0]}$ = arithmetic mean diameter
- $D_{[2,0]}$ = surface area mean diameter
- $D_{[3,0]}$ = volume mean diameter
- $D_{[3,2]}$ = area–volume mean diameter (Sauter)
- $D_{[4,3]}$ = volume weighted mean diameter (De Brouckere)

Other ways of assessing particle size is by population quantiles, especifically D_{10}, D_{90} and median (D_{50}) are used in quality control and product specification. The values of the quantiles are expressed in the same unit as the average size and represent the size that lies below 10, 50 and 90% of the population of particles (XU, 2002). The mode is less sensitive to outliers because it reports only the most frequent size in the particle population, likewise, the median can be biased. There is no single value that

can be used to represent particle size distribution therefore, the width of the distribution can be reported alongside. The equation 2.12 is used to partially solve this problem by taking in consideration the interval between D_{90} and D_{10} divided by the median to give the width of the distribution. The higher the value of *span* is, larger will be the width of the size distribution. Only populations with 90% of particles within a variability of $\pm$ 5% of the median can be considered monodisperse (MERKUS, 2009).

$$Span = \frac{D_{90} - D_{10}}{D_{50}} \tag{2.12}$$

Optical microscopy, although a practical, simple and accessible technique has some disadvantages when used to determine particle size and morphology. The clear disadvantages are the micrographs resolution and the large depth of field that preclude the definition of maximum diameter for emulsion droplets. These disadvantages can be resolved with more precise and sensitive equipments but a better practice is to use advanced techniques such as confocal microscopy, scanning electron microscopy, transmission electron microscopy, polarized light microscopy that allow not only the determination of size but also more intricate morphology studies (KIM; MASON, 2017).

Laser diffraction is a fast and practical technique with a broad interval of detectable particle sizes. The particle size distribution is calculated according to the intensity and angle of diffracted light. Small particles scatter light with smaller angles than larger particles and the intensity of light difracted is proportional to the volume of particles in said size (MERKUS, 2009). Multiple scattering (when light is spread by mutiple particles before reaching the detector) should be avoided as to not result in incorect measurements, the adjustment is done via obscuration level. The obscuration is a measurement of the percentage of incident light that has been removed by the dispersed particles, it varies depending on particle size and dispersion concentration (XU, 2002).

Particle size is calculated using the Mie theory that makes the assumptions that particles are spherical; dispersion is diluted enough to not present multiple scattering; particles have homogeneous composition and optical properties of the dispersed and dispersant are known (XU, 2002).

When the laser diffraction equipments started being manufactured, Mie theory was still a computational obstacle, therefore the Fraunhofer appoximation was created, a simpler and widespread model at the time. In Fraunhofer diffraction it is assumed that particles behave as opaque circular disks; light is scattered in narrow angles; particles of all sizes diffract light with the same intensity and efficiency and the difference between refraction index of dispersed and dispersing phase is infinite (MERKUS, 2009; XU, 2002).

The Fraunhofer approximation is used when it is impossible to obtain optical properties of both phases. It is valid when particles lie within 10 to 100 µm (XU, 2002), however, as particle size decreases below that range, the Fraunhofer approximation can over or underestimate particle size therefore it may be necessary to use other methods to determine droplet size for a macroemulsion (> 0.1 µm)

Laser diffraction methods are used to aid in the optimization of emulsion homogenization (SANTOS; CALERO; MUÑOZ, 2016); ostwald ripening and coalescence rates evaluation (SANTOS; CALERO; TRUJILLO-CAYADO, et al., 2017); colloid system physical stability in cosmetic and food indutries (KOWALSKA; ZBIKOWSKA, 2013) and droplet size assessment for O/W (BRAISCH et al., 2009; CHABNI et al., 2018) as well as W/O emulsions (ZAPATA; RODRÍGEZ-BARONA; GÓMEZ, 2015) but since Fraunhofer approximation assumes that particles dispersed are spherical, aggregates and deformed particles will affect measurements so it is necessary that samples are properly prepared prior to particle sizing (MASON, 1999; BON et al., 2007; MERKUS, 2009; CHUN; POLOSKI; HANSEN, 2010).

3 MATERIAL AND METHODS

To simplify the text, in this document, formulas and their respective batches will be represented as the following: ${}^{y}\mathbf{X}_{z}^{0d}$. Where **X** represents the formula, z represents the batch, $0d$ represents the storage time of the sample or the condition it was evaluated and y represents the approximate mass fraction of the formula as described in Table 1.

3.1 MATERIALS

In this section are listed the raw materials used in all formulations as well as the relevant identification information.

COMMERCIAL NAME: Butylated hydroxytoluene;
INCI NAME: butyl hydroxytoluene, BHT;
BHT is an antioxidant agent that acts retarding or inhibiting the propagation of free radicals by diverse mechanisms (YEHYE et al., 2015).
CAS: 128-37-0

COMMERCIAL NAME: Cetiol 868©;
INCI NAME: octyl stearate;
The Cetiol 868© (BASF) is an ester with chemical formula $C_{26}H_{52}O_2$, used as an emollient in cosmetic formulations. The batch purchased had a apparent density of $0.853\,\mathrm{kg\,m^{-3}}$ and a viscosity of $0.314\,\mathrm{Pa\,s}$
CAS: 22047-49-0

COMMERCIAL NAME: Dimeticone USP 350 cSt;
INCI NAME: dimeticone;
Polysiloxane is a low molecular weight silicon oil that has the function of creating an occlusion layer and waterproofing the skin (MITSUI, 1997). The batch purchased had a apparent density of $0.980\,\mathrm{kg\,m^{-3}}$ and a viscosity of $9.184\,\mathrm{Pa\,s}$
CAS: 9006-65-9

COMMERCIAL NAME: Ethylenediaminetetraacetic acid;
INCI NAME: edetate disodium, EDTA;
EDTA is a metallic ion sequestering agent whose function is to prevent oil oxidation and fragances reaction with residual ions in the formulation (MITSUI, 1997).
CAS: 139-33-3

COMMERCIAL NAME: Germall®115, imidurea;
INCI NAME: imidazolidinyl urea;
This substance is an antimicrobial preservative that acts as a formaldehyde releaser (PAYE; MAIBACH, 2013). The cosmetics industry has been replacing it due to its relationship to contact dermatitis (LEHMANN et al., 2006).
CAS: 39236-46-9

COMMERCIAL NAME: Nipagin™ M, Nipasol™ M;
INCI NAME: methylparaben, propylparaben;
Both metylparaben and propylparaben are anti fungal agents widely used in cosmetic and food industries (BŁEDZKA; GROMADZIŃSKA; WASOWICZ, 2014). Both have also started to be replaced in cosmetic products due to signs of carcinogenic and estrogenic activity the class of parabens has presented (OISHI, 2001; DARBRE et al., 2004).
CAS: 99-76-3, 94-13-3

COMMERCIAL NAME: Mineral oil;
INCI NAME: paraffinum perliquidum, mineral oil;
Colorless and odourless the mineral oil is a mixture of alkenes with chain between 9–16 carbons, that can include ramifications and rings. they are generally a product of petroleum extraction (WEBER et al., 2018). The batch purchased had a apparent density of 0.868 $kg\,m^{-3}$ and a viscosity of 0.589 Pa s
CAS: 8012-95-1

COMMERCIAL NAME: Polawax©;
INCI NAME: emulsifying wax NF, cetearyl alcohol, polysorbate 60;
Emulsifying wax is defined as a waxy solid prepared with cetyl and stearyl alcohol (emulsion stabilizer) and a polyoxyethylene derived from a sorbitan fatty acid ester (polysorbate 60, non-ionic surfactant) (USP, 2005; CASAGRANDE et al., 2006). The polysorbate has an approximate HLB value of 15 (SCHRAMN, 2005) and formula is owned by Croda™. The proportion of these substances was not quantified.
CAS: 67762-27-0, 9005-67-8

COMMERCIAL NAME: Propylene glycol;
INCI NAME: propylene glycol;
Propylene glycol is a viscous transparent liquid pratically odourless. It is used in pharmaceutical and cosmetics industries as a solvent and as a vehicle to water-insoluble substances. It has weting effect and can act as a co-emulsifier in non-ionic surfactant systems (PAYE; MAIBACH, 2013).

CAS: 57-55-6

3.2 EMULSION DESTABILIZATION

Strategies in emulsion destabilisation were to the increase of oily phase mass in relation to aqueous phase from 20 wt. % to 70 wt. % and to reduce the emulsifying system concentration. Preliminary tests demonstrated that reducing the emulsifying system concentration resulted in formulas that had lotion consistency and would hardly be rheologically comparable to the creams with the desired consistency. Therefore, it was chosen to increase oil concentration as a method of emulsion destabilization because the formulas produced achieved desired consistency and the emulsifying system would be under stress due to the higher oil content.

According to the manufacturer specifications (CRODA, 2010), oil phase content should not be above 15 wt. % when using Polawax NF™. The ratio between emulsifier and dispersed phase should be enough to generate droplets with a bigger diameter that in turn will be seen as more unstable creams (MCCLEMENTS; GUMUS, 2016).

In the Section 2.3.1.3 the possibility of molecules within dispersed phase migration to dispersant was explored as a function of the higher LaPlace pressure in the droplet deformed regions, thus increasing coalescence and Ostwald ripening. Since creams with higher oil content deform more due to its volume fraction it is expected that the combination of this phenomena and gravitational separation propensity will result in physical destabilization.

Homogenization during emulsification steps also has a determining importance in emulsion stability (TAL-FIGIEL, 2007) but since the commercial emulsifier is known to be extremelly stable, homogenization was relatively mild. To minimize variables, homogenization remained as unchanged as possible for the various batches of the formulas prepared.

3.3 CREAM PREPARATION

Preparation was conducted as described in the Brazillian Pharmacopoeia National Form (2012) with some modifications. Oily phase (P_{Oil}) and Aqueous phase (P_{Aq}) components were weighted separately and put into beckers with a 500 mL capacity. Complementary phase was weighted in watch-glass. Cream preparation was conducted in three steps: pre-emulsification, emulsification and cooling, one immediatelly after the other:

I. **Pre-emulsification:** both P_{Aq} and P_{Oil} were heated to 80 °C and mixed constantly

so the components would be completely homogenized. As soon as both phases were at 80 °C, P_{Aq} was poured over P_{Oil} with a flow rate of 5.45 mL s^{-1} under mechanical stirring with a helix paddle at 50 rpm.

II. **Emulsification:** the mixture was homogenized with a Silverson® L4RT (Silverson Machines Inc., USA) high shear mixer with a Square Hole High Shear Screen at 3000 rpm for 2 minutes.

III. **Cooling:** mechanical homogenization at 50 rpm with helix paddle for the time it took for the cream to reach ambient temperature. Complementary phase (imidazolidinyl urea solution) was added at temperatures lower than 40 °C.

Formulas were covered with PVC paper and left inside becker at ambient temperature ($\approx$ 25 °C) for 24 hours, for cream maturation. After maturation, cream was separed into 30 g fractions and packed in double-walled, opaque, plastic jars with a capacity of 60 g. Jars were stored within the laboratory at ambient temperature throughout the whole study and jars designated for accelerated studies were stored in incubator at 40 °C for 14 days.

Eight distinct formulas were prepared with distinct P_{Oil} and P_{Aq} concentrations. Quantitative description of formulas is shown in Table 1

Table 1 – CREAMS QUANTITATIVE FORMULA

	A	**B**	**C**	**D**	**E**	**F**	**G**	**H**
Component Name	wt. %							
P_{Aq}								
Parabens solution	3.30	–	–	–	–	–	–	–
EDTA	0.10	–	–	–	–	–	–	–
Water	76.30	66.30	56.30	46.30	41.30	36.30	31.30	26.30
P_{Oil}								
Polawax NF	10.00	–	–	–	–	–	–	–
Dimeticone	2.00	–	–	–	–	–	–	–
Cetiol 868	2.00	–	–	–	–	–	–	–
BHT	0.05	–	–	–	–	–	–	–
Mineral Oil	5.65	15.65	25.65	35.65	40.65	45.65	50.65	55.65
Complementary phase imidazolidinyl urea solution 50 % (m/v)	0.6	–	–	–	–	–	–	–
Approximate Mass fraction (w_i)	0.20	0.30	0.40	0.50	0.55	0.60	0.65	0.70
Approximate Volume fraction (ϕ)	0.21	0.33	0.44	0.56	0.62	0.67	0.73	0.79

SOURCE: Brasil (2012); the author, (2020).

3.4 OGRANOLEPTIC ASSAYS

The organoleptic assays were conducted according to ANVISA (2007). Color, odor and general appearance were evaluated over the time of experimentation. Formulas

were evaluated based on what was expected of a commercial product and sensory parameters. These assays have the function of determining macroscopic structural instability as well as indicators of chemical instability based on odours and color. The structural instability in this case is defined as a clear separation of emulsified and dispersing phases caused by the aforementioned destabilization mechanisms and will be used as comparison to rheological methods.

3.5 PHYSICO-CHEMICAL ASSAYS

3.5.1 Conductivity and pH

Hydrogenionic potential was measured for the samples diluted in purified water at the concentration of 10 % (m/v) homogenized with vortex for 2 minutes, using a calibrated mPA210 MS (TECNOPOM Instrumentação) pH measurer. Value of the measurement was recorded once fluctuations stopped.

Conductivity was assesed to identify coalescence over time. Conductivimetry was realized with a ANALION® C 708 in the same time intervals as all other measurements. Value of the measurement was recorded once fluctuations stopped.

3.5.2 Centrifugation Test

Samples centrifugation is performed to identify phase separation in cosmetic products on developing stages. This test must be conducted at constant temperature, time and speed. Recomended centrifugation speed and duration is of 3000 rpm for 30 minutes but due to differences in the centrifuges' rotor sizes, relative centrifugal force was set at 2000 g for the same duration.

Approximately 1.5 g of the sample was weighted in microtubes with a capacity of 2 mL. Equipment used for this test was a 8011152 Digital Minicentrifuge (BioPet Technologies). Any signs of creaming or phase separation were assessed.

3.6 DROPLET SIZE DETERMINATION

3.6.1 Laser Difraction

To evaluate P_{Oil} droplet size changes over time, creams were diluted to 1.0 % (m/v) in purified water in two steps:

I. One gram of the cream was weighted and put to a 50 mL centrifuge tube. An amount of 25 mL of purified water was transfered to the tube and the mixture was agitated with vortex for 60 s.

II. All the volume of the redispersed cream was transfered to a volumetric flask with a capacity of 100 mL and the volume was completed with purified water. This dispersion was homogenized with magnetic stirrer for 1.5 hours.

Sample analysis was conducted in the Grupo Boticário Particle Size Analysis Laboratory of the Quality Control Department with a Mastersizer 3000 (Malvern Panananalytical) at 20 °C. Fraunhofer difraction method was used with an obscuration range of 10 to 12 %. Results reported are the mean of 3 measurements, each with a duration of 30 seconds. Droplet size was reported as the volume weighted mean diameter (De Brouckere), calculated according to Eq. 2.11.

3.6.2 Optical Microscopy

One of the techniques utilized for droplet size determination was optical microscopy with digital imaging. Samples were diluted with the same methodology described in Section 3.6.1 and homogenized before placing over the microscope slide. Approximatelly 10 µL of the diluted sample were used for each slide and photomicrographs were taken at 10 and 40 times magnification. A calibration slide was used to define the *pixel per millimeter* ratio and droplet diameters were calculated using ImageJ2 open source software (RUEDEN et al., 2017).

3.7 RHEOLOGY

Rheological assays were performed in two distinct equipments. Tension curves, amplitude and frequency sweeps were conducted in a HAAKE™RheoStress™1 (Thermo Fischer) rheometer with a titanium 60 mm diameter, 2° cone-plate geometry (CP60/2) located on BIOPOL – M^{a}. R. Sierakowski Laboratory. Temperature cycle tests were conducted on a Discovery HR-1 rheometer (TA Instruments) with a steel 50 mm diameter, 1° cone-plate geometry (CP50/1), availabe from the Grupo Boticário Analytical Development laboratory.

3.7.1 Amplitude and frequency sweeps

Amplitude sweeps were performed with the control stress mode for all samples in a range of 5×10^{-2} to 5×10^{2} Pa under a constant shear frequency of 5 Hz. Gap height between bottom plate and upper cone was set to 105 µm which is the standard for CP60/2 geometry. For cone-plate geometries, gap height must be finely controlled to avoid miscalculations so the option *Thermo Gap* was activated so the software would correct output based on dilatation coefficient of the geometry and bottom plate. In the experiments without temperature swings, temperature value was set at 25 °C.

Decreasing frequency sweeps were performed on all samples in the range of 5×10^{1} to 10^{-2} Hz at the same temperature and gap conditions of amplitude sweeps, with τ value defined from previous amplitude sweeps within LVER.

3.7.2 Tension curves

Tesion curves were performed in the rotational mode using CP60/2 with RheoStress RS1 in a range of 0.01 to 200 Pa for all samples in all measurement times with the same gap and temperature conditions as other dynamic experiments.

3.7.3 Temperature swing

This experiment was performed within LVER with a fixed tension of 5 Pa and oscillation frequency of 10 Hz. Ten consecutive heating and cooling temperature ramps with a 30 seconds interval between them were programmed in the DHR-1 software with a rate of 5 °C min^{-1} within a range of 5 to 45 °C for a experiment time of roughly 1 hour and 20 minutes. To minimize evaporation, a solvent trap was used with purified water as the solvent.

3.8 SAMPLE HANDLING AND STORAGE

As recomended by the Cosmetic Product Stability Guide (2004), prior to any experiments the top layer of the cream was carefully removed to discard any portion of the material that underwent physico-chemical changes due to dehydration. The bottom portion was mildly homogenized with a spatula before all analysis and sample was placed over the rheometer bottom plate with a spatula to minimize structure disruption. Samples were stored inside the laboratory for a total of 182 days, where temperature and humidity were monitored.

After sample loading onto the rheometer, gap was adjusted and excess cream removed. The aliquot of the cream was left resting for 60 seconds prior to the measurements.

3.9 DATA ANALYSIS

All statistical analysis, data wrangling and treatment and data visualization were done using open source software R 3.6.1 (R CORE TEAM, 2013) and the R package tidyverse 1.3.0 (WICKHAM et al., 2019).

4 RESULTS AND DISCUSSION

In this section, firstly we will explore the macroscopical properties of the formulas and then move towards the traditional methods of cream stability assessment, which include pH measurement centrifugation and microscopy. It is worth noting that optical and polarized light microscopy are not usually conducted in cosmetics industry's quality control routine but they are classified here as traditional methods of characterizing emulsions. Secondly, the rheological data will be explored and discussed, with the inclusion of new equations to assess the structural strength of the formulas and finally it will be discussed the formula's temperature sensitivity.

4.1 MACROSCOPIC STABILITY

In three cases it was possible to observe premature phase separation. The samples ${}^{.50}\mathbf{D}_c$, ${}^{.60}\mathbf{F}_a$ and ${}^{.70}\mathbf{H}_a$ separated phases within 24 hours of preparation. The sample ${}^{.50}\mathbf{D}_c$ took longer than the others and it is not known exactly how long it took before separation but the sample presented an opaque white liquid on the bottom of the becker and a gelled semitransparent structure at the top. In sample ${}^{.60}\mathbf{F}_a$ it was possible to observe the contents of P_{Oil} migrating to the top soon after the cooling stage of cream preparation. The sample was homogenized promptly in an attempt to prevent the full phase separation of the system and macroscopically was perceived as uniform. The centrifugation conducted after cream preparation indicated the that the P_{Oil} incorporated was only trapped inside the structure of the cream and not emulsified. Finally, the sample ${}^{.70}\mathbf{H}_a$ started phase separation during cooling step and it was irrecoverable with mechanical stirring. It was seen that a fraction of the P_{Oil} had been emulsified but most of it was mixed with P_{Aq} as the dispersing phase.

The phase separation seen soon after cream preparation can be explained by both cooling rate and homogenization step. In waxy systems, once temperature drops, surfactant molecules can organize themselves in liquid crystals before their adsorption on the liquid-liquid interface. When the cooling rate is high these structures can be formed before all P_{Oil} interface is covered by the surfactant system hence resulting in coalescence. Alternatively, another mechanism of premature destabilization can be the homogenization inefficiency. If homogenization is not efficient to produce droplets that are small enough and mix the surfactant with it, coalescene will inevitably occur. This was observed in sample ${}^{.50}\mathbf{D}_c$ during the emulsification step.

The Table 2 shows the samples that exhibited phase separation macroscopically and after centrifugation. The emulsifying wax system turned out to be immensely stable

even with high content of P_{Oil}. The samples contained in Table 2 were classified as unstable for this test, however investigations continued even when phase separation was perceived except for those that were stored in climatic chamber at 40 °C for 14 days.

Table 2 – MACROSCOPIC AND CENTRIFUGATION PHASE SEPARATION TIMES FOR DISTINCT FORMULAS AND ITS RESPECTIVE BATCHES

Sample	Centrifugation [days]	Macroscopic [days]
$^{.50}\mathbf{D}_c$	1	1
$^{.60}\mathbf{F}_a$	1	1
$^{.50}\mathbf{D}_b$	28	182
$^{.55}\mathbf{E}_a$	42	–
$^{.65}\mathbf{G}_a$	56	–
$^{.40}\mathbf{C}_a{}^{40^\circ C}$	14	–
$^{.40}\mathbf{C}_b{}^{40^\circ C}$	14	–
$^{.50}\mathbf{D}_a{}^{40^\circ C}$	14	14
$^{.50}\mathbf{D}_b{}^{40^\circ C}$	14	14
$^{.50}\mathbf{D}_c{}^{40^\circ C}$	14	14
$^{.55}\mathbf{E}_a{}^{40^\circ C}$	14	14
$^{.60}\mathbf{F}_a{}^{40^\circ C}$	14	14
$^{.65}\mathbf{G}_a{}^{40^\circ C}$	14	14

LEGEND: Cells identified with – represent times where there was no phase separation observed.
SOURCE: the author, (2020).

Aside from the samples mentioned, none other suffered destabilization in the observed time interval. All incubaded samples showed condensed water at the container lid and all batches of the formulas $^{.50}\mathbf{D}$, $^{.55}\mathbf{E}$, $^{.60}\mathbf{F}$ and $^{.65}\mathbf{G}$, showed water and oily phase contents separated over the top of the cream. Considering that this is one of the tests described in the Cosmetic Products Stability Guide (2004) it is possible to assert that the cited samples have failed the classical stability tests in this condition. For high viscosity creams such as these it is likely that the reduction in the viscosity due to a higher temperature facilitated the migration of the oily phase to the top. Additionally, the higher temperature can alter the properties of the waxy surfactant system by melting it and thus facilitating the coalescence.

The semissolid properties of the emulsion prepared are a result of the high droplet concentration and the liquid crystalline phase surrounding them. The strength of this structure is given by the strength of the inter droplet forces and their arrangment as well of organization of the mesophase (ANVARI; JOYNER (MELITO), 2017).

Most samples did not gone through macroscopic phase separation and centrifugation tests were able to detect phase separation only for the samples with high oil content. It is likely that for some samples, the P_{Oil} was trapped inside the dense structure of the cream which can be seen as pockets of oily phase inside the cream (RAFANAN; ROUSSEAU, 2019). This was not possible to observe macroscopically and neither through centrifugation. Is is believed that the samples that showed destabilization, did so because homogenization steps were not efficient in mixing all the components from P_{Aq} and P_{Oil} especially in formulas with higher oil content.

The focus of the study was determining physical stability so chemical stability of the formulations was not assessed, however pH and organoleptic measurements can indicate a change in the chemical composition. These results will be discussed in Section 4.3.1.

All formulas had an oily feel when applied and spreaded over the skin, however the formulations $^{.50}\mathbf{D}$, $^{.55}\mathbf{E}$, $^{.60}\mathbf{F}$ and $^{.65}\mathbf{G}$ had a specially poor sensory perception when accounting oiliness and spreadability due to its high oil content in the formulation. The original formula described in the National Form does not contain either mineral or vegetable oil in its composition, hence it does not have the same oily sensation. This cream, after it has been prepared and matured, is used as a base to incorporate drugs that are in liquid state or have been solubilized in a compatible, usually aqueous, solvent (BRASIL, 2012).

The centrifugation is an accelerated stability test based on the principle that substances with distinct densities will separate given an increase in the relative gravitational force applied over them. The results of a centrifugation test is either creaming or sedimentation of the dispersed phase. It does not necessarily indicate real physical stability but it is a screening tool to determine whether or not the formulation should procede to the other accelerated and shelf-life stability tests (ANVISA, 2004). The life span of a product can be predicted by the phase separation observed when it is submitted to a gravitational force (WITTERN et al., 1985; IDSON, 1993). If there is no phase separation with centrifugation it can be asserted that when the formulation is conditioned to normal gravitational forces it has a physical stability (TADROS, 2004).

In this study most of the formulations remained stable against the centrifugation tests with the exception of the ones represented in Table 2. The high viscosity of the formulated creams surely has an influence in the kinetics of phase separation. For these systems it is possible that creaming or sedimentation is very unlikelly as long as the solid-like structure of the cream remains unchanged, therefore coalescence may be hardly observed at the surface or the at the bottom of the cream and instead will be observed as pockets of the dispersed phase within the cream.

4.2 BATCH REPRODUCIBILITY

The formulas were not produced using industrial grade equipment and temperature control in the cooling step was not controlled. With that, the cooling rate may have been one important factor in emulsion structure. The parameters least affected by batch irreproducibility were pH and conductivity, and we can observe that rheological data was highly affected.

These results will be discussed in the following sections, however it is important to note that the batch c of the formula $\mathbf{D}$ was produced exactly like the other batches and still presented phase separation. The Figure 29 demonstrates how different is the rheological behaviour of the batches in frequency sweeps, the Table 6 reflects the high variance in the E_{coh} measurements between batches and in Table 5 it is possible to see that ${}^{.40}\mathbf{C}_c$ has a bigger mean diameter when compared to the other batches and ${}^{.20}\mathbf{A}_c$ has a smaller mean diameter when compared to other batches.

The difference between batches is not necessarily a bad thing. In the attempt of classifying creams in a binary, *stable–unstable* system, having a wider variety of samples can be interesting as long as a positive stable control and a negative unstable control are also present.

4.3 PHYSICO-CHEMICAL TESTS

4.3.1 Cream pH values evaluation

The hydrogenionic potential was measured with samples diluted to 10 % (m/v) in purified water due to the high viscosity of the cream. The pH is used in stability assessment to identify potential chemical reactions within the system and it is also used as an exclusion parameter for samples that are too acidic or basic. The measured pH values exhibit a downward trend (Fig. 14) over the 182 days of analysis for all formulas but still lie within the skin pH value range. For non-ionic emulsification systems the pH value of the medium should not have an effect on the stability and this parameter was only used to determine if a sample should be excluded from the experiment.

Figure 14 – HYDROGENIONIC POTENTIAL VALUES AS A FUNCTION OF TIME FOR ALL SAMPLES

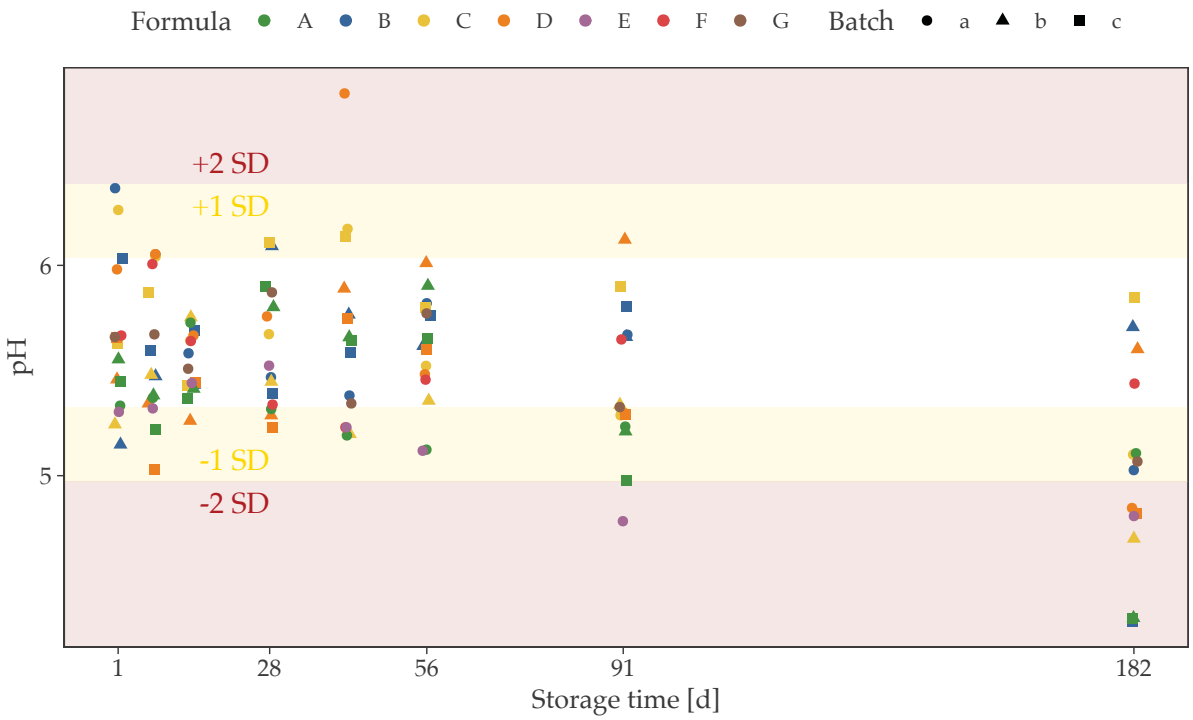

LEGEND: Areas without shading represent values up to ±1 standard deviation (SD), yellow shaded areas represent values that are between ±1 and ±2 SD and red shaded areas contain values that are higher than ±2 SD.

SOURCE: the author (2020).

The samples that were incubaded for 14 days at 40 °C had no observable change in pH values, which indicates that there was no sign of components chemical degradation within this time span under higher temperatures. None of the formulas was excluded from the experiments based on skin compatibility pH values because all remained within a range of 4 and 7, (BROOKS; IDSON, 1991; SCHNEIDER et al., 2007), however it is possible to observe that samples ${}^{.20}\mathbf{E}_a^{91d}$ and ${}^{.50}\mathbf{D}_a^{42d}$ steered away from -2 SD and +2 SD respectively. Several other samples had the same behaviour for the storage time of 182 days, including ${}^{.20}\mathbf{A}$, ${}^{.30}\mathbf{B}$ and ${}^{.40}\mathbf{C}$.

Table 3 – HYDROGENIONIC POTENTIAL VALUES FOR ALL FORMULATIONS AND BATCHES OVER THE PERIOD OF 182 DAYS

Formula	Storage Time [days]														
	1			14			56			91			182		
	Batch														
	a	*b*	*c*	*a*	*b*	*c*	*a*	*b*	*c*	*a*	*b*	*c*	*a*	*b*	*c*
[20]**A**	5.33	5.55	5.45	5.73	5.41	5.37	5.12	5.90	5.65	5.23	5.21	4.98	5.11	4.32	4.32
[30]**B**	6.37	5.15	6.03	5.58	5.43	5.69	5.82	5.62	5.76	5.67	5.66	5.80	5.03	5.71	4.31
[40]**C**	6.26	5.24	5.63	5.64	5.75	5.43	5.52	5.36	5.80	5.29	5.34	5.90	5.10	4.70	5.85
[50]**D**	5.98	5.46	5.66	5.67	5.26	5.44	5.48	6.01	5.60	5.30	6.12	5.29	4.85	5.60	4.82
[55]**E**	5.30	–	–	5.44	–	–	5.12	–	–	4.78	–	–	4.81	–	–
[60]**F**	5.67	–	–	5.64	–	–	5.46	–	–	5.65	–	–	5.44	–	–
[65]**G**	5.66	–	–	5.51	–	–	5.77	–	–	5.33	–	–	5.07	–	–

SOURCE: the author, (2020).

4.3.2 Conductivity evaluation

The conductivity is useful to observe the stability of systems stabilized by ionized surfactants, to assess the whether the formulation prepared is of the O/W or the W/O type and to verify phase inversion. Formulations with water as the continuous phase are have much higher conductivity than W/O emulsions (SAKAMOTO et al., 2017). The creams prepared in this study were too dense and viscous to properly execute conductivity measurements without dilution. By diluting the creams the conductivity measurements did not reflect the real conductivity of the cream, preventing the assessment of phase inversion and emulsion type. The emulsion dispersed phase was defined macroscopically by observing the migration of oily droplets to the top of the diluted dispersion.

Table 4 – CONDUCTIVITY [$\mu S\,cm^{-1}$] VALUES FOR ALL FORMULATIONS AND BATCHES OVER THE PERIOD OF 182 DAYS

Formula	Storage Time [days]														
	1			14			56			91			182		
	Batch														
	a	*b*	*c*	*a*	*b*	*c*	*a*	*b*	*c*	*a*	*b*	*c*	*a*	*b*	*c*
[20]**A**	40.2	31.5	41.3	69.2	35.4	52.5	42.6	44.6	41.8	54.1	39.4	43.7	43.1	29.0	50.3
[30]**B**	76.5	43.5	41.5	27.7	40.3	51.0	31.6	56.5	50.9	48.0	39.5	45.6	40.1	40.2	54.4
[40]**C**	40.5	44.2	30.8	35.7	43.0	36.1	29.5	37.1	39.2	43.7	38.5	41.3	45.6	47.7	40.9
[50]**D**	47.5	32.4	43.5	24.0	37.3	42.5	30.5	34.6	54.1	47.9	29.6	49.6	50.3	50.4	34.4
[55]**E**	35.2	–	–	43.7	–	–	39.8	–	–	–	–	–	40.2	–	–
[60]**F**	32.5	–	–	33.6	–	–	40.6	–	–	34.5	–	–	48.2	–	–
[65]**G**	45.6	–	–	51.3	–	–	47.3	–	–	49.3	–	–	46.4	–	–

SOURCE: the author, (2020).

4.4 DROPLET SIZE MEASUREMENTS

4.4.1 Optical microscopy

Through optical microscopic evaluation with 10 X magnification it was possible to notice that formulations with higher oil content form more aggregates than others even when submitted to the same homogenization and dilution procedure. Droplet size and morphology also changed as oil phase content increased. The diameters were calculated in both 10 X and 40 X magnification with a conversion scale of 1.877 px µm^{-1} and 7.285 px µm^{-1} with a standard deviation of 29.2 px and 122.0 px respectively.

Formulas with lower P_{Oil} content presented spherical and small droplets whilst the ones with higher P_{Oil} had deformed large droplets, that indicate the presence of a gelled structure and many aggregates. In Figure 15 photomicrographs are labelled with the respective formula, batch and storage time.

With microscopy results it is proven that the systems with higher oil content have larger droplets hence inducing colloidal destabilization. The bigger droplet size for formulations with higher oil content can be related to an inneficient homogenization process that failed to provide enough energy to deform the drop to a point of rupture. Additionally, since the concentration of the surfactant system was constant throughout the formulations, it is possible that a depletion of the emulsifier system was in place for formulations with higher oil content. This depletion could have caused the coalescence during homogenization as droplets not completely coated with surfactant were more prone to coalescence when colliding with themselves (TADROS, 2005). Either way, the objective of destabilization was achieved. The size distributions for all samples were multimodal, this can be seen in the photomicrographs as well as in the laser diffraction experiments (Section 4.4.3).

Figure 15 – PHOTOMICROGRAPHS WITH 10 X MAGNIFICATION FOR VARIOUS SAMPLES WITH 7 DAYS OF STORAGE

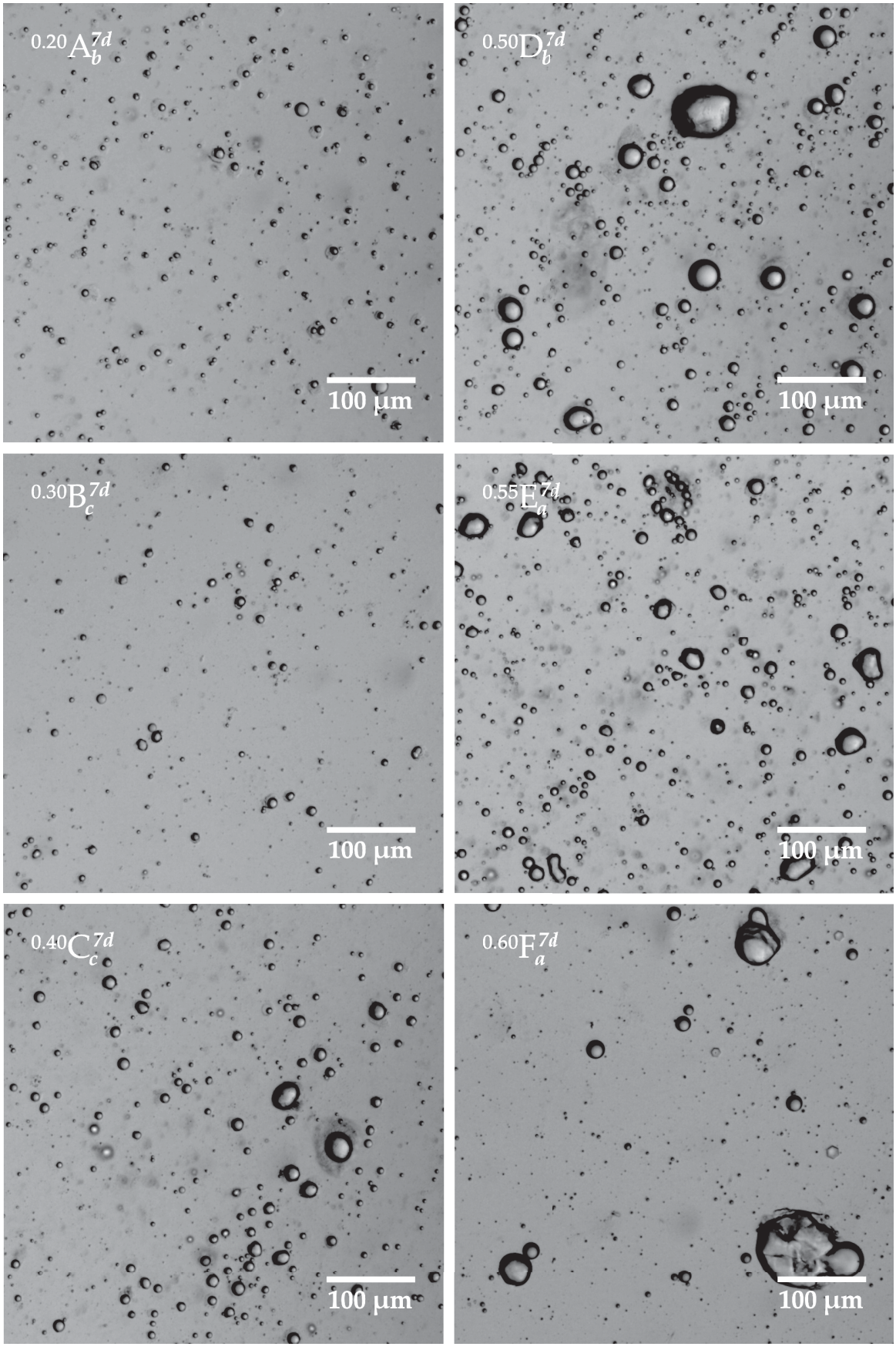

SOURCE: the author, (2020).

Structures other than emulsified droplets were obseved through optical microscopy (Fig. 17*a*). These structures were found dispersed and surrounding the drop interface. It was not possible to determine with photomicrographs the nature of these structures, however since it is widely described in literature that oil-in-water systems formed with cetostearyl alcohol contain a liquid crystals both dispersed in the water bulk phase and surrounding droplets (BARRY, 1975; JUNGINGER, 1984; ANDRADE et al., 2007; SAKAMOTO et al., 2017; TERESCENCO et al., 2018) this was taken to be true.

A negative effect of using optical microscopy for drop size determination is the need of dilution of the systems. The dilution and homogenization most likely changes the structure, morphology and size of the drops in the system. Drops that could have been deformed and compacted within the cream, become spherical once diluted (HU et al., 2017).

4.4.2 Polarized light microscopy

It was possible to observe through polarized light microscopy that the creams contained cetostearyl liquid crystals on the interface as well as dispersed in continuous phase. These liquid crystals can be seen in Figure 16 as a white regions deposited on droplet interface and dispersed on the continuous phase. The white arrows indicated by *a*, represent areas of crystal build up at the interface. In the Figure 16b.1 and 16b.2 it is observed that there is a large layer that may be causing the droplet deformation to an oval shape. These photomicrographs were taken with diluted samples at a concentration of 10 wt. % and still it is possible to observe that droplets become entangled in the network of the liquid crystal phase, thus decreasing droplet mobility. The anisotropy patterns observed in Fig.16 are a characteristic of the lamellar bilayers formed on the interface between the droplet and continuous phase as well as dispersed liquid crystals (MACIEL et al., 2016).

Figure 16 – COMPARISON BETWEEN POLARIZED AND NORMAL LIGHT MICROSCOPY FOR THREE DISTINCT SAMPLES

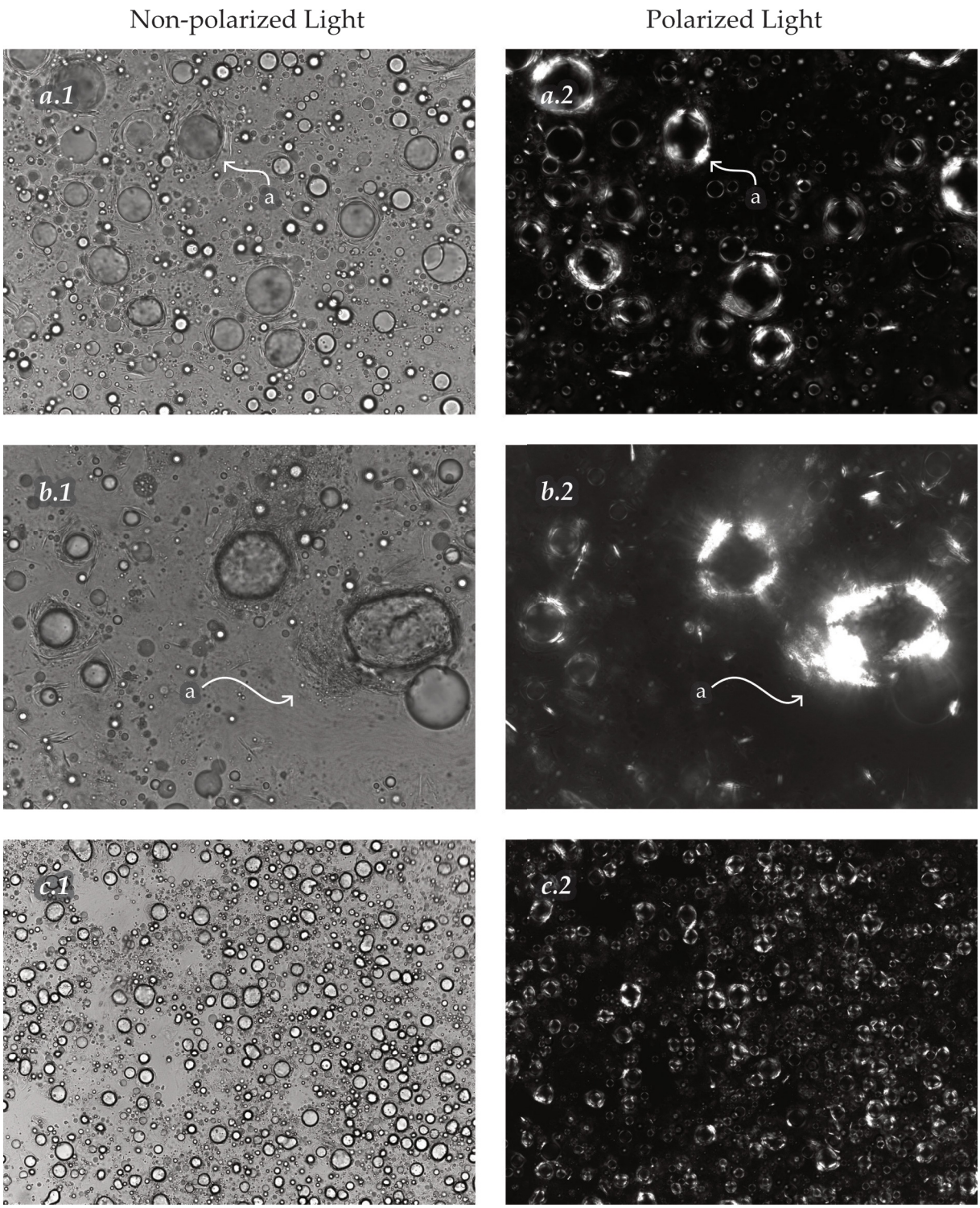

SOURCE: the author, (2020).

4.4.3 Laser multiple scattering

The droplet sizes were determined to verify destabilization phenomena that might be occuring over time. In the Table 5 there is a summary of the De Brouckere

mean diameter for distinct formulas over a period of 42 days of storage in ambient temperature. We can see from this data that the average sizes do not change over the time observed with the exception of $^{.50}\mathbf{D}_c$ that appears to show a constant increase from 83 to 94 µm in the observed storage times. The other formulas exhibit some variability between batches, especially $^{.40}\mathbf{C}_c$ that has a higher average size for all storage times when compared to $^{.40}\mathbf{C}_a$ and $^{.40}\mathbf{C}_b$, however this size difference for $^{.40}\mathbf{C}_c$ did not influence on stability over time as this sample did not destabilize macroscopically or by centrifugation at room temperature.

Table 5 – VOLUME WEIGHTED MEAN DIAMETER FOR DISTINCT FORMULAS STORED AT AMBIENT TEMPERATURE OVER THE PERIOD OF 42 DAYS

		$D_{[4;3]}$ [µm]				
		Storage Time [d]				
Formula	Batch	1	7	14	28	42
$^{.20}\mathbf{A}$	*a*	25	24	26	31	25
	b	24	18	17	14	21
	c	15	16	19	17	18
$^{.30}\mathbf{B}$	*a*	25	25	26	31	30
	b	31	25	28	24	19
	c	25	25	30	28	29
$^{.40}\mathbf{C}$	*a*	24	26	27	29	29
	b	28	27	28	21	23
	c	52	48	54	54	51
$^{.50}\mathbf{D}$	*a*	23	23	25	29	28
	b	35	37	37	37	32
	c	83	86	89	92	94

SOURCE: the author, (2020).

The stability of the creams appears to have no correlation to droplet size with the exception of $^{.50}\mathbf{D}_c$ that had separated phase during cream preparation and thus had bigger droplets and dispersed structures. It is likely that the there is a gelling phenomena in place that arrest droplets and prevent them from coalescing. Additionally, as seen and discussed from polarized microscopy (Fig. 16), the build up of surfactant on the interface can be very effective in preventing coalescence and Ostwald Ripening, thus reducing droplet growth.

Figure 17 – PHOTOMICROGAPHS IN 40 X MAGNIFICATION FOR VARIOUS SAMPLES WITH 7 DAYS OF STORAGE

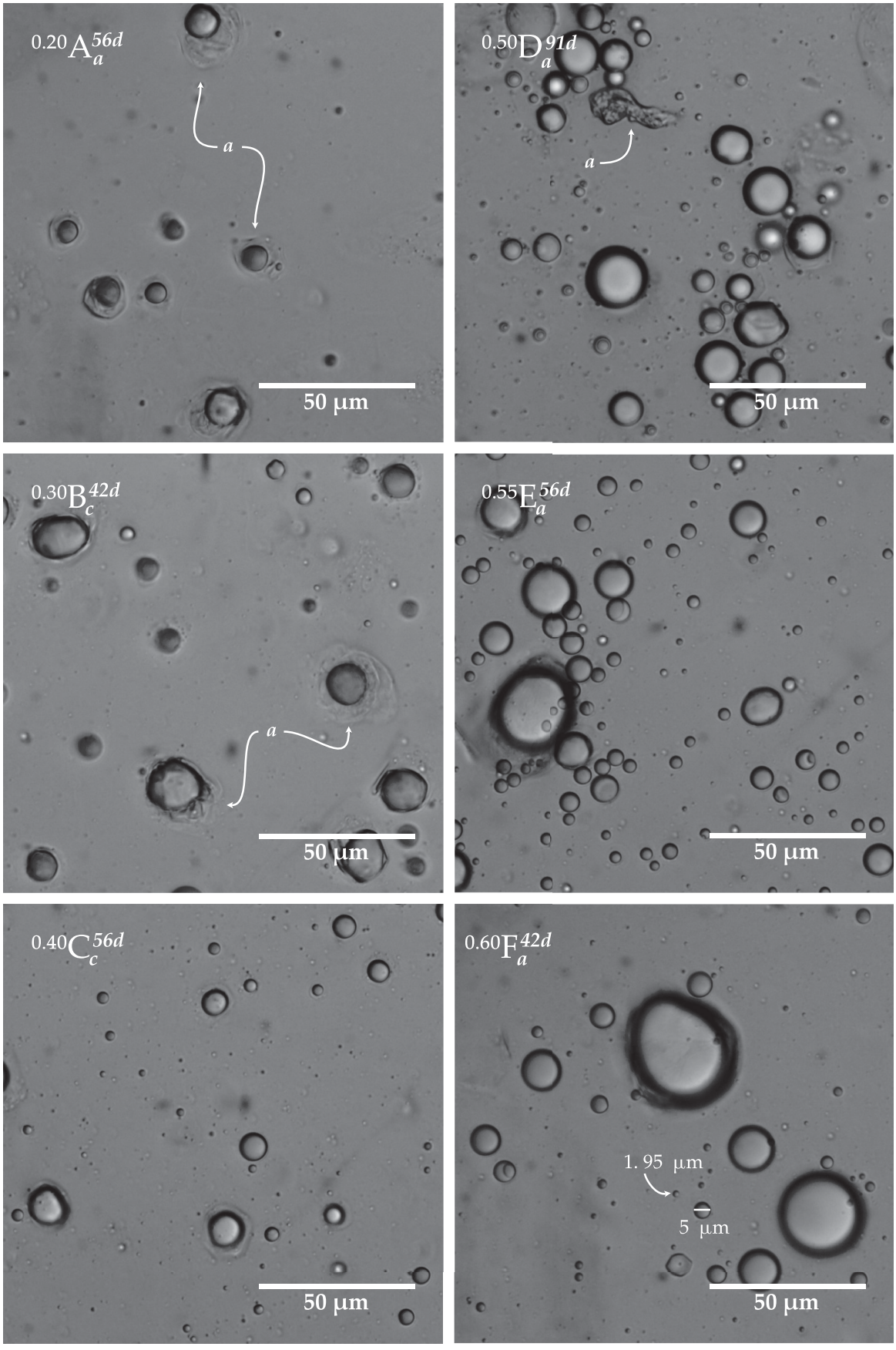

SOURCE: the author, (2020).

The Figure 18 shows that there is a difference in the size distribution as function of P_{Oil} contents, with ${}^{.50}\mathbf{D}_b$ having droplet distribution towards higher sizes and ${}^{.20}\mathbf{A}_b$ to lower sizes when compared to formulas ${}^{.30}\mathbf{B}$ and ${}^{.40}\mathbf{C}$. The dashed line represents the median of the distribution and for the sample ${}^{.50}\mathbf{D}_b^{14d}$ it is higher than the other samples. All samples went through the same dilution and redispersion process but all batches of formula ${}^{.50}\mathbf{D}$ and other formulas with higher oil content (${}^{.60}\mathbf{F}$, ${}^{.65}\mathbf{G}$) showed signs of macroscopic aggregates, that were excluded from the measurements.

Figure 18 – DROPLET SIZE DISTRIBUTION OBTAINED FROM FRAUNHOFER METHOD FOR THE BATCH b IN DISTINCT FORMULAS STORED FOR 14 DAYS

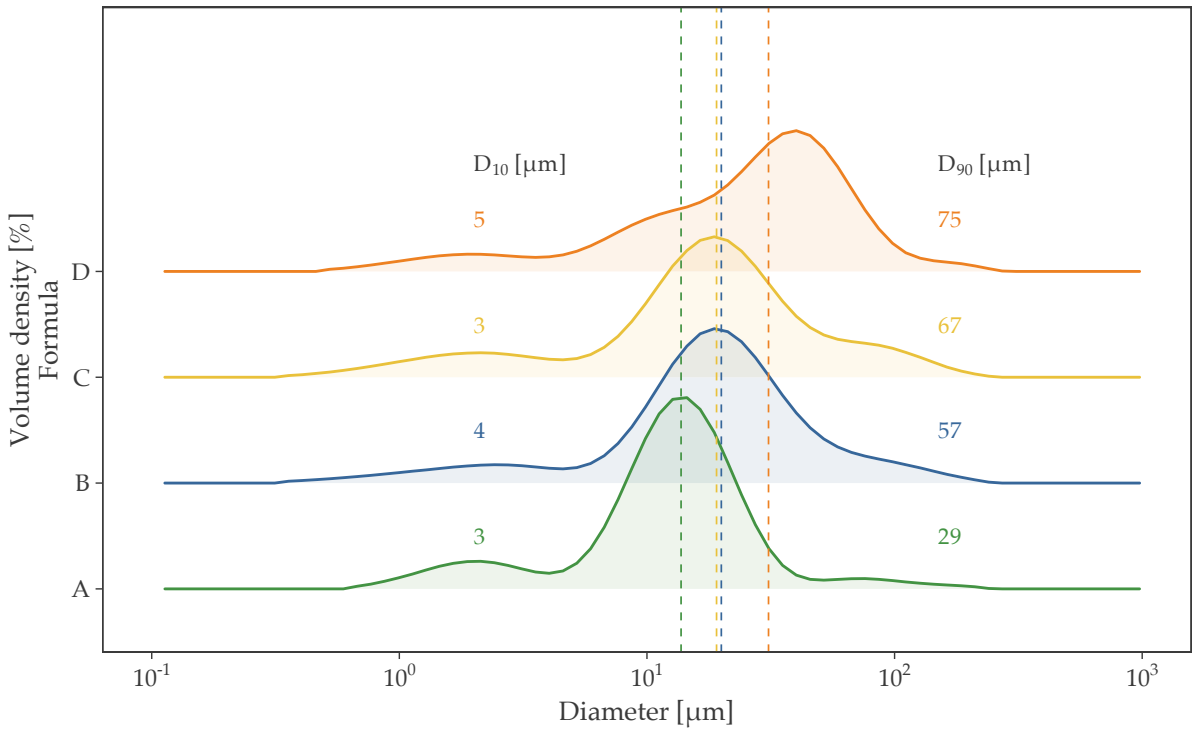

LEGEND: Dashed line represents the D_{50}
SOURCE: the author, (2020).

It was observed that there was minimal change in droplet diameter over storage time (Fig. 19) for formulas with distinct oily phase concentration. All samples exhibited a multimodal droplet size distribution with a high central peak, a small left-shifted peak in the range of 0.5 to 8 µm and a rightmost peak usually not above 100 µm. The leftmost peak is present in all samples and it can be either a population of droplets that were under a higher shear in the cream emulsification steps but it can also be an artifact of the Fraunhofer approximation that performs poorly for diameters in this range (XU, 2002). The left peak increase in 19C that appears on 182 days of storage is a measurement below the technical sensitivity of the equipment and it is most likely an experimental artifact that do not represent the droplet size distribution. In the photomicrographs with magnification of 10 X (Fig. 15) it is possible to observe smaller droplets dispersed and

in the 40 X magnification (Fig. 17) it is possible to visualize and measure their diameters. The shifted peak to the right in formula $^{50}\mathbf{D}$ occurs most likely to aggregates that did not redisperse during the dilution and homogenization steps and large droplets, when associated with the photomicrographs it is possible to determine the nature of these larger population of particles.

Figure 19 – DROPLET DIAMETER EVOLUTION OVER STORAGE TIME FOR THE BATCH *c* OF FORMULAS WITH DISTINCT OILY PHASE MASS FRACTION

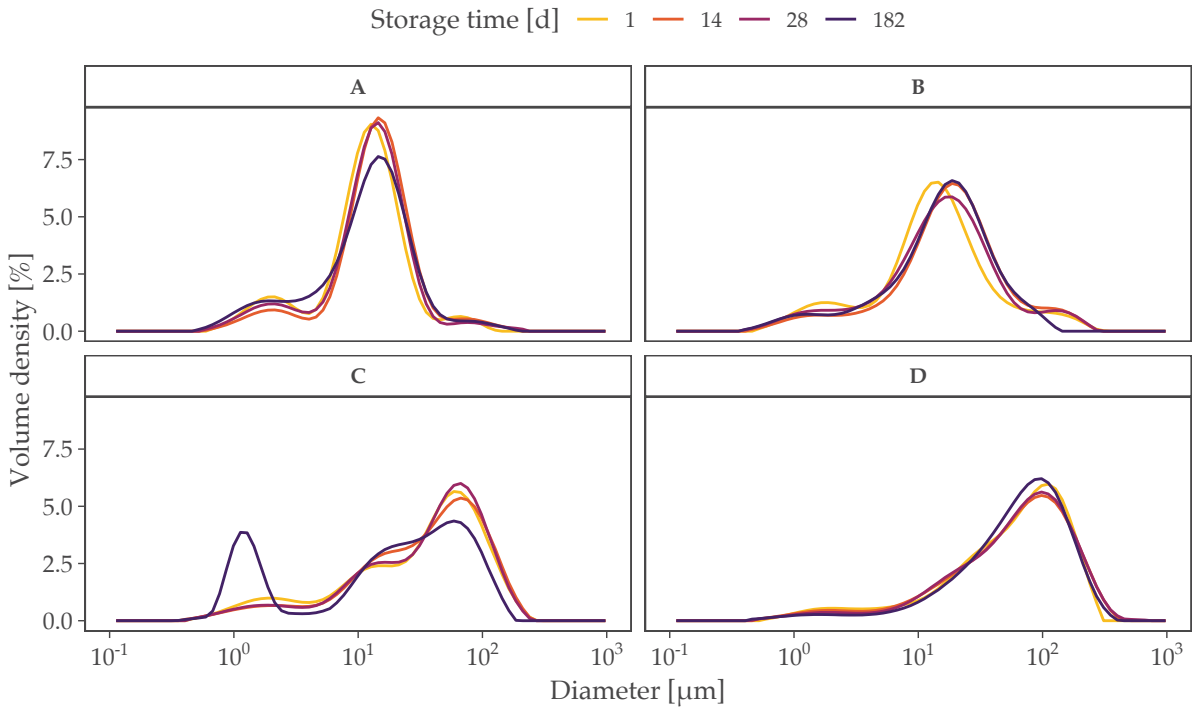

SOURCE: the author, (2020).

The photomicrographs in Figure 20 corroborate to the affirmation that there little difference in droplet size over the storage time, for the formulas as shown in Figure 19. Formula $^{55}\mathbf{E}$ has deformed droplets which indicate gelling of this structure. The formulas with lower oil rarely contain deformed droplets, which leads to believe that the deformation is due to the high concentration of droplets in the emulsion.

The droplet size determined by optical microscopy was done for selected samples to compare to Fraunhofer diffraction sizing. The results showed that for a n = 500 of diameters measured, the microscopy distribution is shifted to lower values when in comparison to the Fraunhofer method (Appendix C). This difference can be explained by two perspectives: the first is that when manually measuring droplet diameters from photomicrographs the inner edge of the droplet interface was chosen and not the outer edge identified by *a* in Figure 17. Secondly, the equipment does not distinghish between aggregates and individual droplets, hence when manually measuring, aggregates that are inherently larger were not considered as an individual droplet.

Figure 20 – DROPLET DIAMETER AND MORPHOLOGY EVOLUTION OVER STORAGE TIME FOR THE BATCH *a* OF FORMULAS WITH DISTINCT OILY PHASE MASS FRACTION STORED IN AMBIENT TEMPERATURE

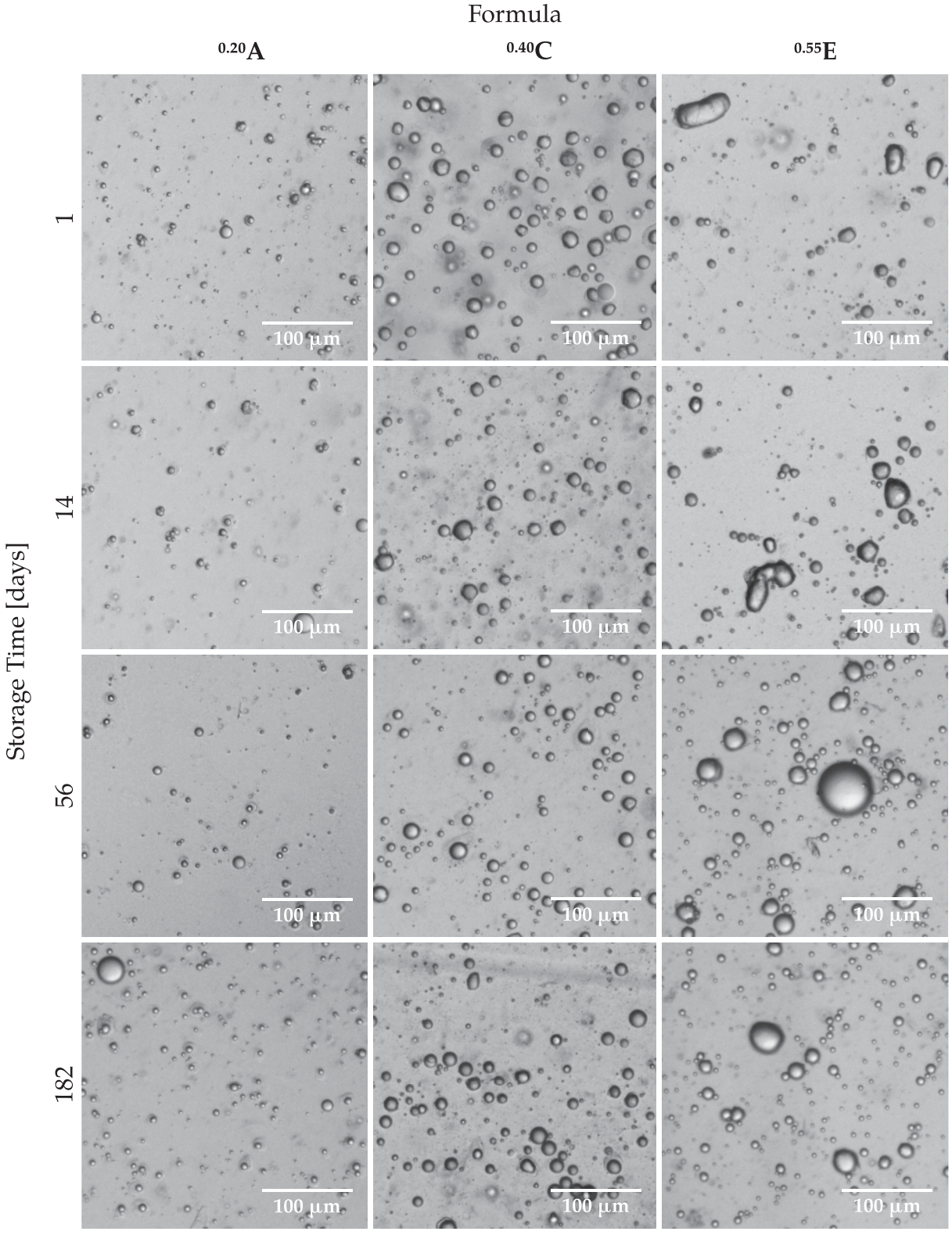

SOURCE: the author, (2020).

As discussed in previous sections, the physical stability of creams was verified

by the traditional methods, with the exception of sensory properties. These more traditional methods were not capable of determining prematurely the destabilization of the formulas with the exception of those that had already separated phases within 24 hours of production ($^{.50}\mathbf{D}_c$, and $^{.60}\mathbf{F}_a$). Centrifugation was the method that gave the most premature data to identify phase separation but even so, at 28 days after production for sample $^{.50}\mathbf{D}_b$ and over 42 days for other samples (Tab. 2). It appears that using traditional methods, instability was sooner assessed using the climatic chamber method, where samples are stressed at the temperature of 40 °C for 14 days. Even so, some of these samples did not underwent macroscopic phase separation and destabilization could only be assessed through a posterior centrifugation. It is expected that using rheological methods it is possible to assess instabilities with a smaller timespan. Data obtained will be discussed in the next sections.

4.5 RHEOMETRY GAP SELECTION

There is conflicting information in literature relating to optimum gap height, so testing should be conducted before experiments are performed. As a “rule of thumb” the gap height should be 3 (SCHRAMM, 1994); 10 (TA INSTRUMENTS, 2019) or 20 times (MCCLEMENTS, 2007) higher than the diameter of the largest particle. A test batch was prepared to standardize and optimize experiment parameters. It was prepared exactly as described in the National Form without the addition of mineral oil and it had a maximum diameter no bigger than 30 µm[1] so a gap height was chosen accordingly.

Geometry selection was based on the sensitivity limits of the equipments. For the RheoStress™1, a geometry with a higher diameter was necessary (60 mm) to work in the torque range of the equipment. For the Discovery HR-1 the geometry chosen was the one with the diameter closest to 60 mm which was 50 mm. The gap chosen was based on frequency sweeps conducted with a test batch, at 25 °C, that was not analyzed over time. The frequency sweeps (Fig. 21) show that in the range of 0.105 to 0.300 mm the curve profile is overlaid and G' values (●) decrease in the whole frequency range for gaps above 0.750 mm. The $\tan\delta$ value (○) was overlaid between all tested gap heights.

Based on these results it was determined that the default gap of 0.105 mm for the geometry CP60/2 was adequate for measurements and since the gap height for cone-plate geometries should not be changed from the default this was optimum. Unfortunately the same was not possible for measurements performed with the DHR-1 rheometer. The CP50/1 geometry chosen had a default gap of 50 µm which lies under the diameter of a fraction of the droplet population thus it had to be adjusted and the gap chosen was of 0.105 mm to match the gap used in the RS1 rheometer.

[1] Data not shown, diameter measured by optical microscopy.

Figure 21 – FREQUENCY SWEEPS IN DISTINCT GAP HEIGHTS

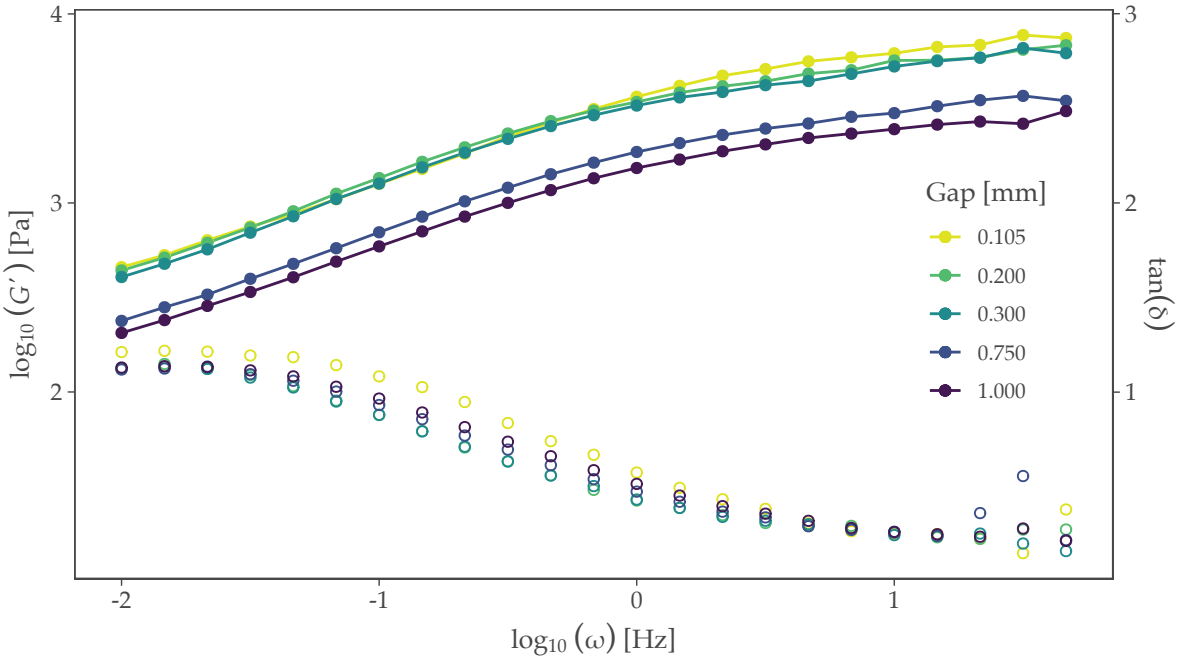

LEGEND: • – G'; ○ – $\tan\delta$

SOURCE: the author, (2020).

4.6 OIL PHASE CONTENT INFLUENCE ON RHEOLOGY

4.6.1 Amplitude sweeps

Amplitude sweeps were performed to verify elastic modulus values inside LVER; determining the yield point (τ_y) and calculating the cohesive energy density (E_{coh}). For all prepared creams it was observed that within LVER, the storage modulus was always higher than viscous modulus, suggesting that formulations behave as solids in the linear viscoelastic region. As tension apllied increases, G' starts do decrease and after the crossover between G' and G'' it is said that the material is flowing. The critical tension (τ_y) was different for various samples as well as the elastic modulus as observed in Figure 22.

The determining factor in cream rheology is not the interaction between droplets but in the formation of viscoelastic networks and its behaviour in the continuous phases (BARRY, 1975), since concentration of surfactant system remains constant in distinct formulas, the ratio between P_{Aq} and P_{Oil} are the factors determining the formation of the structure. From Figure 22 it is possible to notice that formula ${}^{.65}\mathbf{G}_a^{14d}$ has higher G' and a τ_y value close to ${}^{.40}\mathbf{C}_a^{14d}$, both higher than all the other formulas. This can be explained by the higher oil content of the formulation, that has more droplets dispersed and interact more intimately. For samples with lower oil content, such as ${}^{.55}\mathbf{E}_a^{14d}$ the G'

and τ_y values are lower because there is more bulk water between the structures of the system that results in a lower bulk elasticity.

Figure 22 – AMPLITUDE SWEEPS COMPARISON FOR THE BATCH a OF DISTINCT FORMULAS STORED FOR 14 DAYS

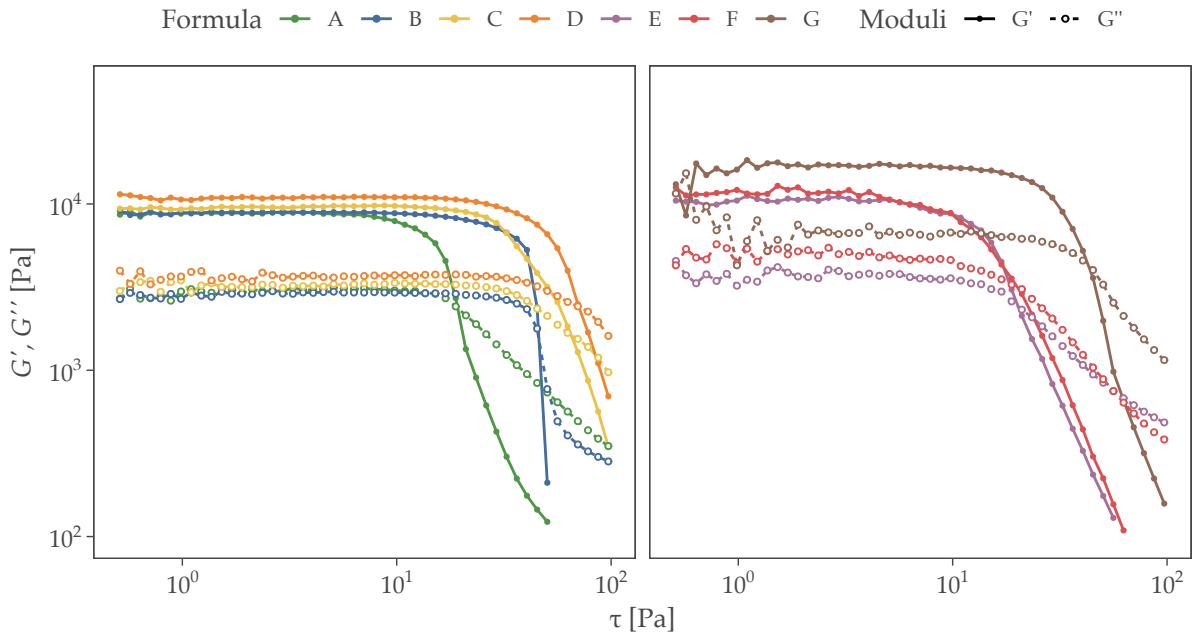

SOURCE: the author, (2020).

It is said emulsions with $G' \gg G''$ within LVER are more stable (JAGER-LÉZER et al., 1998; MASMOUDI et al., 2006) because this solid-like property in lower tensions means that the droplets are arrested in place, however the formulations of this study did not exhibited this relationship. In fact, as a general trend, the samples that presented the higher G' values in viscoelastic region usually destabilized before the ones with lower G' values.

In this study it was seen that the formulation elasticity is affected by the P_{Oil} concentration. The Figure 23 shows G' in LVE region as a function of the P_{Oil} mass fraction (w_i), the ratio between P_{Oil} mass (including Polawax) and total mass of the cream. Data used in Figure 23 were points within LVER in an amplitude range of 1 to 5 Pa for the batch a. Data normality was verified by Shapiro-Wilk, Anderson-Darling and Lilliefors tests and a significative difference was found between all formulas by ANOVA and Tukey except for the pairs $^{.20}\mathbf{A}$-$^{.30}\mathbf{B}$, and $^{.50}\mathbf{D}$-$^{.55}\mathbf{E}$. The higher G' values shown by the samples with higher oil content ($^{.50}\mathbf{D}$, $^{.55}\mathbf{E}$, $^{.60}\mathbf{F}$ and $^{.65}\mathbf{G}$) was perceived in the sensory tests and when retrieving the sample from the container with a spatula (GILBERT; SAVARY, et al., 2013).

Figure 23 – COMPARISON BETWEEN G' VALUES WITHIN LVER FOR THE SAME BATCH IN DISTINCT FORMULAS STORED FOR 14 DAYS

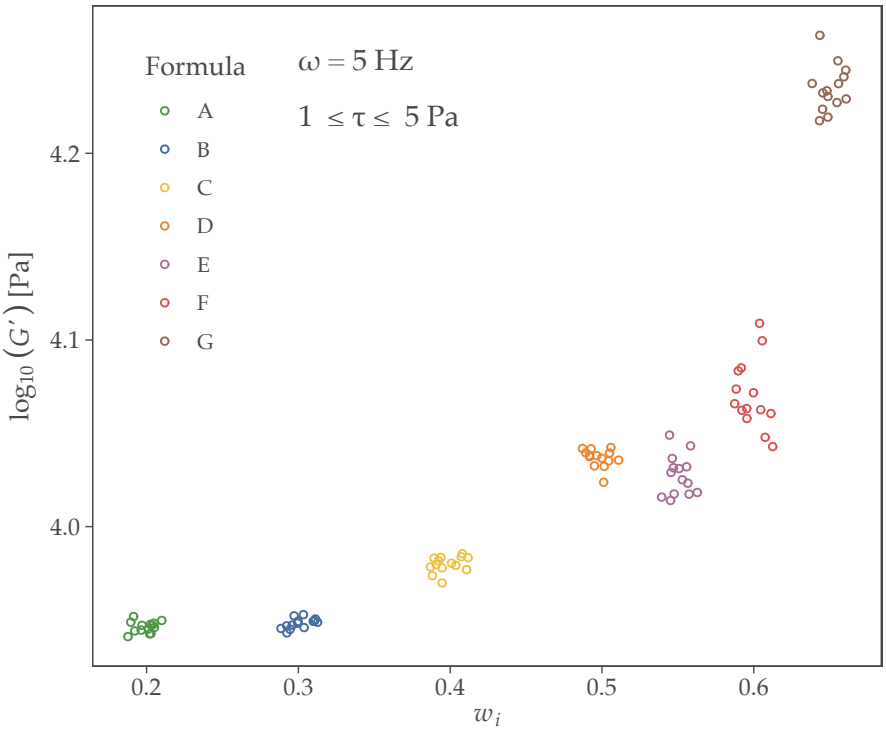

SOURCE: the author, (2020).

The Figure 23 shows the effect of oil content has over G' within LVER. This relationship is directly proportional and was perceived sensorially as well. Likewise the complex viscosity (η^*) follows that trend (See section 4.6.4).

Higher G' values in the formulations with higher oil content can be explained by the increase in the interface elastic force due to droplets deformation and accomodation and the reduction of the thickness of interlamellar water layers (JUNGINGER, 1984; ECCLESTON, 1997; SAVIC; VULETA, et al., 2005). A deformed droplet has more points of contact with its neighboring counterparts, this results in a higher interaction and the formation of a weak gel (BOHLIN, 1980; GABRIELE; DE CINDIO; D'ANTONA, 2001). As the thickness of the interlamellar water is reduced, intermolecular resistance against deformation can increase.

4.6.2 Yield point

The yield point is the minimal tension needed by a material to start flowing, there are standards that define the yield point as the first point where G' value is lower than 5 %[2] or 10 %[3] of the plateau. It can be determined by oscillatory or rotational measurements. The Figure 24 represents the scattered distribution for the oscillatory τ_y

[2]ISO 6721-10; EN/DIN EN 14770
[3]ASTM D7175; DIN 51810-2

versus the rotational τ_y for samples stored up to 28 days. These points were determined as the shear tension where a critical shift in the angular coefficient of the deformation as function of shear tension increase.

The rotational analysis usually returns higher τ_y values than the oscillatory and it has a wider distribution of data while for the oscillatory method the values of oscillatory τ_y seem to be contained between 5 to 25 Pa. Dinkgreve et al. (2016) found that different methods of determining τ_y return different results and the oscillatory methods usually return lower values than values from a tension growth curve, which agrees with the experimental data retrieved in this study. There is no general grouping of data points for distinct formulas and it is hardly possible to make any correlation between yield stress and formulation stability with the gathered data (SAKAMOTO et al., 2017).

It appears that the rotational method is less sensitive to the determination of τ_y, than the oscillatory method. The wide distribution of values measured by the rotational method can be a result of the way the experiment was performed and how the τ_y is calculated. In this case, for these formulas, the oscillatory method was more adequate and returned the most reliable and precise results.

Figure 24 – SCATTERPLOT OF ROTATIONAL AND OSCILLATORY YIELD POINT FOR FORMULAS STORED UP TO 28 DAYS

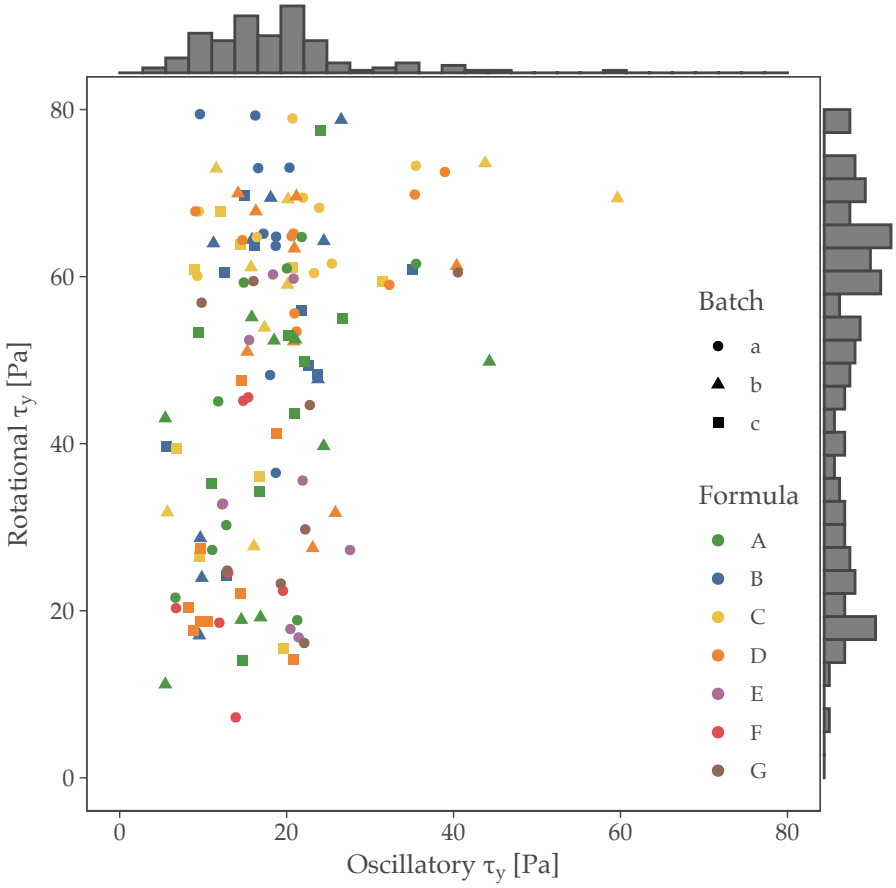

SOURCE: the author, (2020).

4.6.3 Cohesive Energy

The E_{coh} is a measurement of the strength of the dispersed structure (TADROS, 2010). This parameter was calculated using the Equation 2.9[4], γ_y and G'_0 values were extracted from amplitude sweeps using the RheoWin™V.4 software. The E_{coh} values of samples stored for 14 days are displayed in Table 6 and it is possible observe a high standard deviation between batches and no general trend as function of oil content. It was not possible to distinguish, classify or infer formulations stability using E_{coh}.

The cohesive energy is calculated using the equation 2.9 that depends both on τ_y and G'. The yield point values obtained had a high variance with no difference between formulas and storage time so it is expected that the values for E_{coh} would also have high variance.

Table 6 – AVERAGE AND STANDARD DEVIATION OF COHESIVE ENERGY VALUES BETWEEN BATCHES FOR DISTINCT SAMPLES STORED FOR 14 DAYS

Formula	E_{coh} [mJ m^{-3}]	SD
$^{.20}$**A**	26.6	16.8
$^{.30}$**B**	21.4	14.9
$^{.40}$**C**	120.8	165.6
$^{.50}$**D**	33.2	35.7
$^{.55}$**E**	12.2	–
$^{.60}$**F**	16.6	–
$^{.65}$**G**	18.0	–

SOURCE: the author, (2020).

The E_{coh} values for O/W systems varies depending on the nature of the surfactant, droplet size and composition of the system. In the literature these values range from 2.5×10^{-4} mJ m^{-3} in an emulsion prepared with polyethylene oxide and polypropylene oxide block copolymer as the emulsifier and 3.13×10^{2} mJ m^{-3} for oil-in-water emulsions prepared with glucopyranoside (ABEN et al., 2012; NIRAULA et al., 2004). Aben et al. (2012) also claimed that the τ_y has a large error even in triplicate measurements of the same sample, which affects the calculation of E_{coh}, so it was expected that for three distinct batches this error would be even larger.

4.6.4 Frequency sweeps

After determination of the LVER, frequency sweeps were performed with the tension of 5 Pa for all samples in all storage times. This experiment returns the response of the sample's viscoelastic moduli against an oscillatory frequency interval, which can be interpreted as the viscoelastic behavior as a function of observation time. High

[4]Equation displayed in page 36.

frequencies represent a short window of observation while low frequencies represents a long observation window in time (FERNANDEZ-NIEVES et al., 2016).

Frequency dependence was observed in all samples in the viscoelastic regime. Emulsions were characterized as solid-like in frequencies above 1 Hz seen by the predominance of G' over G''. This behaviour is typical of emulsions when under stress because at higher frequencies there is not enough time for droplets to rearrange between oscillation cicles (DIFTIS; BILIADERIS; KIOSSEOGLOU, 2005). In lower frequencies the creams exhibit a lower elastic and viscous moduli but no crossover is found for samples stored for 24 hours (Fig. 25). The clear relationship between the mass fraction (w_i) and G' is expected and indicates a stronger structure for creams with higher oil content. Taking ${}^{.60}\mathbf{F}_a^{1d}$ and ${}^{.30}\mathbf{B}_a^{1d}$ as examples from Figure 25, it is observed that the frequency dependence of ${}^{.30}\mathbf{B}_a^{1d}$ is more noticeable especially in lower frequencies, tending to the crossover, this means that as the time of observation increases it is possible to see the structure relax. The ${}^{.60}\mathbf{F}_a^{1d}$ elastic modulus curve appears to form a plateau as it reaches a frequency of 1×10^{-2} Hz. As a result of the higher concentration of droplets in creams with higher w_i, the crossover point can be shifted to extremely low frequencies, the solid structure formed in ${}^{.60}\mathbf{F}_a^{1d}$, despite of presenting phase separation, is stronger than formulations with less oil (GABRIELE; DE CINDIO; D'ANTONA, 2001).

Figure 25 – FREQUENCY SWEEPS FOR THE BATCH a OF DISTINCT FORMULAS 24 HOURS AFTER PREPARATION

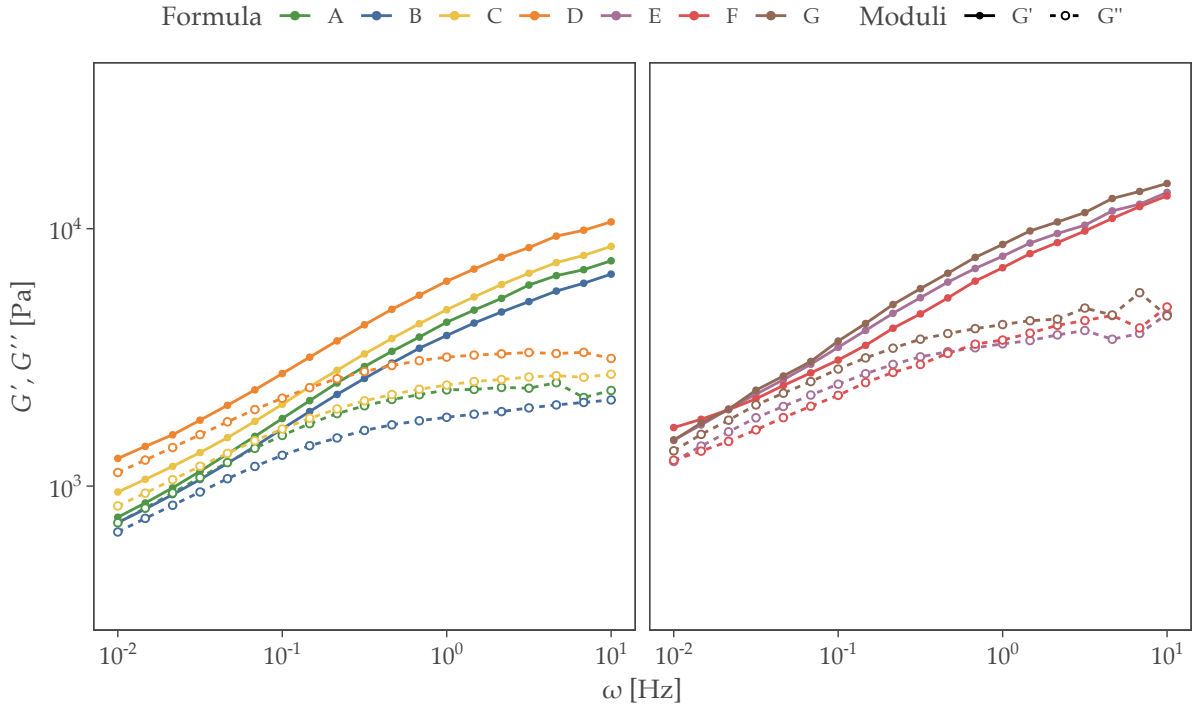

SOURCE: the author, (2020).

To demonstrate the relationship between complex viscosity and the oil loading

of the samples, the frequency of 10 Hz was chosen because it lies within the solid-like state of the cream. The data shown in Figure 26 is from samples stored for 14 days. This time was chosen because it represents a time where creams had already gone through maturation. Even though the volumetric fraction (ϕ) was not approximated, higher mass fractions inherently mean higher volumetric fraction, therefore the concept of droplet packing can be used to explain the higher viscosity of these formulations (TADROS, 2004).

The Figure 26 demonstrates that $\eta^* \propto w_i$ in the determined oscillation frequency. Along with the results from Figure 25 it is possible to state that the formulations with higher oil load have a stronger structured network.

Figure 26 – COMPLEX VISCOSITY MEASURED AT 10 Hz RELATIONSHIP TO MASS FRACTION FOR SAMPLES STORED FOR 14 DAYS

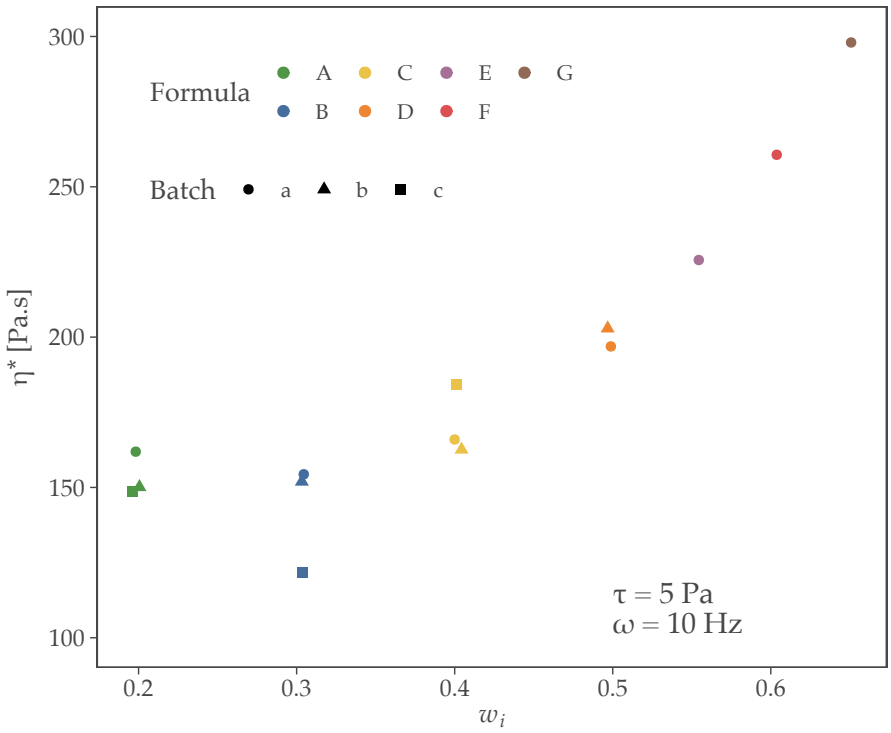

SOURCE: the author, (2020).

4.7 STORAGE TIME INFLUENCE ON RHEOLOGY

It was expected that the vicoelastic properties of the creams would change over time as a result of dehydration, relaxation and colloidal destabilization. The change on viscoelastic properties over time could elucidate whether or not they are good indicators of shelf-life stability. The first effect observed as function of storage time was the cream maturation. Cream maturation was visualized differently for distinct formulas but it was observed as an increase in both G' and G'' in frequency sweeps. The Figure 27 shows

grid of frequency sweeps experiments for two batches of the formulas $^{.20}\mathbf{A}$ and $^{.50}\mathbf{D}$ between 1 and 28 days of storage time. There is a leap in the values for elastic and viscous modulus for both batches of formula $^{.20}\mathbf{A}$. This leap observed between these storage times indicate that there must be a change in the cream network. The formula $^{.50}\mathbf{D}_a$ appears to have a smaller influence of time in comparison to both $^{.20}\mathbf{A}$ batches, whilst the structure of $^{.50}\mathbf{D}_b$ keeps changing over this period.

Figure 27 – FREQUENCY SWEEPS FOR BATCHES a AND b OF FORMULAS A AND D UP TO 28 DAYS OF STORAGE

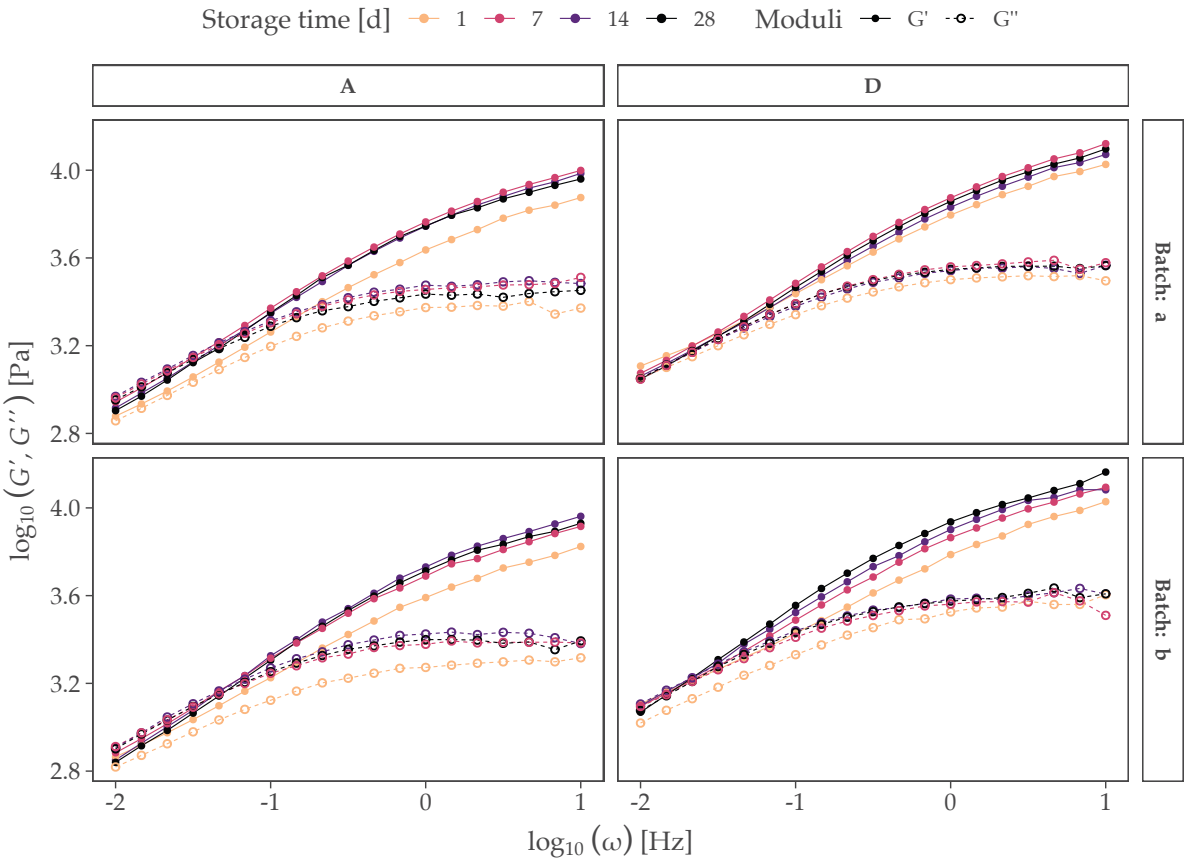

SOURCE: the author, (2020).

This maturation time can be the result of droplet accomodation and initial coarsening of the emulsion by flocculation, Ostwald ripening and coalescence or engulfment (RHEIN et al., 2006).

4.7.1 Crossover frequency as function of storage time

Independent of oil fraction it was possible to observe that ω_c was smaller in the first day of storage, when compared to the following times, indicating bigger relaxation times for samples that were not yet fully mature. The ω_c shift to lower frequencies as function of storage time can indicate that the cream rigidity is increasing due to the

increasing efficiency of the surfactant layers in protect droplets against deformation and the appearance of other dispersed structures that have stronger elastic properties than droplets (TAN; MISRAN; KHOO, 2011), in this case it is likely that the dispersed structures are becoming more connected as bulk water evaporates (SAKAMOTO et al., 2017).

In the Figure 28 it is possible to observe that the ω_c is not influenced by storage time. In 28D and 28F it is possible to observe a higher variance in the crossover frequency than for the other formulas. Frequency sweeps for ${}^{.50}\mathbf{D}_c$ were very irregular (Fig. 29) when compared to other batches and formulas, gave unreliable ω_c values and the same was observed for ${}^{.60}\mathbf{F}_a$. Both of these formulations had separated phase within 24 hours of cream preparation and the irregularities found with frequency sweeps are a result of the large droplets formed (in ${}^{.60}\mathbf{F}_a$ sometimes larger than the geometry gap) and heterogeneity of the system that suffered phase separation.

Figure 28 – CROSSOVER FREQUENCY AS A FUNCTION OF STORAGE TIME FOR DISTINCT FORMULAS

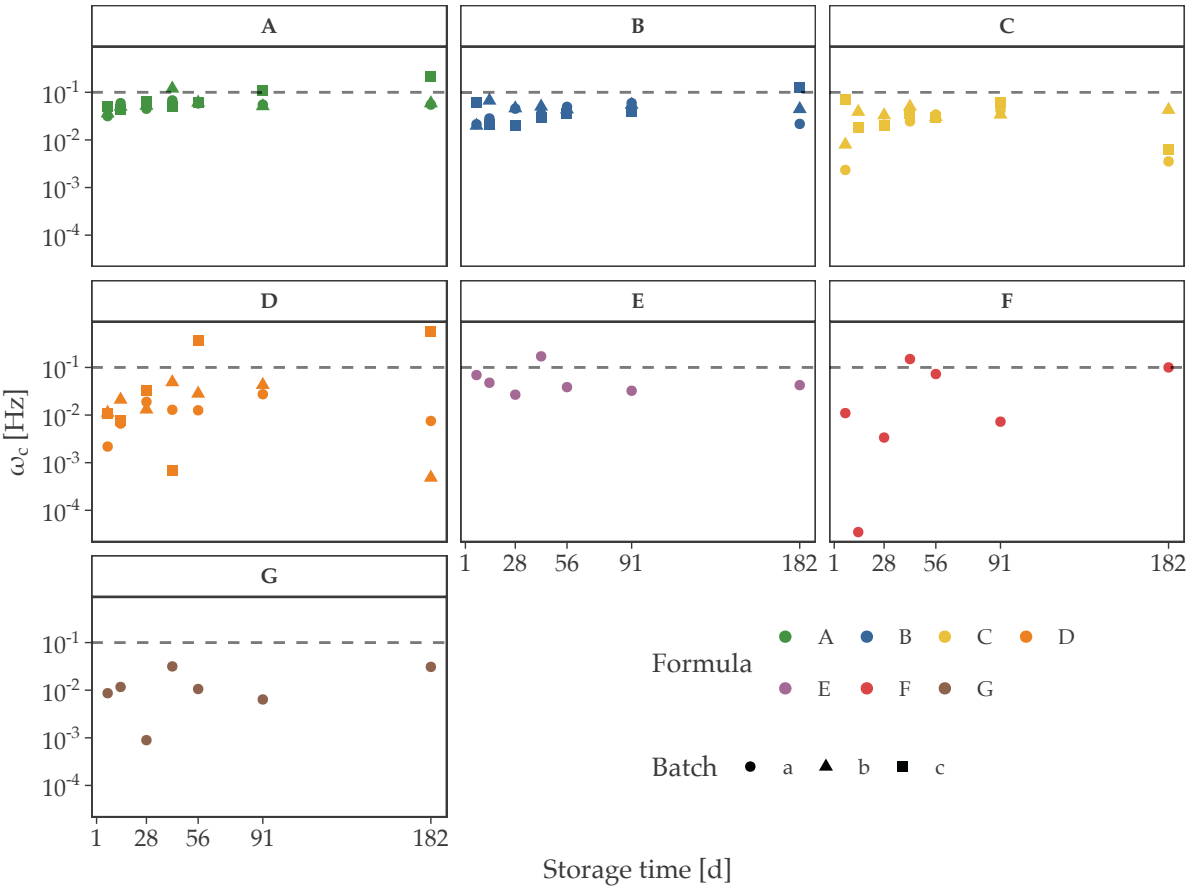

LEGEND: The dashed line plotted is a reference at 0.1 Hz to facilitate the comparison between formulas.
SOURCE: the author, (2020).

The relaxation time is the inverse of the crossover frequency and it represents the time it takes for the structure of the material to relax. According to Aben et al. (2012),

it can be a predictor of emulsion physical stability, however, with the gathered data, no correlation was found between relaxation time and stability.

Figure 29 – RELATIVE DIFFERENCE BETWEEN BATCHES a AND c FOR THE FORMULA D UP TO 42 DAYS OF STORAGE

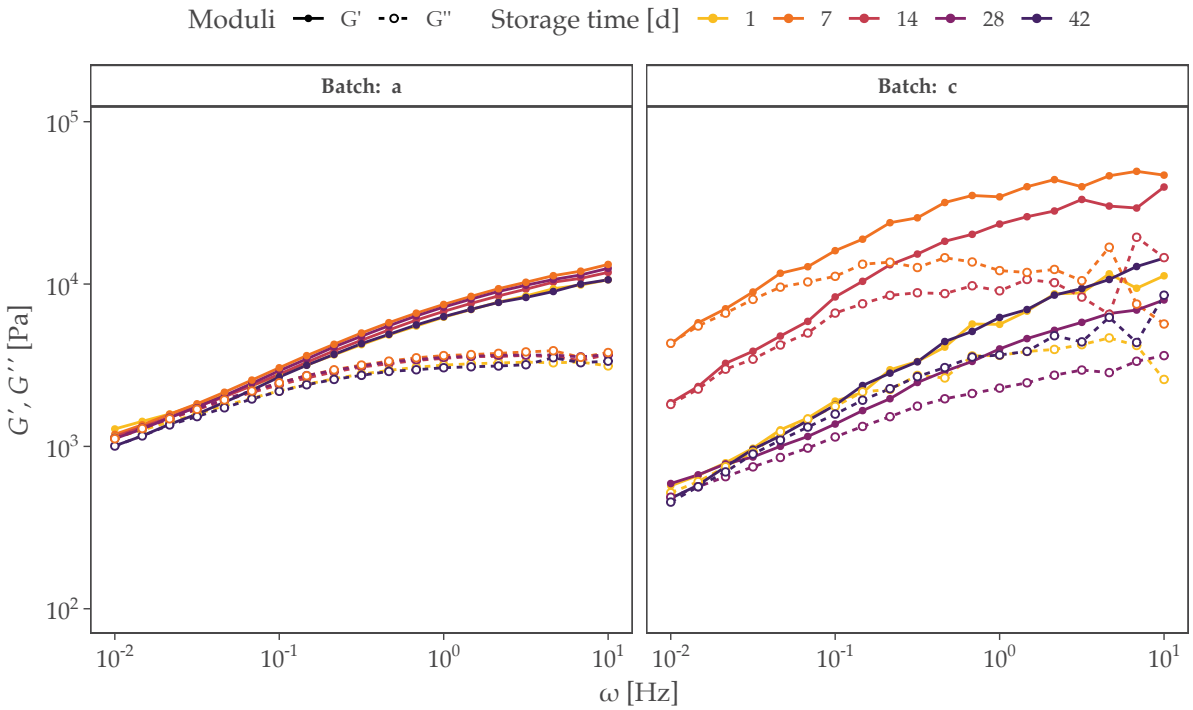

SOURCE: the author, (2020).

The structural properties of emulsions can also be modelled by the power law Equation 4.1, where the parameter $\mathcal{A}$ represents the proportional coefficient in Pa and z the coordination number that is dimensionless (GABRIELE; DE CINDIO; D'ANTONA, 2001). According to Bohlin (1980) emulsions are modelled as a network of rheological units that interact to form a structure. The coordination number z is a measure of the points of interaction between these rheological units and the parameter $\mathcal{A}$ is related to the strength of said interaction (LACA; PAREDES; DÍAZ, 2012).

$$G^* = \mathcal{A}\,\omega^{1/z} \tag{4.1}$$

In the Table 7 it can be observed that as oil content increases ($A \rightarrow H$), so does the parameter $\mathcal{A}$. This model thus confirms the stronger structures found in the samples ${}^{.50}\mathbf{D}$, ${}^{.55}\mathbf{E}$, ${}^{.60}\mathbf{F}$ and ${}^{.65}\mathbf{G}$. However, as a function of time there seems to be no relationship with the network strength. The z values displayed on Table 7 have a maximum value of 4.55 for ${}^{.20}\mathbf{A}_a^{91d}$ and a minimum value of 3.59 for ${}^{.55}\mathbf{E}_a^{91d}$ indicating that the number of points of interactions between the droplets and other dispersed structures does not vary much even for more concentraded formulas indicating that the strength of the structure

does not come from the number of interactions between rheological units (GABRIELE; DE CINDIO; D'ANTONA, 2001).

Table 7 – POWER LAW PARAMETERS DESCRIBING FREQUENCY SWEEPS

	Storage Time [d]					
	1		28		91	
	$M\mathcal{A}$ [Pa]	z	$M\mathcal{A}$ [Pa]	z	$M\mathcal{A}$ [Pa]	z
$^{.20}\mathbf{A}_a$	6.13	4.17	7.48	4.21	7.89	4.02$*$
$^{.30}\mathbf{B}_a$	5.35	4.13	70.5	4.13	7.25	4.17$*$
$^{.40}\mathbf{C}_a$	6.84	4.09	8.65	4.12	8.84	4.09
$^{.50}\mathbf{D}_a$	8.73	4.32	9.83	4.07	11.47	4.06
$^{.55}\mathbf{E}_a$	10.75	4.09	12.02	3.89	9.79	3.59
$^{.60}\mathbf{F}_a$	10.29	3.82	9.35	3.85	10.26	3.64
$^{.65}\mathbf{G}_a$	12.05	4.01	13.23	3.99	13.22	3.73

LEGEND: Cells marked with an $*$ represent power law regressions with R^2 of 0.98. All other have an $R^2 \geq 0.99$.

SOURCE: the author, (2020).

4.7.2 Yield point evolution in time

It was discussed in Section 4.6.2 that no relationship was found between the yield point of the formulations. This relationship has also not been found as function of storage time. In Figure 30 the solid line (—) represents the mean between all batches and the dashed lines (- - -) represent the standard deviation. It is possible to observe that over the period of 182 days there is no trend in the points and that there is a high variance. This variance can be attributed to the non reproducibility of the cream preparation method that resulted in batches with distinct rheological and particle size properties. In the Figures 30F and 30H it is observed that a single batch has a narrower standard deviation. Some of the variance can be explained through experimental errors as well. A way to improve reproducibility in rheological experiments is to add a pre-shear step to assure that there is no shear-history effect associated with measured data (SCHRAMM, 1994). The cosmetic emulsions were characterized as having a time-dependent behaviour and the resting time prior to yield point determination may not have been enough to reduce shear-history of the sample thus resulting in a high variance.

Figure 30 – YIELD POINT VALUES FOR DISTINCT FORMULAS OVER TIME

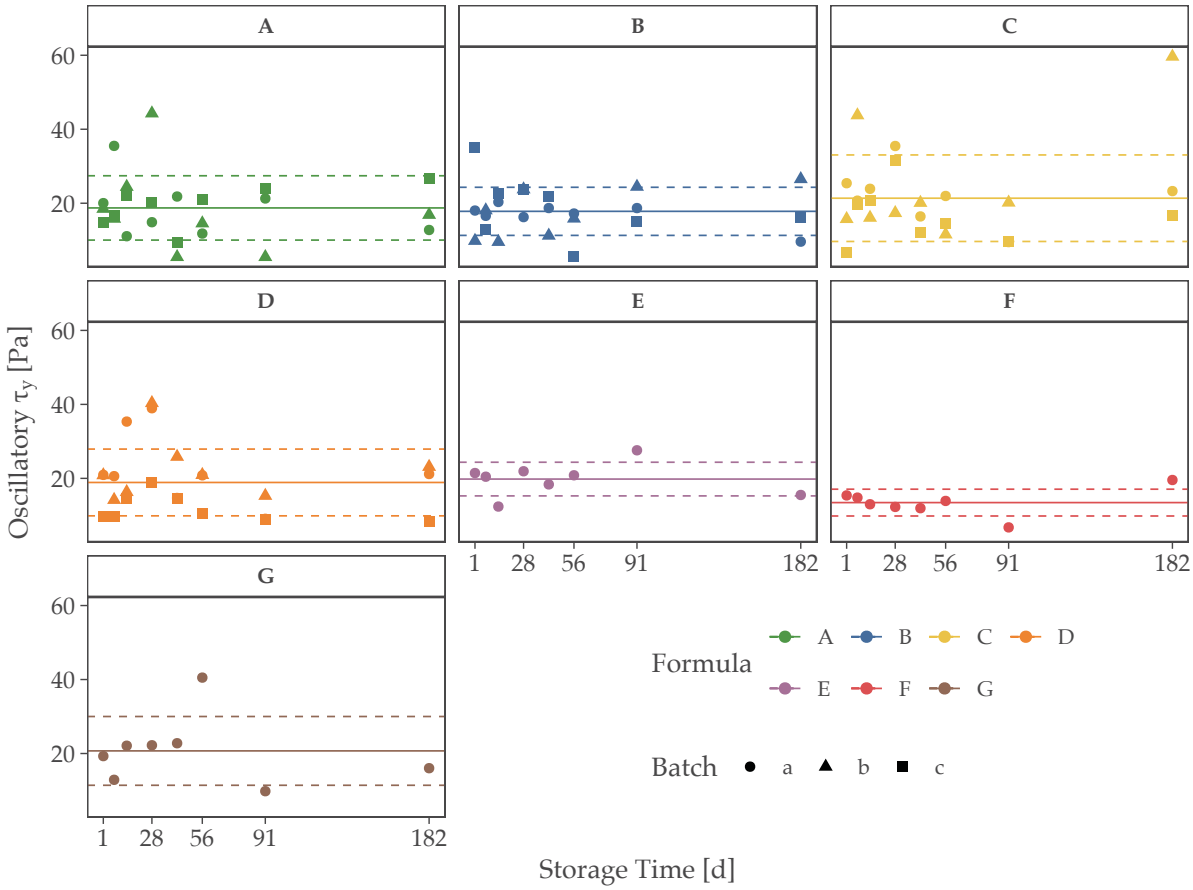

LEGEND: Solid line represent average between all batches and storage times. Dashed lines represent the SD between batches and storage times.
SOURCE: the author, (2020).

With the data gathered it is not possible to conclude that the τ_y is a good predictor of cream physical stability. The differences between samples are not enough evidence to claim that the τ_y can be used to predict emulsion stability.

4.8 TEMPERATURE SWINGS

It can be seen that the dependence of elastic and viscous moduli increases as a function of the oily fraction concentration of the creams. Samples with higher oil content have elastic and viscous moduli with higher dependence of temperature.

According to Tadros (2004), when a material, being suspension or emulsion has a viscous modulus greater than elastic, this system is stable because it is in a gel state, without droplet migration within the dispersion.

For creams with higher oily fraction it was observed that after the experiments the cream appeared as a practically gelled cohesive material (Figure 31A represents ${}^{.55}\mathbf{E}_a^{42d}$) while the other samples maintained their creamy macroscopic appearance

(Figure 31B represents ${}^{\cdot 30}\mathbf{B}_{b}^{56d}$). This phenomenon is the result of bulk and interlamellar water evaporation, which causes the shortening of the distance between surfactant lamellae and dispersed structures, increasing the cohesiveness of the material.

Figure 31 – PHOTOGRAPHS OF THE APPEARENCE OF DISTINCT CREAMS AFTER TEMPERATURE CYCLES

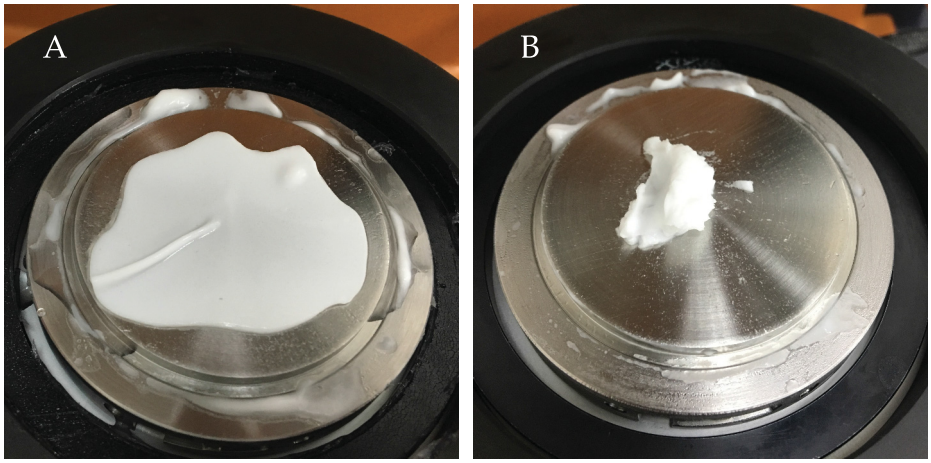

SOURCE: the author, (2020).

The moduli inversion in higher temperatures can be explained by the melting of the crystalized surfactant layers. As temperature decreases, both moduli start to increase indicating a partial solidification of the structure. In the range of 20 to 25 °C appears a small valley on the curve profile that indicates a phase transition of the material. This transition may be a result of the the presence of multiple types of crystalline phases within the formulation (MACIEL et al., 2016).

Through the results from temperature swings it was possible to determine that the temperature dependence of both G' and G'' is different for distinct formulas. As an example, the Figure 32 displays this dependence for three distinct formulas of the batch a after 24 hours of cream preparation in two consecutive heating cycles. The ${}^{\cdot 50}\mathbf{D}_{a}^{1d}$ has a higher dependence on temperature when compared to the other formulas and for the second cycle displayed there is a moduli crossover indicated by the black dots. that does not appear for ${}^{\cdot 40}\mathbf{C}_{a}^{1d}$ and ${}^{\cdot 30}\mathbf{B}_{a}^{1d}$.

Figure 32 – CONSECUTIVE COOLING RAMPS OF THE BATCH a FOR DISTINCT FORMULAS WITH 24 HOURS OF STORAGE TIME

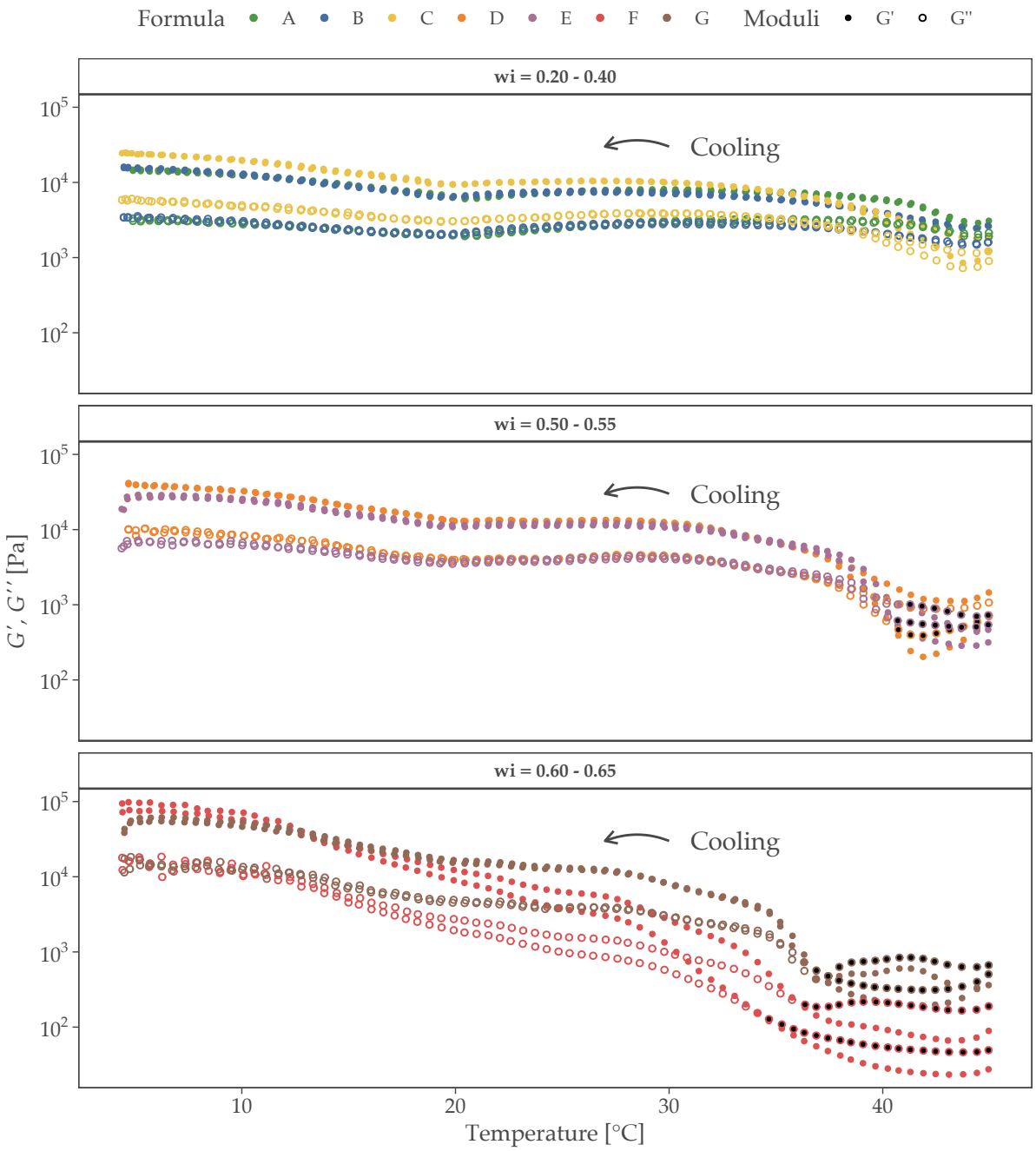

LEGEND: Black filled circles represent points where $\tan\delta > 1$. The arrows indicate the direction of the passage of time in the plot.

SOURCE: the author, (2020).

When the same samples are plotted as a function of time, it is possible to see that aside from the temperature dependence there is a temperature cycle dependence, meaning that after each cycle, the structural properties of the cream change. For instance, there is no crossover in ${}^{40}\mathbf{C}_a^{1d}$ in the first step of the experiment and in the subsequent steps it is possible to observe that in higher temperatures G' becomes

lower than G'' (indicated by the black dots in Fig. 33). Additionally, the G' lowest points decrease as a function of the temperature cycles.

Figure 33 – ELASTIC AND VISCOUS MODULI DEPENDENCE ON TEMPERATURE CYCLES FOR DISTINCT FORMULAS STORED FOR 24 HOURS

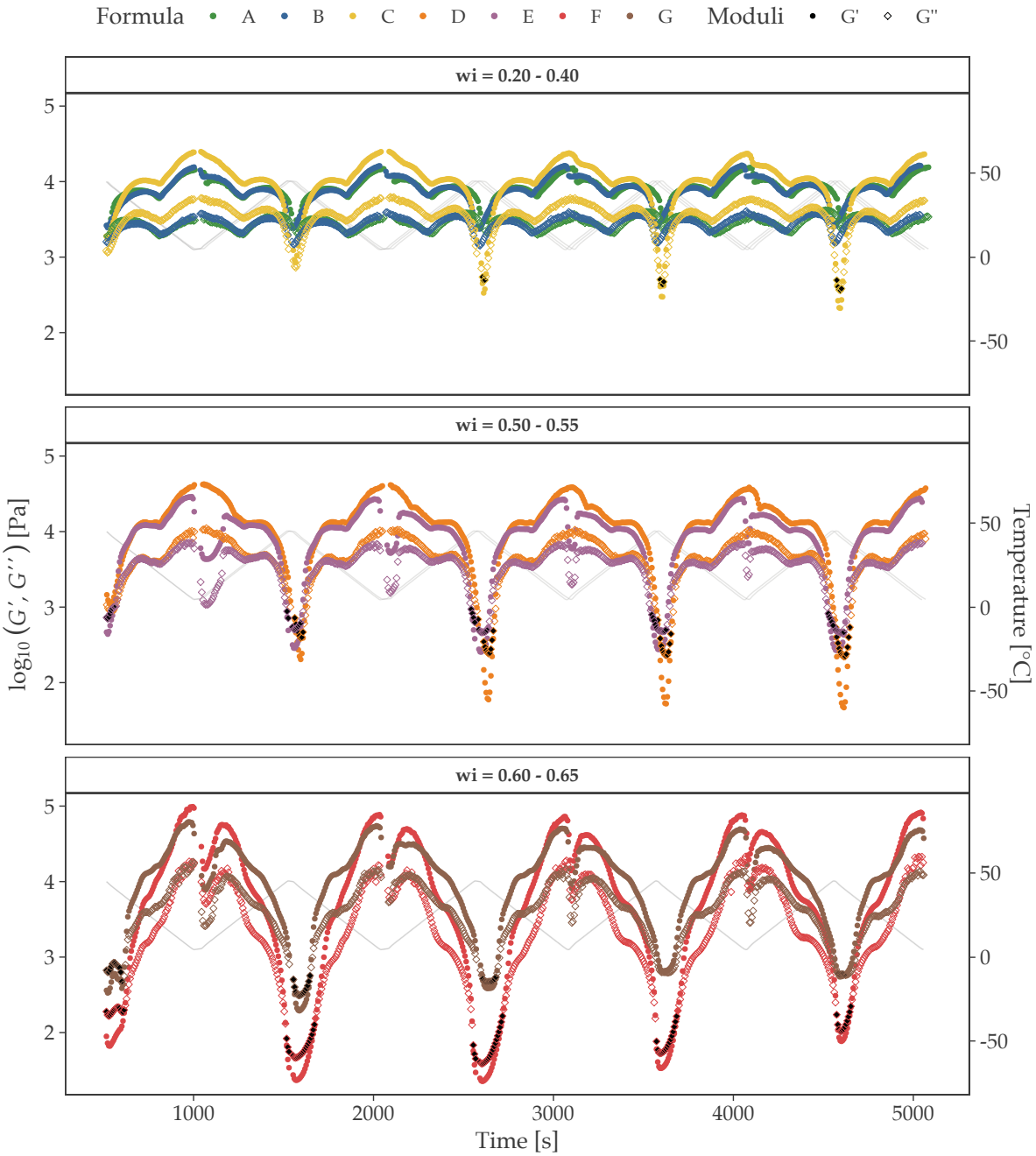

LEGEND: Black filled diamond shapes represent points where $\tan\delta > 1$. Gray lines represent the temperature ramps.

SOURCE: the author, (2020).

It is not visually interesting to show the raw results of all experiments performed to discuss them individually so it was necessary to develop creative visualizations that allow a better understanding of the information extracted from the raw data. The section

4.8.1 will focus on explaining data handling and visualization.

4.8.1 Temperature swings analysis

One way to assess whether material structure changes as a function of temperature cycles is to check the maximum and minimum values of G' and G'' following heating and cooling ramps. Brummer (2006) demonstrated that for unstable formulations, there is considerable variation and irregularity of moduli as a function of cycles.

This is a novel model of determining formulation structure over temperaure cycles so there is no standardized methodology to assess this effect, however, Bernzen (2008) developed a way to translate the change of the structure over temperature cycles, that was used by Cekic, Savic, and Savic (2019) and Karasu et al. (2015). This method observes the relative structure differences between the cycles by calculating the ratio of G' maximum value from the current cycle by the G' of the first cycle using the equation 4.2. With this method it is possible to verify which of the samples varies more with the temperature cycles. According to Brummer (2006) a formula can be classified as stable if both G' and G'' have identical values in consecutive temperature cycles at constant frequency and amplitude independent of how many cycles are applied.

$$\Xi = \frac{G'_{max}\ i}{G'_{max}\ 1};\ i = 1 \text{ to } 10 \tag{4.2}$$

Where: i is the index of the temperature ramp (2 to 10) and $G'_{max}i$ is the storage modulus maximum (or minimum) value at the i^{th} temperature ramp. Ξ was also calculated for G'' in both maximum and minimum.

In order to reduce the experiment time the temperature sweeps were not performed in temperature equilibrium, therefore it was noticed that that for ascending and descending temperature ramps the values of G' and G'' were different in consecutive maximum or minimum temperatures (5 °C and 45 °C). Because of that it was necessary to group the data points in three variables: *Modulus* (G' or G''); *Step* (heating or cooling); *Temperature* (min of max) totaling 8 groups of points for each experiment. The Figure 34 represents 4 of the 8 groups of points.

The second method was to perform a least-squared linear regression model on these groups of points extracted from temperature swings. The angular coefficient (α) and the coefficient of determination (R^2) were obtained to visualize the tendency of cream structure over cycles.

The higher the absolute value of α, the greater the tendency of cream strucure change over the temperature cycles. Values closer to 0 indicate that the cream suffers smaller change over the temperature cycles. The R^2 was used to filter out regressions

that did not have a good coefficient of determination. In this case, all regressions with a $R^2 < 0.75$ were removed.

Figure 34 – SCHEMATIC REPRESENTATION OF THE LINEAR REGRESSION MODEL APPLIED TO EACH OF THE GROUPED POINTS IN TEMPERATURE SWINGS

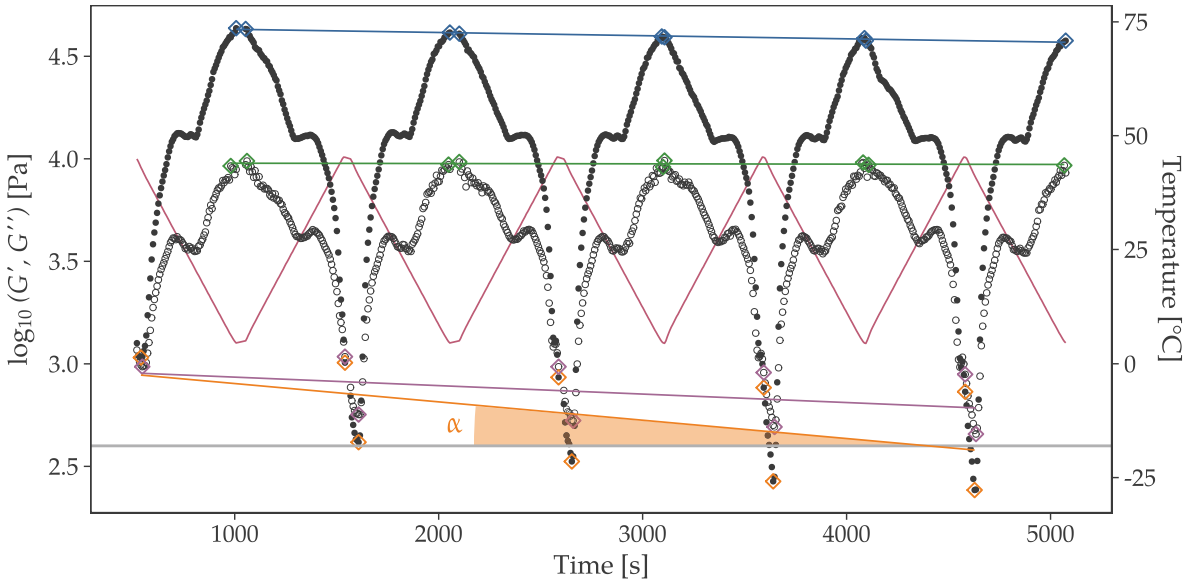

LEGEND: The coloured lines represent the linear regression model applied in G'_{max}, G''_{max}, G'_{min}, and G''_{min} on consecutive temperature ramps. In this diagram α represents angular coefficient of the G'_{min} regression line.

SOURCE: the author, (2020).

The analysis performed by the two methods are represented on the Figures 35 and 36. On the Figure 35 a kernel density plot was created to summarize the values of the ratio between the i^{th} of the analysis and the first cycle (Ξ). The data had a wide distribution with many outliers especially for the formula ${}^{.60}\mathbf{F}_a$, so the x-axis was plotted on a $\log_{10}$ scale. It is possible to observe that formulas with higher oil content (${}^{.50}\mathbf{D}$, ${}^{.55}\mathbf{E}$, ${}^{.60}\mathbf{F}$ and ${}^{.65}\mathbf{G}$) have a wider distribution of Ξ than those with lower oil content (${}^{.20}\mathbf{A}$, ${}^{.30}\mathbf{B}$ and ${}^{.40}\mathbf{C}$), this is noticeable in both, 1 day and 56 days of storage. These formulas with higher oil content were observed to be less stable by macroscopic methods in comparison to the ones with lower oil content and for the formulas that were characterized as less stable, a wider distribution of Ξ that can be viewed as formulas that undergo greater structural changes.

Figure 35 – DISTRIBUTION OF Ξ VALUES FOR DISTINCT FORMULAS

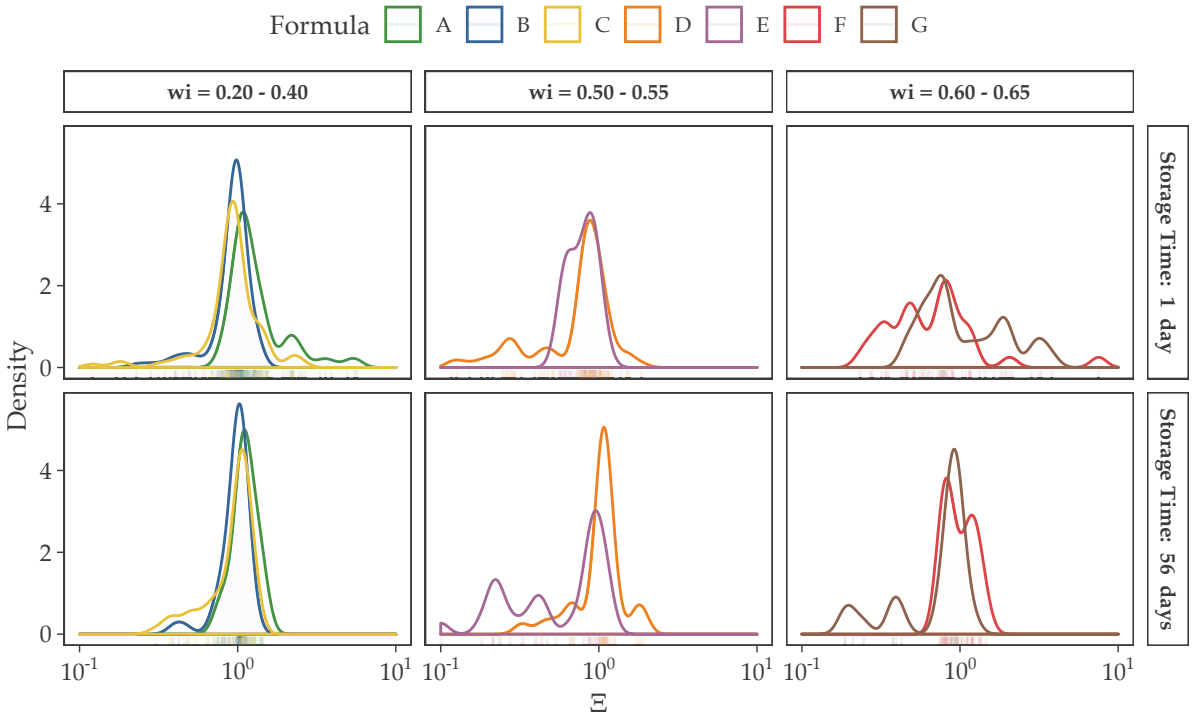

SOURCE: the author, (2020).

In the Figure 36 on the y-axis are plotted the $\log_{10}$-transformed values of α, which means that wider distributions have a higher range of angular coefficients whether they are positive or negative, meaning higher structural change over the temperature cycles. With this second visualization method, it is possible to observe that formulas with higher oil content generally have wider distributions when compared to thos with less oil content. In the subfigure 36B, there is missing data for the formula $^{.55}\mathbf{E}$ and $^{.60}\mathbf{F}$, which means that the regression line for the viscous modulus in these formulas in this condition is lower than 0.75, which by itself is an indication that the formula behaves unpredictably when going through the temperature cycles. The same is observable in subfigures 36D and 36A, the missing data indicates that the linear regression was not a good fit to the data. Although these values have not been found to be significantly different between samples, from Fig. 36 it is observed that the distribution of α tends to be narrower for $^{.20}\mathbf{A}$ and $^{.30}\mathbf{B}$ when in comparison with other formulas, with $^{.20}\mathbf{A}$ having α values slightly above 0.

Figure 36 – DISTRIBUTION OF α VALUES FOR DISTINCT FORMULAS OVER THE ANALYSIS DURATION

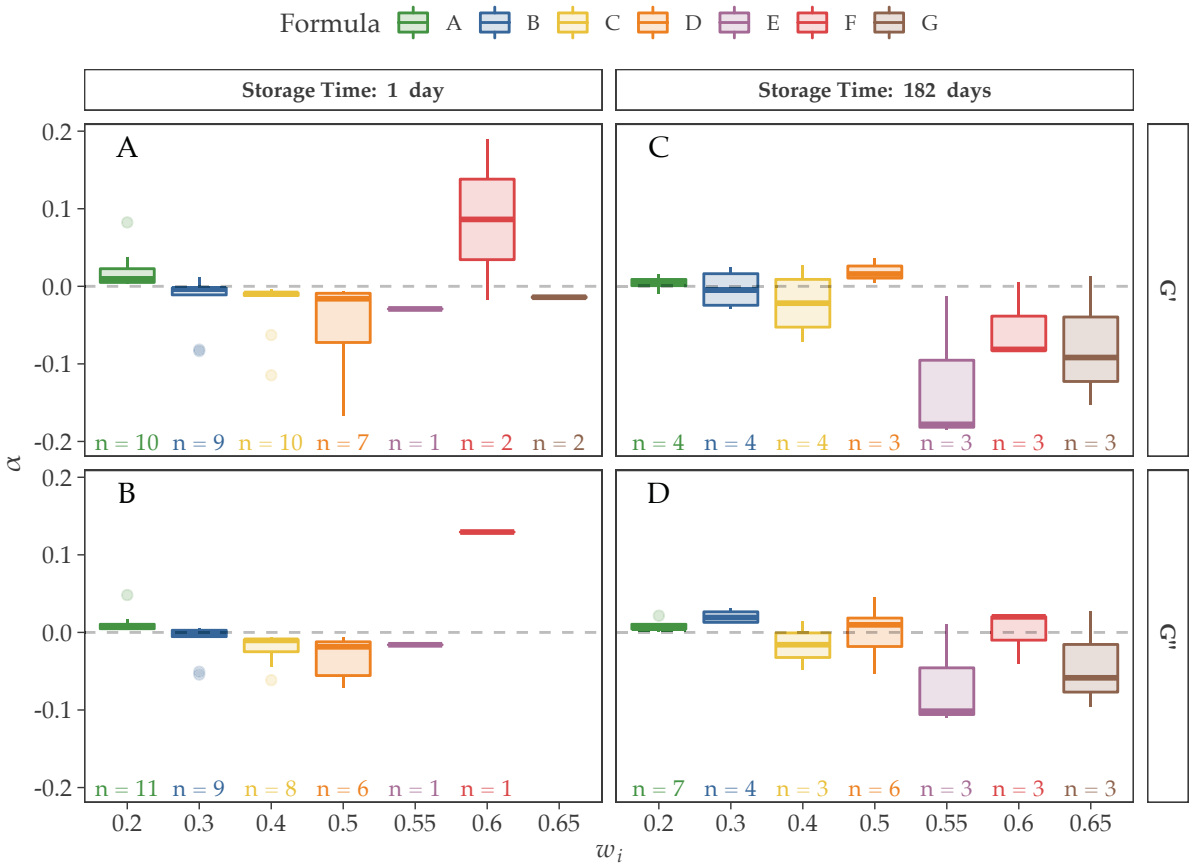

SOURCE: the author, (2020).

This can indicate that this sample is undergoing dehydratation over the temperature cycles. The subfigure 36A represents the evolution of the elastic modulus over the temperature cycles in the first 24h of storage time. A downward trend is observed as a function of oily mass fraction with the exception of formula $^{.60}\mathbf{F}$. The same is observed for viscous modulus in subfigure 36B. This can indicate that the creams are loosing its structural properties over the period of the experiment.

In the following storage times, this behaviour is no longer observed but the width of the distribution starts to increase in time for all the formulas excepts $^{.20}\mathbf{A}$. The median of the distribution no longer follows a trend as function of w_i but becomes more erratic and more distant from 0, which indicates that the angular coefficient is becoming larger.

The α parameter is an attempt to visualize the differences between formulas in a summarized way with the intent to translate the curve profile observed in temperature swing experiment to easier to assess the data. However, little information could be extracted from this method since it depends on a linear regression model that may not describe the trend of storage and viscous moduli maximum and minimum over the duration of the experiment. There is a small indication that this method is able to classify

samples as physically stable or unstable. A better way may be to analyse the G' and G'' curve profiles individually as a function of experiment duration (Fig. 33) or as function of temperature (Fig. 32).

5 FINAL CONSIDERATIONS

This work was a result of the necessity the cosmetics industry face to develop new methods to increase efficiency and efficacy in the production and development sectors. Predictive tests have been a tool to reduce resource waste, especially development time. The traditional, widely used conventional methods have been lacking on helping the industry to predict the stability of new products and so new methods have been seeked. The experimental data obtained showed that:

- as expected, extremelly stable creams were produced even with a high oily phase content;
- destabilization occured likely due to homogenization inefficiency when mixing the formula components and not because of coalescence as observed by microscopy and laser diffraction;
- the cream odour and color did not change for all samples over the period of 182 days and appearance changed due to a dehydratation of the top layers of the cream in the container;
- no correlation was found between stability and yield point and cohesive energy and it was not possible to verify that these rheological parameters changed over time;
- the frequency sweeps experiments were succesful in detecting maturation time and the network strength of formulations, indicating that creams with higher oil content have stronger structures;
- temperature swing analysis demonstrated that creams with higher oil content suffer higher structural changes when compared to those with less oil in its composition which can be seen as an indicator of instability.

BIBLIOGRAPHY

ABEN, Simon et al. Rheological investigations on the creaming of depletion-flocculated emulsions. **Langmuir**, v. 28, n. 21, p. 7967–7975, 2012.

ABIHPEC. **Panorama do Setor de Higiene Pessoal, Perfumaria e Cosméticos**. [S.l.: s.n.], 2015. P. 1–22. Available from: https://abihpec.org.br/publicacao/panorama-do-setor-2015/.

_____._____. [S.l.], 2018. P. 1–22. Available from: https://abihpec.org.br/publicacao/panorama-do-setor-2018/.

AFIFAH, Sharifah Nurfadhlin et al. Development of a kojic monooleate-enriched oil-in-water nanoemulsion as a potential carrier for hyperpigmentation treatment. **International Journal of Nanomedicine**, v. 13, p. 6465–6479, 2018.

ALBUQUERQUE, Priscilla B.S. et al. Investigating a galactomannan gel obtained from Cassia grandis seeds as immobilizing matrix for Cramoll lectin. **International Journal of Biological Macromolecules**, Elsevier B.V., v. 86, p. 454–461, 2016. Available from: http://dx.doi.org/10.1016/j.ijbiomac.2016.01.107.

ALEMÁN, J. et al. Definitions of terms relating to the structure and processing of sols, gels, networks, and inorganic-organic hybrid materials. **Pure and Applied Chemistry**, v. 79, n. 10, p. 1801–1829, 2007.

ALMDAL, K. et al. Towards a phenomenological definition of the term 'gel'. **Polymer Gels and Networks**, v. 1, n. 1, p. 5–17, 1993. Available from: https://www.sciencedirect.com/science/article/pii/096678229390020I.

ANDRADE, F. F. et al. Influence of PEG-12 Dimethicone addition on stability and formation of emulsions containing liquid crystal. **International Journal of Cosmetic Science**, v. 29, n. 3, p. 211–218, 2007.

ANVARI, Mohammad; JOYNER (MELITO), Helen S. Effect of fish gelatin-gum arabic interactions on structural and functional properties of concentrated emulsions. **Food Research International**, Elsevier, v. 102, September, p. 1–7, Dec. 2017. Available from: https://linkinghub.elsevier.com/retrieve/pii/S0963996917306737.

ANVISA. **Conceitos e Definições - Anvisa**. [S.l.: s.n.], 2018. Available from: http://portal.anvisa.gov.br/cosmeticos/conceitos-e-definicoes. Visited on: 8 Oct. 2019.

_____. **Guia de Controle de Qualidade De Produtos Cosméticos**. Ed. by AGÊNCIA NACIONAL DE VIGILÂNCIA SANITÁRIA. 2. ed. Brasília: [s.n.], 2007. P. 130.

ANVISA. **Guia de Estabilidade de Produtos Cosméticos**. Ed. by AGÊNCIA NACIONAL DE VIGILÂNCIA SANITÁRIA. 1. ed. Brasília: Editora Agência Nacional de Vigilância Sanitária, 2004. v. 1, p. 52.

_____. **RESOLUÇÃO - RDC Nº 45 DE 9 DE AGOSTO DE 2012**. [S.l.]: Ministério da Saúde, 2012.

ARAB, Danial; KANTZAS, Apostolos; BRYANT, Steven L. Nanoparticle stabilized oil in water emulsions: A critical review. **Journal of Petroleum Science and Engineering**, v. 163, January, p. 217–242, 2018. Available from: http://www.sciencedirect.com/science/article/pii/S0920410517310549.

BAIS, D. et al. Rheological characterization of polysaccharide-surfactant matrices for cosmetic O/W emulsions. **Journal of Colloid and Interface Science**, v. 290, n. 2, p. 546–556, 2005.

BALLMANN, C.; MÜELLER, B. W. Stabilizing effect of cetostearyl alcohol and glycerylmonstearate as co-emulsifiers on hydrocarbon-free O/W glyceride creams. **Pharmaceutical Development and Technology**, Kiel, v. 13, n. 5, p. 433–445, 2008.

BARNES, Howard A.; HUTTON, J. F; WALTERS, K F R S. **An Introduction to Rheology**. Ed. by K Walters. 1. ed. [S.l.]: Elsevier, 1989. v. 3, p. 199. Available from: http://linkinghub.elsevier.com/retrieve/pii/0377025789850153.

BARRY, B. W. Viscoelastic Properties of Concentrated Emulsions. **Advances in Colloid and Interface Science**, Portsmouth, v. 5, p. 37–75, 1975.

BERNZEN, Monika. **Determination of the Mechanical and Thermal Stability of Skin Cream with Oscillation and Freeze-Thaw Cycle Tests**. [S.l.: s.n.], 2008. P. 4–7. Available from: http://s21.co.kr/m/view.jsp?ncd=3026. Visited on: 10 Nov. 2019.

BŁEDZKA, Dorota; GROMADZIŃSKA, Jolanta; WASOWICZ, Wojciech. Parabens. From environmental studies to human health. **Environment International**, Elsevier Ltd, v. 67, p. 27–42, 2014.

BOHLIN, L. A theory of flow as a cooperative phenomenon. **Journal of Colloid And Interface Science**, v. 74, n. 2, p. 423–434, 1980.

BOM, S et al. A step forward on sustainability in the cosmetics industry: A review. **Journal of Cleaner Production**, Elsevier, v. 225, p. 270–290, June 2019. Available from: https://www.sciencedirect.com/science/article/pii/S0959652619309655.

BON, Stefan A.F. et al. Route to stable non-spherical emulsion droplets. **European Polymer Journal**, v. 43, n. 11, p. 4839–4842, 2007.

BOURNE, Malcolm C. **Food texture and viscosity : concept and measurement**. 2. ed. [S.l.]: Academic Press, 2002. P. 427.

BRAISCH, Brigitte et al. Preparation and flow behaviour of oil-in-water emulsions stabilised by hydrophilic silica particles. **Chemical Engineering and Technology**, v. 32, n. 7, p. 1107–1112, 2009.

BRASIL. **Formulário Nacional da Farmacopéia Brasileira**. 2. ed. Brasília: [s.n.], 2012. P. 224.

BROOKS, G; IDSON, B. Skin lipids. **International Journal of Cosmetic Science**, v. 13, n. 2, p. 103–113, Apr. 1991. Available from: http://doi.wiley.com/10.1111/j.1467-2494.1991.tb00553.x.

BRUMMER, R et al. Rheological Swing Test to Predict the Temperature Stability of Cosmetic Emulsions. In: PROCEEDINGS of the XXIst IFSCC International Congress. [S.l.: s.n.], 2000. P. 476–484.

BRUMMER, Rüdiger. **Rheology Essentials of Cosmetic and Food Emulsions**. 1. ed. Berlin/Heidelberg: Springer-Verlag, 2006. P. 180. (Springer Laboratory). Available from: http://link.springer.com/10.1007/3-540-29087-7.

BUCHOLD, Philipp et al. Structural behaviour of sodium hyaluronate in concentrated oppositely charged surfactant solutions. **Soft Matter**, Royal Society of Chemistry, v. 13, n. 11, p. 2253–2263, 2017.

CALIXTO, Livia Salomão; MAIA CAMPOS, Patricia M B G. Physical–Mechanical characterization of cosmetic formulations and correlation between instrumental measurements and sensorial properties. **International Journal of Cosmetic Science**, v. 39, n. 5, p. 527–534, 2017.

CALIXTO, Lívia Salomão; INFANTE, Victor Hugo Pacagnelli; MAIA CAMPOS, Patrícia M B G. Design and Characterization of Topical Formulations: Correlations Between Instrumental and Sensorial Measurements. **AAPS PharmSciTech**, AAPS PharmSciTech, v. 19, n. 4, p. 1512–1519, 2018.

CARLOTTI, M. E. et al. Photostability and stability over time of retinyl palmitate in an O/W emulsion and in SLN introduced in the emulsion. **Journal of Dispersion Science and Technology**, v. 26, n. 2, p. 125–138, 2005.

CASAGRANDE, Rúbia et al. Protective effect of topical formulations containing quercetin against UVB-induced oxidative stress in hairless mice. **Journal of Photochemistry and Photobiology B: Biology**, v. 84, n. 1, p. 21–27, 2006.

CEKIC, Nebojsa D.; SAVIC, Snezana D. Sanela M.; SAVIC, Snezana D. Sanela M. Dynamic-mechanical thermoanalysis test: a rapid alternative for accelerated freeze-thaw stability evaluation of W/O emulsions. **Drug Development and Industrial Pharmacy**, Taylor & Francis, v. 0, n. 0, p. 1–11, 2019. Available from: https://doi.org/10.1080/03639045.2019.1672718.

CHABNI, Malika et al. Physicochemical properties of concentrated triglyceride-in-water emulsions stabilized with decaglycerol monolaurate and sucrose. **Journal of Materials and Environmental Science**, v. 9, n. 3, p. 986–993, 2018.

CHUN, Jaehun; POLOSKI, Adam P.; HANSEN, Erich K. Stabilization and control of rheological properties of Fe2O3/Al(OH)3-rich colloidal slurries under high ionic strength and pH. **Journal of Colloid and Interface Science**, Elsevier Inc., v. 348, n. 1, p. 280–288, 2010. Available from: http://dx.doi.org/10.1016/j.jcis.2010.04.004.

CRODA. **POLAWAX ™ NF and POLAWAX A-31**. Edison, 2010. P. 3.

DAHER, Cláudia Cecilio et al. Development of O/W emulsions containing euterpe oleracea extract and evaluation of photoprotective efficacy. **Brazilian Journal of Pharmaceutical Sciences**, v. 50, n. 3, p. 639–652, 2014.

DARBRE, P. D. et al. Concentrations of Parabens in human breast tumours. **Journal of Applied Toxicology**, v. 24, n. 1, p. 5–13, Jan. 2004. Available from: http://doi.wiley.com/10.1002/jat.958.

DATTA, Sujit S et al. Rheology of attractive emulsions. **Physical Review E**, v. 84, n. 4, p. 041404, Oct. 2011. Available from: https://link.aps.org/doi/10.1103/PhysRevE.84.041404.

DE FREITAS, Rilton A. et al. Stabilization of Water-in-Water Emulsions by Polysaccharide-Coated Protein Particles. **Langmuir**, American Chemical Society, v. 32, n. 5, p. 1227–1232, Feb. 2016. Available from: https://pubs.acs.org/doi/10.1021/acs.langmuir.5b03761.

DERAKHSHANDEH, Maziar et al. Analysis of network formation and long-term stability in silica nanoparticle stabilized emulsions. **Soft Matter**, v. 14, n. 21, p. 4268–4277, 2018.

DERJAGUIN, B.; LANDAU, L. Theory of the stability of strongly charged lyophobic sols and of the adhesion of strongly charged particles in solutions of electrolytes. **Progress in Surface Science**, v. 43, n. 1-4, p. 30–59, May 1993. Available from: https://linkinghub.elsevier.com/retrieve/pii/007968169390013L.

DERKACH, Svetlana R. Rheology of emulsions. **Advances in Colloid and Interface Science**, Elsevier B.V., v. 151, n. 1-2, p. 1–23, Oct. 2009. Available from: https://linkinghub.elsevier.com/retrieve/pii/S0001868609000517.

DICKINSON, Eric. Food emulsions and foams: Stabilization by particles. **Current Opinion in Colloid and Interface Science**, Elsevier B.V., v. 15, n. 1-2, p. 40–49, 2010. Available from: http://dx.doi.org/10.1016/j.cocis.2009.11.001.

DIFTIS, N. G.; BILIADERIS, C. G.; KIOSSEOGLOU, V. D. Rheological properties and stability of model salad dressing emulsions prepared with a dry-heated soybean protein isolate-dextran mixture. **Food Hydrocolloids**, v. 19, n. 6, p. 1025–1031, 2005.

DINKGREVE, Maureen et al. On different ways of measuring “the” yield stress. **Journal of Non-Newtonian Fluid Mechanics**, Elsevier B.V., v. 238, p. 233–241, 2016. Available from: http://dx.doi.org/10.1016/j.jnnfm.2016.11.001.

ECCLESTON, G. M. Functions of mixed emulsifiers and emulsifying waxes in dermatological lotions and creams. **Colloids and Surfaces A: Physicochemical and Engineering Aspects**, Elsevier Sci B.V., v. 123-124, p. 169–182, May 1997.

ESQUENA, Jordi. Water-in-water (W/W) emulsions. **Current Opinion in Colloid & Interface Science**, Elsevier, Bacelona, v. 25, n. 6, p. 109–119, Oct. 2016. Available from: http://www.sciencedirect.com/science/article/pii/S135902941630142X.

ESTANQUEIRO, M; AMARAL, M H; SOUSA LOBO, J. M. Comparison between sensory and instrumental characterization of topical formulations: impact of thickening agents. **International Journal of Cosmetic Science**, Porto, v. 38, n. 4, p. 389–398, Aug. 2016. Available from: http://doi.wiley.com/10.1111/ics.12302.

EUROPEAN COMMISSION. **Regulation (EC) No 1223/2009 of the European Parliament and of the Council of 30 November 2009 on cosmetic products**. [S.l.: s.n.], 2009. P. 59–209.

FANUN, Monzer. Microemulsions as delivery systems. **Current Opinion in Colloid and Interface Science**, Elsevier Ltd, v. 17, n. 5, p. 306–313, 2012. Available from: http://dx.doi.org/10.1016/j.cocis.2012.06.001.

FARN, Richard. J. **Chemistry and Technology of Surfactants**. 1. ed. Oxford, Reino Unido: Blackwell Publishing Ltd, 2006. P. 315. Available from: http://doi.wiley.com/10.1002/9780470988596.

FERNANDEZ-NIEVES, Alberto et al. **Fluids, Colloids and Soft Materials: An Introduction to Soft Matter Physics**. Ed. by Alberto Fernandez-Nieves and Antonio Manuel Puertas. 1. ed. New Jersey: Wiley, 2016. P. 408.

FILIPOVIC, M et al. Towards satisfying performance of an O/W cosmetic emulsion: screening of reformulation factors on textural and rheological properties using general experimental design. **International Journal of Cosmetic Science**, v. 39, n. 5, p. 486–499, 2017.

FLICK, Ernest W. **Cosmetic and Toiletry Formulations**. Ed. by Ernest. W Flick. 2. ed. Nova Jérsei: Elsevier, 1989. v. 2, p. 51. Available from: http://www.sciencedirect.com/science/article/pii/B9780815512189500072.

FRYD, Michael M.; MASON, Thomas G. Advanced Nanoemulsions. **Annual Review of Physical Chemistry**, v. 63, n. 1, p. 493–518, 2012.

FUKUSHIMA, S.; TAKAHASHI, M.; YAMAGUCHI, M. Effect of cetostearyl alcohol on stabilization of oil-in-water emulsion. I. Difference in the effect by mixing cetyl alcohol with stearyl alcohol. **Journal of Colloid And Interface Science**, v. 57, n. 2, p. 201–206, 1976.

GABRIELE, Domenico; DE CINDIO, Bruno; D'ANTONA, Paolo. A weak gel model for foods. **Rheologica Acta**, Falerna, v. 40, n. 2, p. 120–127, 2001.

GALLEGOS, C.; FRANCO, J. M. Rheology of food, cosmetics and pharmaceuticals. **Current Opinion in Colloid and Interface Science**, v. 4, n. 4, p. 288–293, 1999.

GARRETT, Edward R. Prediction of stability in pharmaceutical preparations VIII. Oil-in-water emulsion stability and the analytical ultracentrifuge. **Journal of Pharmaceutical Sciences**, Chemical Publishing New York, New York, v. 51, n. 1, p. 35–42, 1962.

GILBERT, Laura; PICARD, Céline, et al. Rheological and textural characterization of cosmetic emulsions containing natural and synthetic polymers: Relationships between both data. **Colloids and Surfaces A: Physicochemical and Engineering Aspects**, Elsevier B.V., v. 421, p. 150–163, 2013. Available from: http://www.sciencedirect.com/science/article/pii/S0927775713000137.

GILBERT, Laura; SAVARY, Géraldine, et al. Predicting sensory texture properties of cosmetic emulsions by physical measurements. **Chemometrics and Intelligent Laboratory Systems**, Elsevier B.V., v. 124, p. 21–31, May 2013. Available from: http://www.sciencedirect.com/science/article/pii/S016974391300035X.

GOLEMANOV, Konstantin et al. Remarkably high surface visco-elasticity of adsorption layers of triterpenoid saponins. **Soft Matter**, Vlaardingen, v. 9, n. 24, p. 5738–5752, 2013.

GUARATINI, Thais; GIANETI, Mirela D.; CAMPOS, Patrícia M B G M. Stability of cosmetic formulations containing esters of Vitamins E and A: Chemical and physical aspects. **International Journal of Pharmaceutics**, v. 327, n. 1-2, p. 12–16, 2006.

GUPTA, A; SBRAGAGLIA, M; SCAGLIARINI, A. Hybrid Lattice Boltzmann/Finite Difference simulations of viscoelastic multicomponent flows in confined geometries. **Journal of Computational Physics**, v. 291, p. 177–197, May 2015. Available from: https://www.sciencedirect.com/science/article/pii/S0021979713006012.

HAJ-SHAFIEI, Samira; GHOSH, Supratim; ROUSSEAU, Dérick. Kinetic stability and rheology of wax-stabilized water-in-oil emulsions at different water cuts. **Journal of Colloid and Interface Science**, Elsevier Inc., v. 410, p. 11–20, 2013. Available from: http://dx.doi.org/10.1016/j.jcis.2013.06.047.

HAZT, Bianca et al. Effect of pH and protein particle shape on the stability of amylopectin–xyloglucan water-in-water emulsions. **Food Hydrocolloids**, Elsevier, Curitiba, p. 105769, Feb. 2020. Available from: https://linkinghub.elsevier.com/retrieve/pii/S0268005X19323525.

HONG, In Kwon; KIM, Su In; LEE, Seung Bum. Effects of HLB value on oil-in-water emulsions: Droplet size, rheological behavior, zeta-potential, and creaming index. **Journal of Industrial and Engineering Chemistry**, The Korean Society of Industrial and Engineering Chemistry, v. 67, p. 123–131, 2018. Available from: https://www.sciencedirect.com/science/article/pii/S1226086X18303137.

HU, Yin-ting Ting et al. Techniques and methods to study functional characteristics of emulsion systems. **Journal of Food and Drug Analysis**, Elsevier Ltd, v. 25, n. 1, p. 16–26, 2017. Available from: http://dx.doi.org/10.1016/j.jfda.2016.10.021.

HUANG, John. S; KIM, M. W. Critical behavior of a microemulsion. **Physical Review Letters**, New Jersey, v. 47, n. 20, p. 1462–1465, 1981. Available from: https://journals.aps.org/prl/pdf/10.1103/PhysRevLett.47.1462.

IDSON, B. Stability testing of emulsions. **Drug and Cosmetic Industry**, v. 152, p. 38–38, 1993.

ISAAC, Vera Lucia Borges et al. Protocolo para ensaios físico-quimicos de estabilidade de fitocosméticos. **Revista de Ciências Farmacêuticas Básica e Aplicada**, v. 29, n. 1, p. 81–96, 2008.

JAGER-LÉZER, Nathalie et al. Rheological analysis of highly concentrated w/o emulsions. **Rheologica Acta**, v. 37, n. 2, p. 129–138, 1998.

JUNGINGER, H. The Ratio of Interlamellarly Fixed Water to Bulk Water Used as Quality Criterion in O/W Creams. **Berichte der Bunsengesellschaft für physikalische Chemie**, Wiley-Blackwell, Leiden, v. 88, n. 11, p. 1070–1074, Nov. 1984. Available from: http://doi.wiley.com/10.1002/bbpc.198400010.

KABALNOV, Alexey S.; SHCHUKIN, Eugene D. Ostwald ripening theory: applications to fluorocarbon emulsion stability. **Advances in Colloid and Interface Science**, Moscow, v. 38, n. 100, p. 69–97, 1992.

KANTAR IBOPE MEDIA. **Setores Econômicos – 2015**. [S.l.: s.n.], 2016. Available from: https://www.kantaribopemedia.com/setores-economicos-2015/. Visited on: 8 Aug. 2019.

_____. **Setores Econômicos – Janeiro a Dezembro 2016**. [S.l.: s.n.], 2017. P. 7–10. Available from: https://www.kantaribopemedia.com/setores-economicos-janeiro-a-dezembro-2016/. Visited on: 8 Aug. 2019.

KARASU, Salih et al. Thermal loop test to determine structural changes and thermal stability of creamed honey: Rheological characterization. **Journal of Food Engineering**, Elsevier Ltd, v. 150, p. 90–98, 2015. Available from: http://dx.doi.org/10.1016/j.jfoodeng.2014.10.004.

KARL, Wunsch et al. Effect of surfactant on structure thermal behavior of cetyl stearyl alcohols: DSC and X-ray scattering studies. **Journal of Thermal Analysis and Calorimetry**, v. 123, n. 2, p. 1411–1417, 2016.

KIM, Ha Seong; MASON, Thomas G. Advances and challenges in the rheology of concentrated emulsions and nanoemulsions. **Advances in Colloid and Interface Science**, Elsevier, Los Angeles, v. 247, p. 397–412, 2017. Available from: https://www.sciencedirect.com/science/article/pii/S0001868617301884.

KOWALSKA, M.; ZBIKOWSKA, A. Application of a Laser Diffraction Method for Determination of Stability of Dispersion Systems in Food and Chemical Industry. **Journal of Dispersion Science and Technology**, v. 34, n. 10, p. 1447–1453, 2013.

KRALCHEVSKY, Peter A.; DANOV, Krassimir D.; DENKOV, Nikolai D. Chemical Physics of colloids and interfases. In: HANDBOOK of Surface and Colloid Chemistry. [S.l.: s.n.], 2009. chap. 7, p. 137–344.

KREBS, T.; SCHROËN, C. G.P.H.; BOOM, R. M. Separation kinetics of an oil-in-water emulsion under enhanced gravity. **Chemical Engineering Science**, v. 71, p. 118–125, Mar. 2012.

LACA, Amanda; PAREDES, Benjamín; DÍAZ, Mario. Lipid-enriched egg yolk fraction as ingredient in cosmetic emulsions. **Journal of Texture Studies**, v. 43, n. 1, p. 12–28, 2012.

LANGENFELD, Anne; SCHMITT, Véronique; STÉBÉ, Marie José. Rheological behavior of fluorinated highly concentrated reverse emulsions with temperature. **Journal of Colloid and Interface Science**, v. 218, n. 2, p. 522–528, Oct. 1999. Available from: https://linkinghub.elsevier.com/retrieve/pii/S0021979799964275.

LARSON, Ronald G. **The Structure and rheology of complex Fluids**. 1. ed. [S.l.]: Oxford University Press, 1998. P. 688.

LEHMANN, Søren Vig et al. Characterization and chemistry of imidazolidinyl urea and diazolidinyl urea. **Contact Dermatitis**, v. 54, n. 1, p. 50–58, Jan. 2006. Available from: http://doi.wiley.com/10.1111/j.0105-1873.2006.00735.x.

LERCHE, D.; SOBISCH, T. Direct and accelerated characterization of formulation stability. **Journal of Dispersion Science and Technology**, v. 32, n. 12, p. 1799–1811, 2011.

LI, Fangfang; ZHANG, Wanping. Stability and rheology of W/Si/W multiple emulsions with polydimethylsiloxane. **Colloids and Surfaces A: Physicochemical and Engineering Aspects**, Elsevier B.V., v. 470, p. 290–296, 2015. Available from: https://www.sciencedirect.com/science/article/pii/S092777571500120X.

LIEBERMAN, Norman P.; LIEBERMAN, Elizabeth T. **A Working Guide to Process Equipment**. Ed. by Norman Lieberman and Elizabeth Lieberman. 4. ed. [S.l.]: McGraw Hill Education, 2014. P. 624.

LU, Xiaocun et al. A Robust Oil-in-Oil Emulsion for the Nonaqueous Encapsulation of Hydrophilic Payloads. **Journal of the American Chemical Society**, v. 140, n. 10, p. 3619–3625, 2018. Available from: http://pubs.acs.org/doi/10.1021/jacs.7b11847.

LUKIC, M.; JAKSIC, I., et al. A combined approach in characterization of an effective w/o hand cream: The influence of emollient on textural, sensorial and in vivo skin performance. **International Journal of Cosmetic Science**, v. 34, n. 2, p. 140–149, 2012.

LUKIC, Milica; PANTELIC, Ivana; SAVIC, Snezana. Emulsion systems: From stability concerns to sensory properties. In: ALKYL Polyglucosides: From Natural-Origin Surfactants to Prospective Delivery Systems. [S.l.]: Elsevier Inc., May 2014. P. 73–105.

MACIEL, Naira Rezende et al. A New System of Multiple Emulsions with Lamellar Gel Phases from Vegetable Oil. **Journal of Dispersion Science and Technology**, Taylor & Francis, v. 37, n. 5, p. 646–655, May 2016. Available from: http://dx.doi.org/10.1080/01932691.2015.1054506.

MARKOVITZ, Hershel. **Theory of viscoelasticity. An introduction**. 2. ed. EUA: Academic Press, 2008. v. 98, p. 292.

MASMOUDI, Houda et al. A Rheological Method to Evaluate the Physical Stability of Highly Viscous Pharmaceutical Oil-in-Water Emulsions. **Pharmaceutical Research**, v. 23, n. 8, p. 1937–1947, Aug. 2006. Available from: http://link.springer.com/10.1007/s11095-006-9038-x.

MASON, T. G. New fundamental concepts in emulsion rheology. **Current Opinion in Colloid & Interface Science**, Annandale, v. 4, n. 3, p. 231–238, May 1999. Available from: https://www.sciencedirect.com/science/article/pii/S1359029499000357?via%7B%5C%%7D3Dihub.

MCCLEMENTS, David Julian. Critical review of techniques and methodologies for characterization of emulsion stability. **Critical Reviews in Food Science and Nutrition**, David Julian Mcclements, v. 47, n. 7, p. 611–649, 2007. Available from: https://www.tandfonline.com/action/journalInformation?journalCode=bfsn20.

MCCLEMENTS, David Julian; GUMUS, Cansu Ekin. Natural emulsifiers — Biosurfactants, phospholipids, biopolymers, and colloidal particles: Molecular and physicochemical basis of functional performance. **Advances in Colloid and Interface Science**, Elsevier B.V., v. 234, p. 3–26, Aug. 2016. Available from: http://dx.doi.org/10.1016/j.cis.2016.03.002.

MCCLEMENTS, David Julian; JAFARI, Seid Mahdi. Improving emulsion formation, stability and performance using mixed emulsifiers: A review. **Advances in Colloid and Interface Science**, v. 251, p. 55–79, Jan. 2018. Available from: http://www.sciencedirect.com/science/article/pii/S0001868617303196.

MEDINA-TORRES, Luis et al. Rheology of Sodium Polyacrylate as an Emulsifier Employed in Cosmetic Emulsions. **Industrial & Engineering Chemistry Research**, American Chemical Society, v. 53, n. 47, p. 18346–18351, Nov. 2014. Available from: https://pubs.acs.org/doi/pdf/10.1021/ie503406a.

MERKUS, Henk. G. **Particle Size Measurements**. Ed. by Henk. G Merkus. 1. ed. Dordrecht: Springer, 2009. P. 533. (Particle Technology Series). Available from: http://link.springer.com/10.1007/978-1-4020-9016-5.

MEZGER, Thomas G. **The Rheology Handbook**. Ed. by Thomas G Mezger. 4. ed. Hanover: Vincentz Network, 2014. P. 432.

MIKKONEN, K. S. et al. Determination of physical emulsion stabilization mechanisms of wood hemicelluloses via rheological and interfacial characterization. **Soft Matter**, v. 12, n. 42, p. 8690–8700, May 2016. Available from: http://pubs.rsc.org/en/content/articlelanding/2016/sm/c6sm01557c.

MIRSHEKARI, Fahimeh; PAKZAD, Leila; FATEHI, Pedram. An investigation on the stability of the hazelnut oil-water emulsion. **Journal of Dispersion Science and Technology**, Taylor & Francis, v. 0, n. 0, p. 1–12, May 2019. Available from: https://www.tandfonline.com/doi/full/10.1080/01932691.2019.1614459.

MITSUI, Takeo. **New Cosmetc Science**. Ed. by Takeo Mitsui. 1. ed. [S.l.]: Elsevier, 1997. P. 499.

MORAVKOVA, Tereza; FILIP, Petr. The influence of thickeners on the rheological and sensory properties of cosmetic lotions. **Acta Polytechnica Hungarica**, v. 11, n. 6, p. 173–186, 2014.

MOSCHINI DAUDT, Renata et al. Rheological and physical parameters correlations in formulations with pinhão derivatives stability study: building up an analytical route. **Pharmaceutical Development and Technology**, Taylor & Francis, v. 23, n. 6, p. 620–627, June 2018. Available from: https://doi.org/10.1080/10837450.2017.1334217.

MOULAI MOSTEFA, N. et al. Determination of optimal cream formulation from long-term stability investigation using a surface response modelling. **International Journal of Cosmetic Science**, v. 28, n. 3, p. 211–218, 2006.

MYERS, Drew. **Surfactant Science and Technology**. Ed. by Drew Myers. 3. ed. Hoboken: John Wiley & Sons, Inc., Sept. 2005. v. 13, p. 297. Available from: https://linkinghub.elsevier.com/retrieve/pii/0021979789901070.

NIRAULA, Boris et al. Rheology properties of glucopyranoside stabilized oil-water emulsions: Effect of alkyl chain length and bulk concentration of the surfactant. **Colloids and Surfaces A: Physicochemical and Engineering Aspects**, v. 251, n. 1-3, p. 117–132, 2004.

OISHI, Shinshi. Effects of butylparaben on the male reproductive system in rats. **Toxicology and Industrial Health**, v. 17, n. 1, p. 31–39, Feb. 2001. Available from: http://journals.sagepub.com/doi/10.1191/0748233701th093oa.

ONDRACEK, J et al. Comparison among five methods for testing the physical stability of O/W emulsions. **Acta Pharmaceutica Technologica**, v. 31, p. 42–48, 1985.

OZTURK, Bengu et al. Formation and stabilization of nanoemulsion-based vitamin E delivery systems using natural biopolymers: Whey protein isolate and gum arabic. **Food Chemistry**, Elsevier Ltd, v. 188, p. 256–263, May 2015.

PAL, Rajinder. A new linear viscoelastic model for emulsions and suspensions. **Polymer Engineering & Science**, v. 48, n. 7, p. 1250–1253, June 2008. Available from: http://doi.wiley.com/10.1002/pen.21065.

_____. Rheology of simple and multiple emulsions. **Current Opinion in Colloid & Interface Science**, Elsevier Ltd, Waterloo, v. 16, n. 1, p. 41–60, 2011. Available from: http://www.sciencedirect.com/science/article/pii/S1359029410001135.

PALIERNE, J F. Linear rheology of viscoelastic emulsions with interfacial tension. **Rheologica Acta**, v. 29, n. 3, p. 204–214, 1990. Available from: http://link.springer.com/10.1007/BF01331356.

PAYE, Marc; MAIBACH, Howard I. **Handbook of Cosmetic Science and Technology Second Edition**. [S.l.: s.n.], 2013.

PY, C. et al. Investigation of multiple emulsion stability using rheological measurements. **Colloids and Surfaces A: Physicochemical and Engineering Aspects**, v. 91, n. 100, p. 215–225, 1994.

R CORE TEAM. **R: A Language and Environment for Statistical Computing**. Vienna: [s.n.], 2013. Available from: http://www.r-project.org/.

RAFANAN, Ruby; ROUSSEAU, Derick. Dispersed droplets as tunable fillers in water-in-oil emulsions stabilized with fat crystals. **Journal of Food Engineering**, v. 244, p. 192–201, 2019.

RHEIN, Linda D. et al. **Surfactants in personal care products and decorative cosmetics**. Ed. by Linda D. Rhein. 3. ed. [S.l.]: CRC Press Taylor & Francis Group, 2006. P. 481.

ROBINS, Margaret M; WATSON, Andrew D; WILDE, Peter J. Emulsions - creaming and rheology. **Current Opinion in Colloid and Interface Science**, Elsevier, v. 7, p. 419–425, Nov. 2002. Available from: https://www.sciencedirect.com/science/article/pii/S1359029402000894.

ROSEN, Milton J J. **Surfactants and interfacial phenomena**. 3. ed. Hoboken: John Wiley & Sons, Inc., 2004. P. 347. Available from: http://linkinghub.elsevier.com/retrieve/pii/0166662289800307.

RUEDEN, Curtis T et al. ImageJ2: ImageJ for the next generation of scientific image data. **BMC Bioinformatics**, BMC Bioinformatics, v. 18, n. 1, p. 529, 2017. Available from: https://bmcbioinformatics.biomedcentral.com/articles/10.1186/s12859-017-1934-z.

SAKAMOTO, Kazutami et al. **Cosmetic Science and Technology: Theoretical Principles and Applications**. Ed. by Kazutami Sakamoto. 1. ed. [S.l.]: John Fedor, 2017. P. 1–835.

SANFELD, Albert; STEINCHEN, Annie. Emulsions stability, from dilute to dense emulsions - Role of drops deformation. **Advances in Colloid and Interface Science**, v. 140, n. 1, p. 1–65, 2008. Available from: https://www.sciencedirect.com/science/article/pii/S0001868607001881.

SANTOS, J; CALERO, N; TRUJILLO-CAYADO, L A A, et al. Assessing differences between Ostwald ripening and coalescence by rheology, laser diffraction and multiple light scattering. **Colloids and Surfaces B: Biointerfaces**, Elsevier, v. 159, p. 405–411, Nov. 2017. Available from: https://www.sciencedirect.com/science/article/pii/S0927776517305301.

SANTOS, Jenifer; CALERO, Nuria; MUÑOZ, José. Optimization of a green emulsion stability by tuning homogenization rate. **RSC Advances**, v. 6, n. 62, p. 57563–57568, May 2016. Available from: http://pubs.rsc.org/en/content/articlelanding/2016/ra/c6ra10207g.

SARAMITO, Pierre. A new elastoviscoplastic model based on the Herschel-Bulkley viscoplastic model. **Journal of Non-Newtonian Fluid Mechanics**, v. 158, n. 1-3, p. 154–161, May 2009.

SAVIC, Snezana; TAMBURIC, Slobodanka, et al. Natural surfactant-based emulsion systems: The influence of common pharmaceutical excipients on colloidal structure and physical stability. **Journal of Dispersion Science and Technology**, v. 29, n. 9, p. 1276–1287, 2008.

SAVIC, Snezana; VULETA, Gordana, et al. Colloidal microstructure of binary systems and model creams stabilized with an alkylpolyglucoside non-ionic emulsifier. **Colloid and Polymer Science**, v. 283, n. 4, p. 439–451, 2005.

SAVIĆ, Snezana; TAMBURIĆ, Slobodanka; SAVIĆ, Miroslav M. From conventional towards new natural surfactants in drug delivery systems design: Current status and perspectives. **Expert Opinion on Drug Delivery**, v. 7, n. 3, p. 353–369, 2010.

SCHNEIDER, Lars Alexander et al. Influence of pH on wound-healing: A new perspective for wound-therapy? **Archives of Dermatological Research**, Maienweg, v. 298, n. 9, p. 413–420, 2007.

SCHRAMM, Gebhard. **A Practical Approach to Rheology and Rheometry**. Ed. by Gebhard Schramm. 2. ed. Karlsruhe: Thermo Haake Rheology, 1994. P. 291. Available from: http://www.polymer.cn/bbs/File/UserFiles/UpLoad/200904010309415s.pdf.

SCHRAMN, Laurier. L. **Emulsions, Foams, and Suspensions: Fundamentals and Applications**. 1. ed. Weinheim: Wiley-VCH Verlag GmbH & Co. KGaA, 2005. P. 448.

SHARU, B K et al. Development of microstructure and evolution of rheological characteristics of a highly concentrated emulsion during emulsification. **Colloids and Surfaces A: Physicochemical and Engineering Aspects**, v. 532, p. 342–350, 2017. Available from: http://www.sciencedirect.com/science/article/pii/S0927775717304107.

SJÖBLOM, Johann. **Emulsions and Emulsion Stability**. 2. ed. Boca Raton: CRC Press Taylor & Francis Group, 2006. P. 662.

STEFFE, James F. **Rheological Methods in Food Process Engineering**. 2. ed. East Lansing: Freeman Press, 1996. P. 428.

SUGIURA, Shinji et al. Effect of interfacial tension on the dynamic behavior of droplet formation during microchannel emulsification. **Journal of Colloid and Interface Science**, v. 269, n. 1, p. 178–185, 2004.

TA INSTRUMENTS. **Strategies for Better Rheology Data - Part Two - Exploring Testing Guidelines**. [S.l.: s.n.]. Available from: https://www.youtube.com/watch?v=nwePVkXqAd4. Visited on: 13 Nov. 2019.

TADROS, Tharwat F. Application of rheology for assessment and prediction of the long-term physical stability of emulsions. **Advances in Colloid and Interface Science**, Elsevier, Berkshire, v. 108-109, p. 227–258, May 2004.

_____. **Applied Surfactants: Principles and Applications**. Ed. by Tharwat F Tadros. 1. ed. Germany: Wiley-VCH, 2005. P. 646.

TADROS, Tharwat F. Emulsion Formation, Stability, and Rheology. In: _____. **Emulsion Formation and Stability**. Ed. by Tharwat F Tadros. 1. ed. Weinheim: Wiley-VCH Verlag GmbH & Co. KGaA, Jan. 2013. chap. 1, p. 1–75. Available from: http://doi.wiley.com/10.1002/9783527647941.ch1.

_____. Interparticle interactions in concentrated suspensions and their bulk (Rheological) properties. **Advances in Colloid and Interface Science**, Elsevier B.V., v. 168, n. 1-2, p. 263–277, 2011. Available from: http://dx.doi.org/10.1016/j.cis.2011.05.003.

_____. **Rheology of Dispersions: Principles and Applications**. Ed. by Tharwat F Tadros. Weinheim: Wiley-VCH Verlag GmbH & Co. KGaA, 2010. Available from: http://doi.wiley.com/10.1002/9783527631568.

TAL-FIGIEL, B. The formation of stable W/O, O/W, W/O/W cosmetic emulsions in an ultrasonic field. **Chemical Engineering Research and Design**, v. 85, 5 A, p. 730–734, 2007.

TAN, H. W.; MISRAN, M.; KHOO, S. K. Viscoelastic behavior of olive oil-in-water emulsion stabilized by sucrose fatty acid esters. **Applied Rheology**, Kuala Lumpur, v. 21, n. 5, p. 1–9, 2011.

TAYLOR, P. Ostwald ripening in emulsions. **Advances in Colloid and Interface Science**, Elsevier, v. 75, n. 2, p. 107–163, Apr. 1998. Available from: http://linkinghub.elsevier.com/retrieve/pii/S0001868698000359.

TERESCENCO, Daria et al. Influence of the emollient structure on the properties of cosmetic emulsion containing lamellar liquid crystals. **Colloids and Surfaces A: Physicochemical and Engineering Aspects**, Elsevier B.V., Cedex, v. 536, p. 10–19, Jan. 2018. Available from: http://www.sciencedirect.com/science/article/pii/S0927775717307720.

USP. **The United States Pharmacopeia : USP 29 : the National formulary : NF 24**. [S.l.]: Rockville, Md. : United States Pharmacopeial Convention, 2005. P. 3539.

VADER, David; WYSS, Hans. **Introduction to Rheology**. [S.l.], 2018. Available from: https://weitzlab.seas.harvard.edu/files/weitzlab/files/introductiontorheology2.pdf.

VAN DER GRAAF, S. et al. Influence of dynamic interfacial tension on droplet formation during membrane emulsification. **Journal of Colloid and Interface Science**, v. 277, n. 2, p. 456–463, 2004.

WAQAS, Muhammad K et al. Stability study of a cosmetic emulsion loaded with Tamarindus indica seeds extract. **Latin American Journal of Pharmacy**, v. 33, n. 5, p. 731–738, 2014.

WEBER, Sandra et al. Analytical Methods for the Determination of Mineral Oil Saturated Hydrocarbons (MOSH) and Mineral Oil Aromatic Hydrocarbons (MOAH)—A Short Review. **Analytical Chemistry Insights**, v. 13, p. 16, Jan. 2018. Available from: http://journals.sagepub.com/doi/10.1177/1177390118777757.

WICKHAM, Hadley et al. **Welcome to the Tidyverse**. v. 4. [S.l.: s.n.], Nov. 2019. P. 1686. Available from: https://joss.theoj.org/papers/10.21105/joss.01686.

WITTERN, K. P et al. Stability testing of cosmetic emulsions. **Cosmetics and Toiletries**, New York, v. 100, n. 10, p. 33–39, 1985.

XU, Renliang. **Particle Characterization: Light Scattering Methods**. Ed. by Brian Scarlett. 1. ed. Miami: Kluwer Academic Publishers, 2002. v. 13, p. 121. (Particle Technology Series). Available from: http://link.springer.com/10.1007/0-306-47124-8.

YEHYE, Wageeh A et al. **Understanding the chemistry behind the antioxidant activities of butylated hydroxytoluene (BHT): A review**. v. 101. [S.l.: s.n.], 2015. P. 295–312.

ZAPATA, Angela María Ormaza; RODRÍGEZ-BARONA, Sneyder; GÓMEZ, Gloria Inés Giraldo. Rheological characterization and stability study of an emulsion made with a dairy by-product enriched with omega-3 fatty acids. **Brazilian Journal of Food Technology**, v. 18, n. 1, p. 23–30, Feb. 2015. Available from: http://dx.doi.org/10.1590/1981-6723.2014.

Appendix

APPENDIX A – AMPLITUDE SWEEPS IN SELECTED STORAGE TIMES

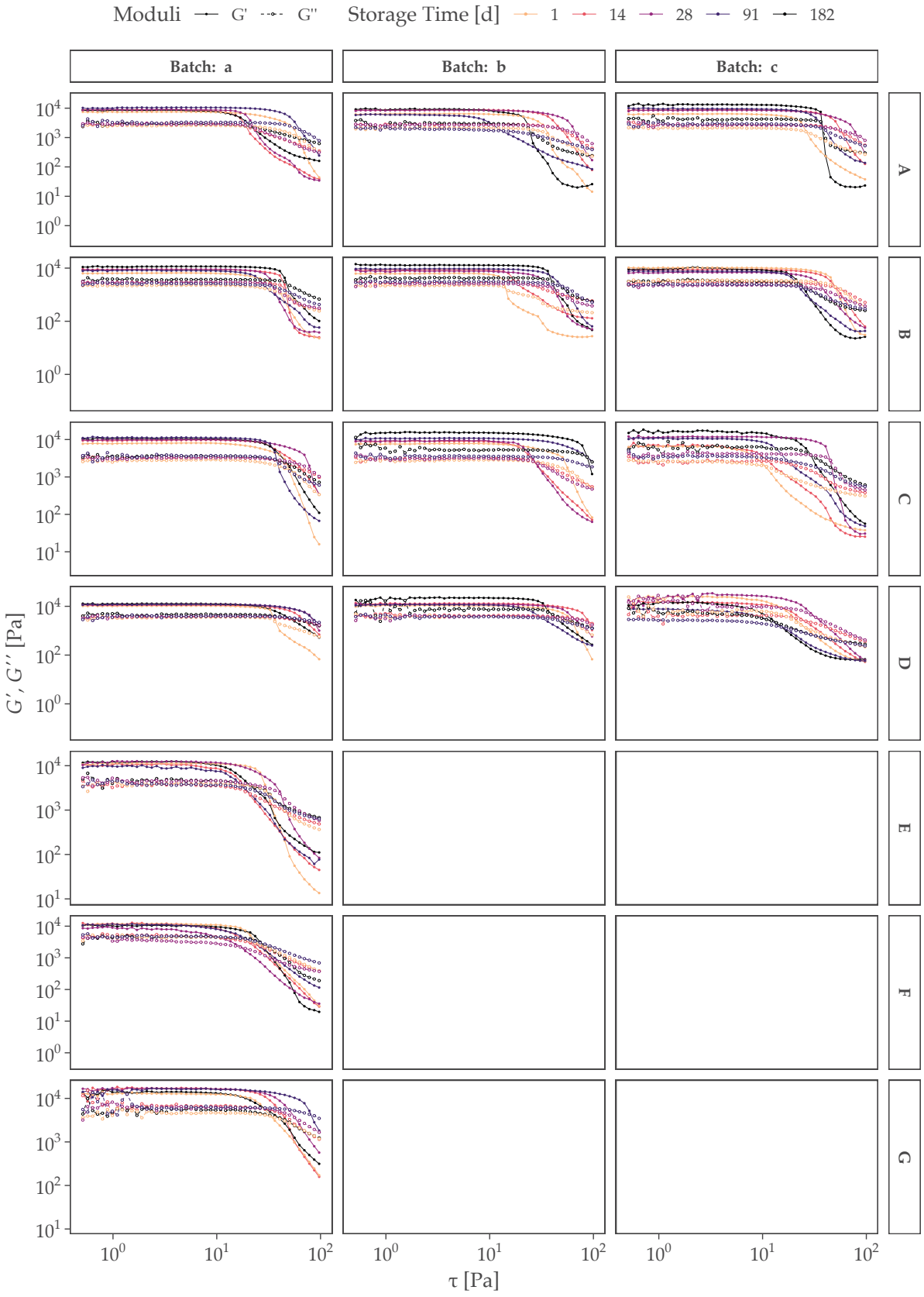

SOURCE: the author, (2020).

APPENDIX B – FREQUENCY SWEEPS IN SELECTED STORAGE TIMES

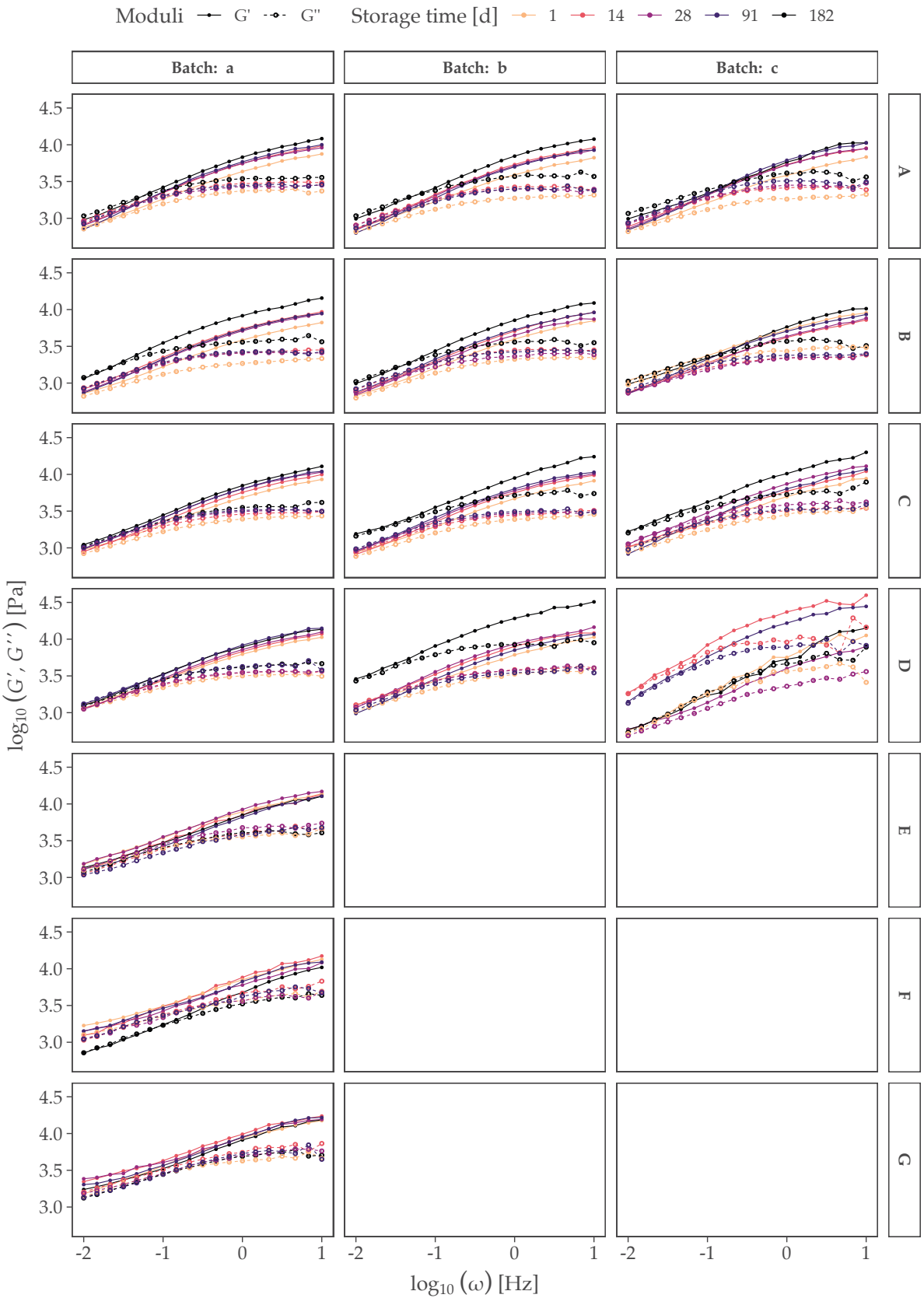

SOURCE: the author, (2020).

APPENDIX C – COMPARISON BETWEEN OPTICAL MICROSCOPY AND FRAUNHOFER DIFRACTION METHODS FOR DROPLET SIZING FOR THE BATCH b OF THE FORMULA B IN DISTINCT STORAGE TIMES AT AMBIENT TEMPERATURE

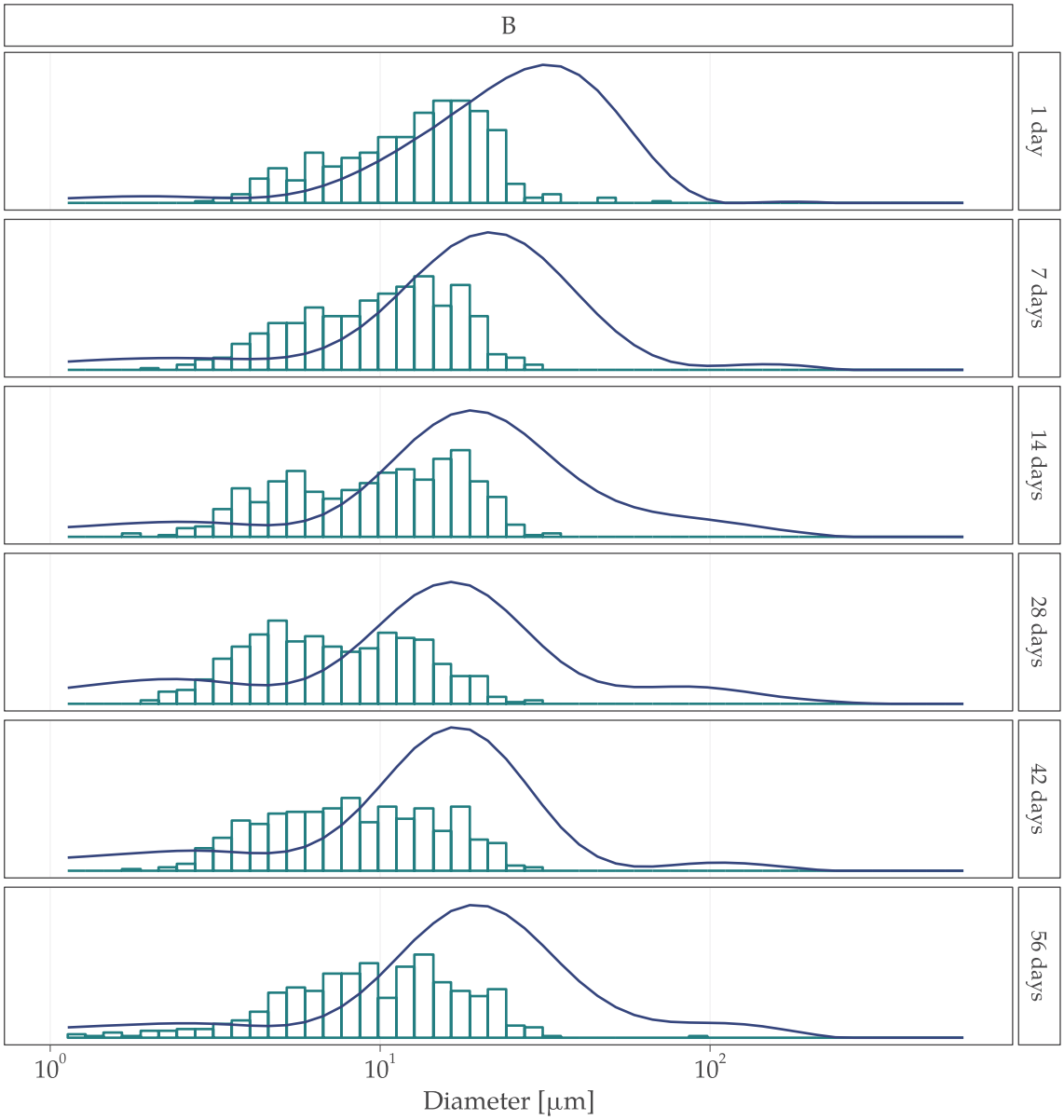

LEGEND: Histogram represents the distribution of droplets as measured by optical microscopy and line represents the distribution of droplets as measured by Fraunhofer diffraction method.
SOURCE: the author, (2020).